Pathophysiology of cerebral ischemia: Role of Cytotoxic T Lymphocytes (CTLs) and Granzyme-b mediated cell death in the rat model of transient focal cerebral ischemia.

Thesis submitted for the degree of
Doctor of Philosophy
in
Animal Sciences

Supervisor
Prof. P. Prakash Babu

By
Ganta Vijay Chaitanya
Enrolment No. 03LAPH07

Department of Animal Sciences and
Department of Biotechnology
School of Life Sciences
University of Hyderabad
Hyderabad 500 046
India

University of Hyderabad
(Central university established in 1974 by the Act of Parliament)
Hyderabad-500046, India

CERTIFICATE
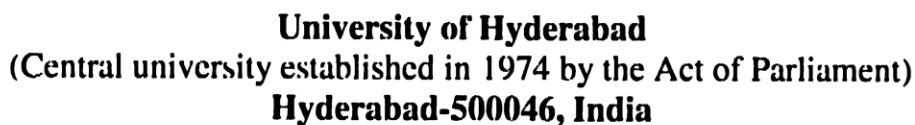
This is to certify that **Mr. Ganta Vijay Chaitanya** has carried out the research work

embodied in the present thesis under my supervision and guidance for a full period

prescribed under the Ph. D. ordinance of this university. We recommend his thesis

"Pathophysiology of cerebral ischemia: Role of Cytotoxic T Lymphocytes (CTLs)

and Granzyme-b mediated cell death in the rat model of transient focal cerebral

ischemia" for submission to the degree of doctor of philosophy of this university

Prof. P. Prakash Babu
Supervisor

Head
Department of animal Sciences

Dean
School of Life Sciences

University of Hyderabad
(Central university established in 1974 by the Act of Parliament)
Hyderabad-500046, India

DECLARATION

I hereby declare that the work embodied in this thesis entitled "**Pathophysiology of cerebral ischemia: Role of Cytotoxic T Lymphocytes (CTLs) and Granzyme-b mediated cell death in the rat model of transient focal cerebral ischemia**" has been carried out by me under the supervision of Prof. P. Prakash Babu and this has not been submitted for any degree or diploma of any other university earlier.

Prof. P. Prakash Babu
(Research Supervisor)

G. Vijay Chaitanya
(Research Scholar)

Dedicated to

Jehovah Jireh

ACKNOWLEDGEMENTS

Abbreviations

AEC	Amino Ethyl Carbazole
AIF	Apoptosis Inducing Factor
ALP	Alkaline phosphatase
ATP	Adenosine 5'-tri phosphate
BCIP	5-bromo-4-chloro-3-indolyl phosphate
Ca^{2+}	Calcium ions
CAMP	Cyclic adenosine mono phosphate
CD	Cluster of Differentiation
Cl_2	Chlorine
CNS	Central Nervous System
COX-2	Cyclo-Oxygenase-2
CPCSEA	Committee for the Purpose of Control and Supervision on Experiments on Animals.
CTL	Cytotoxic T Lymphocyte
Cyt-C	Cytochrome-C
DAB	Di Amino Benzidine
DAPI	4',6-diamidino-2-phenylindole
DNA	Deoxy ribose nucleic acid
DTT	1,4-Dithio-DL-threitol
dUTP	deoxy uridynyl tri phosphate
EDTA	Ethylenediaminetetraaceticacid
FITC	Fluorescein iso-thio-cyanate
GFAP	Glial fibrillary acidic protein
Gra-b	Granzyme-b
H+	Hydrogen ion
H_2O	Water
H_2O_2	Hydrogen peroxide
HCl	Hydrogen Chloride
hrs	Hours

HSP-70	Heat shock protein-70
IBA	Ionized calcium binding adaptor molecule
IL-2	Inter Leukin-2
IκB	Inhibitor of kappa Beta
iNOS	inducible Nitric Oxide Synthase
IP-10/CXCL10	Interferon γ inducible protein-10
JNK	Jun N-terminal Kinase
KCl	Potassium Chloride
kDa	Kilo Dalton
MAP-2	Micro tubule associated Protein-2
MCA	Middle Cerebral Artery
mg	Milligrams
$MgCl_2$	Magnesium Chloride
mins	Minutes
mM	Millimolar
Mn	Manganese
MRI	Magnetic Resonance Imaging
Na^+	Sodium ion
Na_2EDTA	Ethylenediaminetetraacetic acid disodium salt dihydrate
NaCl	Sodium Chloride
NAD+	Nicotinamide adenine dinucleotide
NADP+	Nicotinamide adenine dinucleotide phosphate
NADPH	Nicotinamide adenine dinucleotide phosphate, reduced form
NaEGTA	Ethyleneglycol-bis(β-aminoethylether)-N,N,N',N',-tetraacetic acid tetrasodium salt
NaOH	Sodium hydroxide
NBT	Nitro blue tetrazolium
NF-κB	Nuclear Factor kappa Beta
NK cells	Natural killer cells

nM	Nanomolar
NMDA	N-methyl D-aspartate
nNOS	Neuronal Nitric Oxide Synthase
NO	Nitric oxide
PARP	Poly (ADP)Ribose polymerase
PBN	N-tert-butyl-alpha-phenylnitrone
PBS	Phosphate Buffered Saline
pH	Negative logarithm of hydrogen ion concentration
PI	Propidium Iodide
PMSF	Phenylmethylsufonyl fluoride
PSD-95	Post synaptic density protein-95
ROS	Reactive Oxygen Species
SDS	Sodium dodecyl sulphate
SDS-PAGE	Sodium dodecyl sulphate polyacrylamide gel electrophoresis
tBid	Truncated Bid
Tdt	Terminal deoxy nucleotidyl transferase
TE	Tris EDTA
tg	transgenic
TNF-α	Tumor Necrosis Factor- α
tPA	Tissue Plasminogen Activator
Tris	Tris (hydroxy methyl) amino methane
TRITC	Tetramethyl Rhodamine Iso-Thio-cyanate
TTC	Tetrazolium tri chloride
TUBIII	Tubulin-III
TUNEL	Terminal deoxy Uridine Nick End Labeling
w/v	Weight /Volume

List of Figures:

Fig-60: Schematic representation of the proposed gra-b pathway during the pathology of cerebral ischemia.

List of Tables:

Contents

General Introduction

INTRODUCTION

Stroke is the rapid development of loss of brain functions due to a disturbance in the blood vessels supplying blood to the brain. In medicine, a stroke, fit, or faint is sometimes referred to as an ictus (cerebri; Latin: *icere* "to strike"). In the past, stroke was referred to as cerebrovascular accident or CVA, but the term "stroke" is now preferred. The traditional definition of stroke, devised by the World Health Organization in the 1970s, is "a neurological deficit of cerebrovascular cause that persists beyond 24 hrs or is interrupted by death within 24 hrs". There are mainly two types of strokes, 1) Ischemic stroke and 2) Hemorrhagic stroke.

Ischemic Stroke

Ischemic stroke is caused by an obstruction of an artery supplying blood to the brain, preventing oxygenated blood from reaching the areas supplied by the artery (Fig-1). Ischemic strokes are either thrombotic or embolic, depending on the origin of the obstruction or clot (thrombus or embolus). About 83 percent of strokes are ischemic. Thrombotic ischemic stroke is caused by a thrombus (blood clot) that develops in an artery supplying blood to the brain. There are two types of thrombotic stroke namely, large vessel thrombosis which occurs in the brain's larger arteries and small vessel thrombosis also known as lacunar infarction occurs when blood flow is blocked to a very small arterial vessel. Thrombotic disease accounts for about 60 percent of acute ischemic strokes. Of those, approximately 70 percent are large vessel thrombosis. In case of embolic stroke, the clot forms outside of the brain usually in the heart or large arteries of the upper chest and neck and is transported through the bloodstream to the brain. Many emboli are caused by a cardiac condition called atrial fibrillation, which is an abnormal

rapid heartbeat. 80 percent of embolic ischemic strokes are due to cardiac sources of embolism.

Hemorrhagic Stroke

Hemorrhagic stroke occurs when a vessel in the brain suddenly ruptures and blood begins to leak directly into brain tissue and/or into the clear cerebrospinal fluid that surrounds the brain and fills its central cavities (ventricles). There are two types of hemorrhagic strokes. Intracerebral hemorrhage (ICH) and subarachnoid hemorrhage (SAH). They are differentiated by where the ruptured artery is located and where the resulting blood leakage occurs. About 17 percent of strokes are hemorrhagic. Intra cerebral hemorrhage is also called intraparenchymal hemorrhage or intracranial hematoma. The sudden rupture of an artery or blood vessel within the brain causes this type of stroke (Fig- 2). They occur most commonly in the basal ganglia where the vessels can be particularly delicate. Approximately 10 percent of strokes are intracerebral hemorrhages. Subarachnoid hemorrhage occurs when bleeding from a damaged vessel causes blood to accumulate between the brain and the skull, in the subarachnoid space creating pressure on the surface of the brain instead of dispersing into the tissue (Fig- 3).

Symptoms of stroke

Sudden numbness of the face, arm, or leg, especially on one side of the body, confusion, trouble speaking or understanding speech, trouble seeing in one or both eyes, dizziness, loss of balance or coordination, and/or sudden severe headache with no known cause (most common with hemorrhagic stroke). The symptoms depend on the part of the brain that's affected. Stroke may be associated with a headache, or may be completely painless. Therefore, signs and symptoms vary from person to person (Fig- 4).

Fig-1

Ischemic Stroke

)ccurs when oxygen rich blood flow to the brain
is restricted by a blood clot or other blockage

Blood clot in
the middle
cerebral artery

Blockaye in
the interna
carotid arte
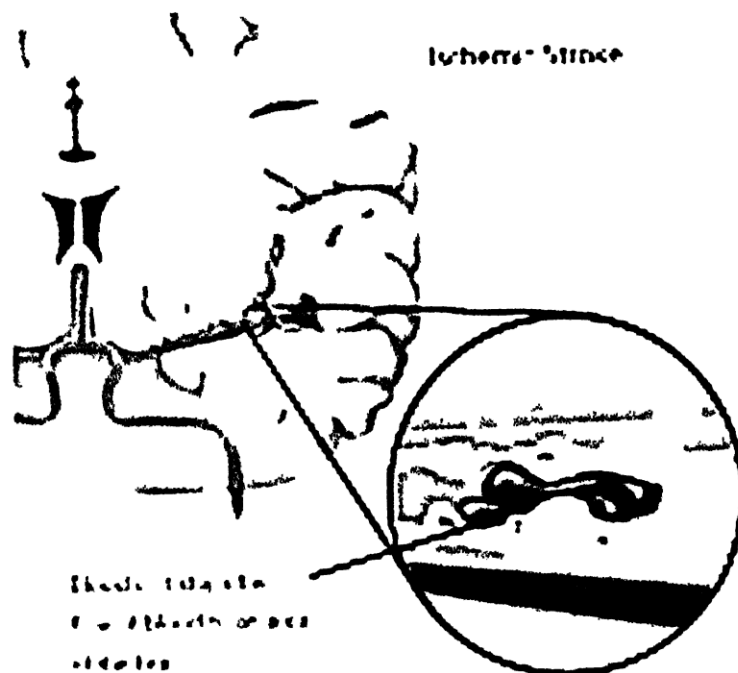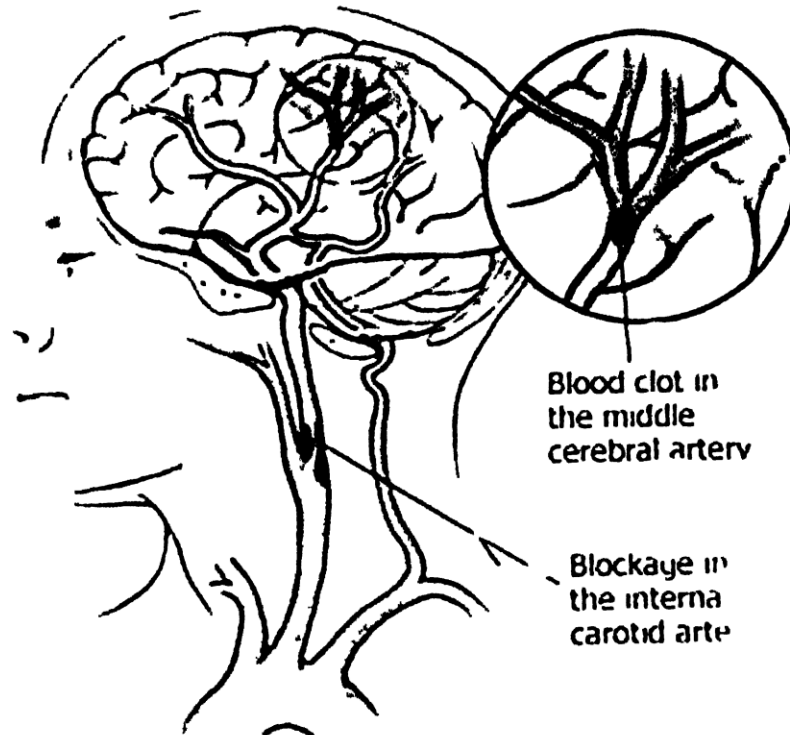
Fig-2

Intracerebral Hemorrhage
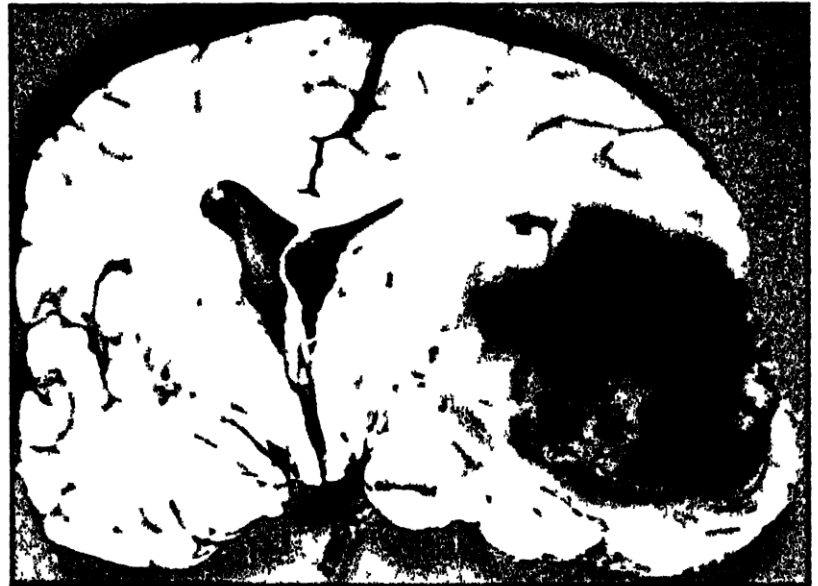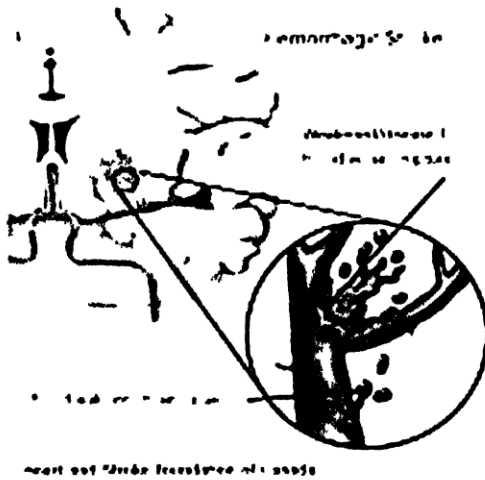
Fig-3

Subarachnoid hemorrhage

The meninges are the membranes covering the brain and spinal cord

Dura mater (2 layers)
Arachnoid
Pia mater
Brain
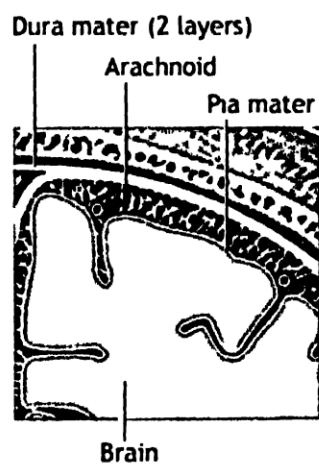
Fig-4

Symptoms of cerebral ischemia (Stroke)

Sudden severe headache ——
with no known cause

Unexplained dizziness, ——
unsteadiness or sudden falls,
especially with any of the
other signs

Sudden difficulty speaking or ——
trouble understanding speech

Sudden dimness or loss of ——
vision, particularly in one eye

Sudden weakness or numbness
of the face, arm or leg on one
side of the body

General Introduction

Risk Factors

A healthy lifestyle and diet along with preventive medical care where appropriate can significantly reduce the risk of suffering a stroke. By modifying certain behaviors and getting treatment for risky medical conditions, it is possible to prevent or control many of the conditions that commonly lead to stroke. Some of the risk factors for stroke are

- Diet & Nutrition
- Physical activity
- Smoking: Risk of stroke increases incrementally depending on the number of cigarettes a person smoke per day.
- Substance Abuse
- Alcohol consumption: Studies suggest that two drinks or more a day may increase more than tenfold the chances of suffering a subarachnoid hemorrhage (SAH).
- Obesity: Modest weight gain over the ideal weight, such as 24 to 43 pounds over 16 years, doubles the chances of suffering a stroke
- Abnormal blood vessel connections (arteriovenous malformations and arteriovenous fistulas)
- Cerebral aneurysms (unruptured)
- Cholesterol level (high levels of "bad" cholesterol and/or low levels of "good" cholesterol)
- Diabetes: People with diabetes are two to four times more likely to suffer strokes. Hardening of the Arteries (Atherosclerosis/Arteriosclerosis)
- Heart Disease (Cardiovascular Disease): About 15 percent of strokes occur in people with atrial fibrillation.

General Introduction

- ➤ High Blood Pressure (Hypertension)

- ➤ Age: The chance of suffering a stroke more than doubles for each decade of life after age 55.

- ➤ Ethnicity

- ➤ Heredity/family history of stroke

- ➤ Gender: Men have a higher risk for stroke (1.25 times that of women), but more women die from stroke.

Current statistics of stroke survival rates

- Worldwide, stroke is the second leading cause of death, responsible for 4.4 million (9 percent) of the total 50.5 million deaths each year.

- Stroke incidence in India is put at about 800 per 100,000 population. Current

statistics of stroke survival, disability and the mortality due to different types of strokes are shown in Fig- 5.

Data and figures for general introduction are obtained from

- ❖ University Hospital of Newark,

- ❖ National Institute of Neurological Disorders and Stroke (NINDS) - National Institutes of Health.

Figures obtained from

- ↓ www.heartandstroke.com

- ↓ www.medhelp.org

Fig-5

Percentage of patients suffering with disability after stroke

Minor impairments

Require Personal care

40
35
30
25
20
15
10
5

Survive — Experience moderate to severe impairments — Die shortly
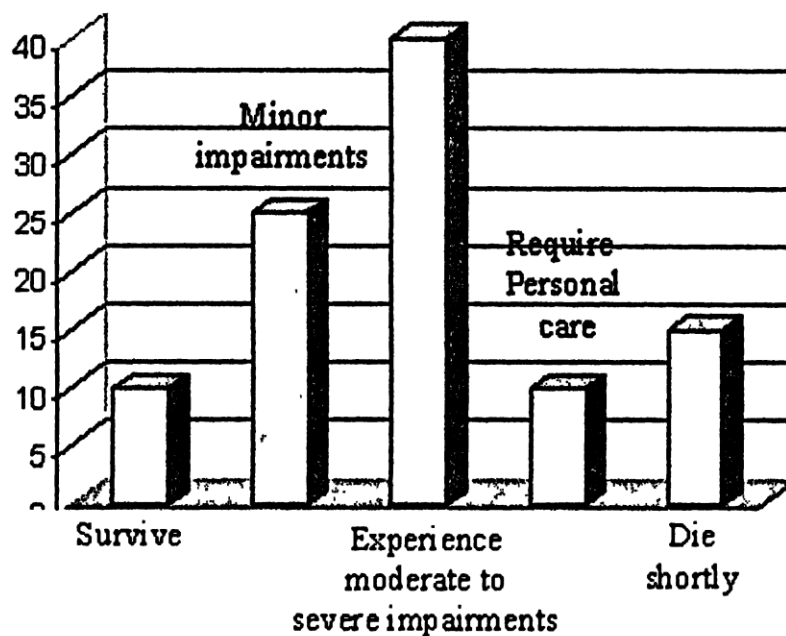
Mortality rate of ischemic, hemorrhagic and Sub-arachnoid strokes

50
45
40
35
30
25
20
15
10
5
0

Ischemic — Hemorrhagic — Sub arachnoid
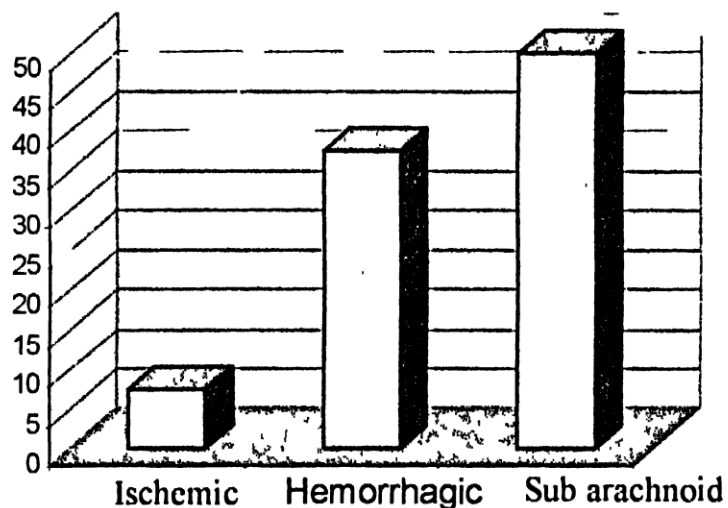
Though subarachnoid hemorrhage constitutes 7% of strokes mortality rate is high in sub-arachnoid strokes (50 %)

General Introduction

Animal models of cerebral ischemia

To predict the value and effect of therapeutic approaches in human subjects, use of appropriate animal models is very essential. Focal (stroke) and global (cardiac arrest) cerebral ischemia represents neurodegenerative disorders that are common in the humans. Experimental models for cerebral ischemia are characterized as global, focal, and multifocal ischemia depending upon the occlusion of type and number of cerebral blood vessels (Fig-6). The major blood vessels of cerebral blood flow and circle of Willis are depicted in Fig-7. Global ischemia occurs when cerebral blood flow (CBF) is reduced throughout the brain for varying time periods, whereas focal ischemia is represented by a reduction in blood flow to a very distinct, specific brain region. In multifocal ischemia, a patchy pattern of reduced CBF occurs. With complete ischemia, global blood flow ceases completely; whereas with incomplete global ischemia, global blood flow is severely reduced but the amount of flow is insufficient to maintain cerebral metabolism and function. In focal cerebral ischemia, usually no blood flows in the central core but there will be some blood flow that reaches the periphery via collateral circulation (Fig-8). Hence there will be a gradient of blood flow from the inner core to the outer penumbra of the ischemic area.

Focal cerebral ischemia models involve occlusion of one major cerebral blood vessel such as the middle cerebral artery (MCA) (Fig-9) (Garcia 1984; Hossmann 1991; Ponten et al. 1973). MCA occlusion (MCAo) results in a reduction of CBF in both the striatum and motor cortex, but the degree and distribution of blood flow reduction depends on the duration of MCAo, the site of occlusion along the MCA, and the amount of collateral blood flow into the MCA territory. Different types of MCAo models exist,

and for the most part they are either a permanent or temporary (reperfusion) occlusion with MCA occlusion at either the proximal or distal part of the vessel. These MCAo models have been used extensively because of their purported relevance to human thrombo-embolic stroke. There is widespread use of these models in studying pharmacological neuroprotection and mechanisms of injury from ischemia, and for characterization of genes and proteins involved in stroke.

Animal model for present study

In the present study we employed transient focal cerebral ischemia. In this model middle cerebral artery is occluded distally using a nylon monofilament of 3-0. The benefit of this model is, it mimics human focal ischemia to a large extent, and the injury to the animal is highly reproducible. Further, most of the human focal cerebral ischemic strokes were due to middle cerebral artery occlusion either by thrombus or embolus. Detailed surgical procedure indicating the surgical procedure is given in the materials and methods section under surgical procedure and photographs were presented in Fig-10.

Fig-6: Animal models of cerebral ischemia are divided into global or focal depending on the number of blood vessels being occluded. Further they are subdivided into transient or permanent depending on whether the blood vessel is being occluded permanently or for some specific period of time allowing the blood to reperfuse again.

Fig-7: Major blood vessels of the brain. ACA- Anterior carotid artery, IC-internal carotid artery, MCA-middle cerebral artery, PCA-posterior carotid artery, BA-basilar artery, VA-Vertebral Artery.

Fig-6

Animal models of cerebral ischemia


```
            ┌──── Permanent
Complete ───┤
            └──── Global ischemia
                │
             Transient
                │
            ┌──── Incomplete
            │
            └──── Focal ischemia
                  Permanent
```

Fig-7

Major blood vessels of the brain

The Circle of Willis

Anterior

Frontal lobe

Optic chiasma — into brain

Middle cerebral artery

Internal carotid artery — into brain

Pituitary gland

Temporal lobe — into brain

Pons

Occipital lobe

into brain

Circle of Willis
• Anterior communicating artery

• Anterior cerebral artery

• Posterior communicating artery

• Posterior cerebral artery

Basilar artery

Vertebral artery

Cerebellum

(d)

Posterior

Fig-8: Ischemic infarct. Any obstacle in the blood vessel carrying blood to the brain results in an infarct comprising of necrotic core surrounded by physiologically ill penumbra which gradually merges into the core if suitable pharmacological intervention is not provided. Usually anoxic conditions prevail in necrotic core and hypoxic conditions prevail in penumbra.

Fig-8

Ischemic infarct during focal cerebral ischemia

Penumbra

Core

Thrombus

Internal carotid artery

External carotid artery

Common carotid artery

CORE ⟶ PENUMBRA

Time
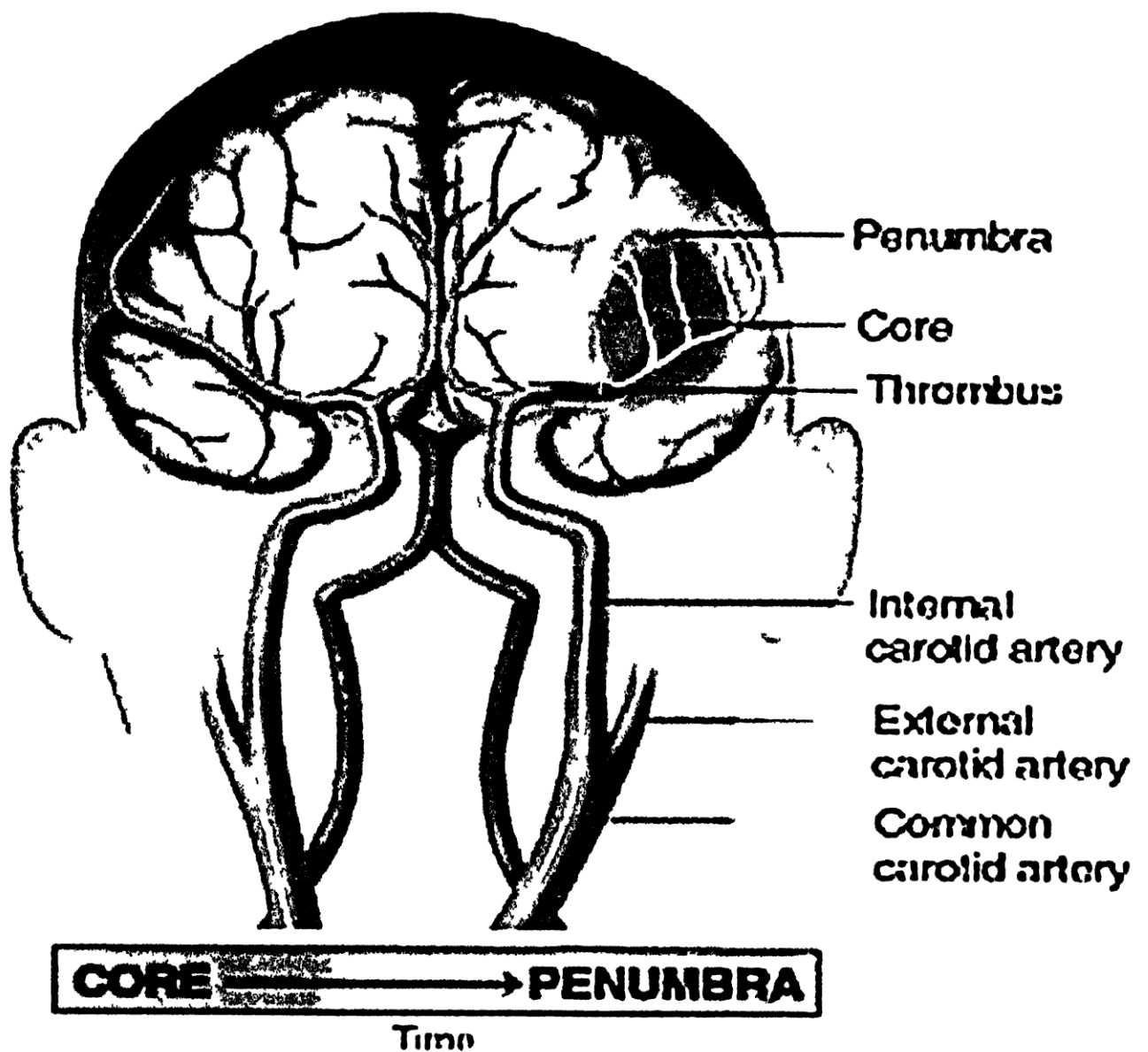
Fig-9: Schematic representation of MCA occlusion model in rat. The major blood vessels and the path of the nylon monofilament insertion and travel are depicted. The insertion of nylon monofilament to an appropriate distance via the external carotid artery into the internal carotid results in an ischemic infarct in rat that mimics the ischemic infarct in humans to a large extent.

Fig-9

Schematic representation for the
animal model of focal cerebral ischemia

Middle Cerebral
Artery (MCA)

Anterior cerebral
artery

Internal
carotid
artery

Posterior
cerebral
artery

Tympanic
bulla

Superior
thyroid
artery

Occipital
artery

External
carotid
artery

Pterygopalatine
artery

Nylon mono-
filament
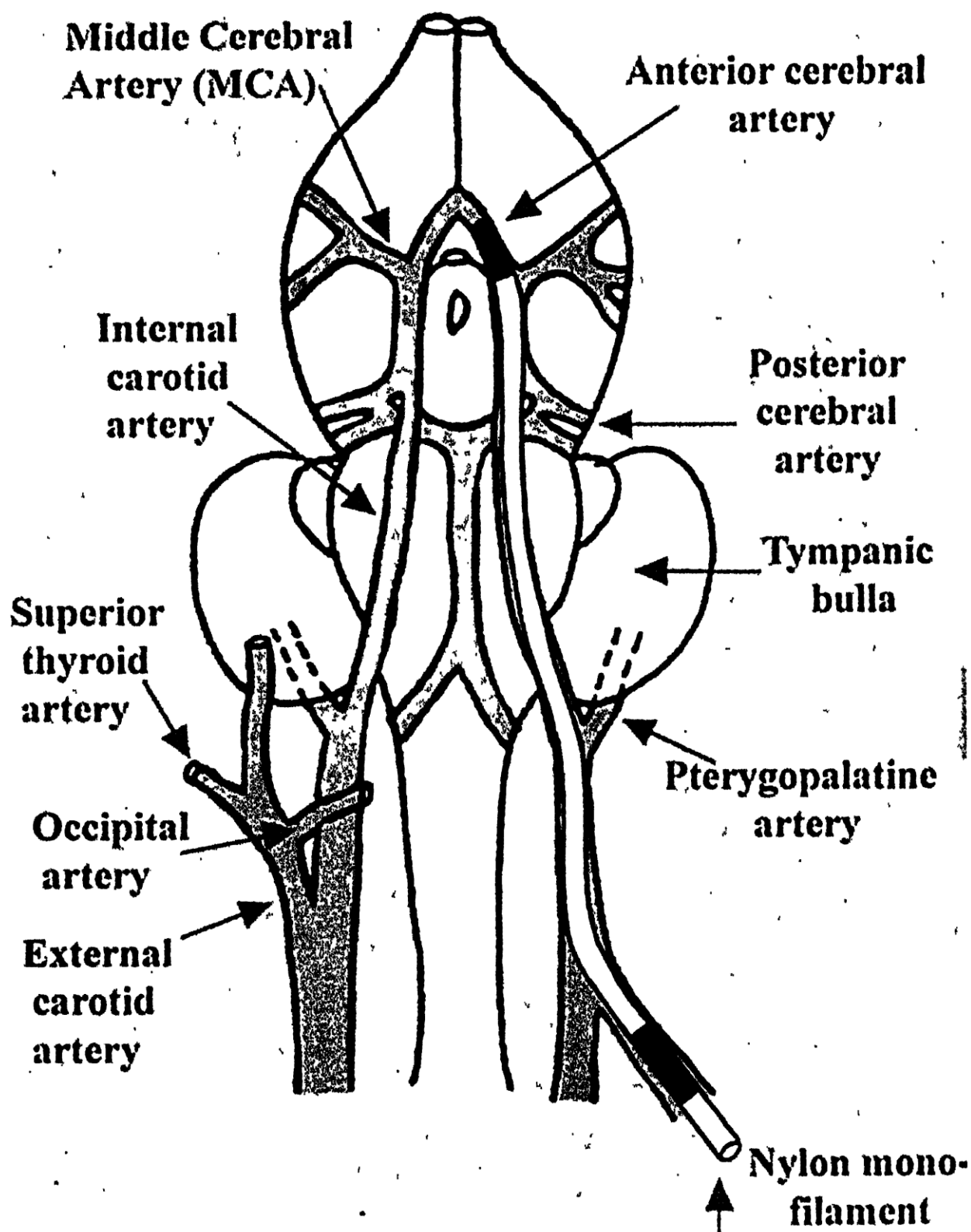
Experimental Procedures

Experimental Procedure

Surgical procedure

All experiments were performed according to the guidelines of Institutional Animal Ethical Committee (IAEC). Male Wistar rats, weighing 300-350g, were used in the present study. Rats were randomly divided into 6 groups. 1- Sham group; 2- permanently occluded for 3 hrs; 3- 1hr reperfused; 4- 12 hr reperfused; 5- 1 day reperfused; 6- 3 days reperfused groups which were 3 hr MCA occluded. MCA occlusion was achieved by the nylon suture method (Longa et al., 1989), in which the left middle cerebral artery (MCA) was occluded by inserting a nylon monofilament through the external carotid artery to occlude origin of MCA for 3 hrs. The animals were anesthetized using N_2O-halothane mixture through facemask. Briefly a midline neck incision was made and the bifurcation of the left common carotid artery was visualized. The bifurcation of the left internal carotid artery, and the left external carotid artery were exposed and the external carotid artery was ligated distally. A 3-0 monofilament suture (50 mm in length) was inserted through an arteriectomy of the external carotid artery. The nylon suture was gently advanced from the external carotid artery into the internal carotid artery. The path of the suture toward the base of the skull was visualized. Approximately 17.5 to 18 mm of suture was inserted past the common carotid artery bifurcation to block the origin of the left MCA. The occlusion of the MCA was felt. For the sham-operated rats, the carotid arteries were exposed; suture was inserted but not extended to occlude the MCA. The animals were allowed to recover from anesthesia. After the occlusion period the animals were re-anaesthetized and the filament was removed from the artery at various reperfusion time periods.

3 rats from 1 hr reperfusion time period were perfusion-fixed with saline followed

Experimental Procedure

by 4% paraformaldehyde and the brains were dissected out for immunohistochemical analysis. Group of 4 rats from each group were killed with an overdose of pentobarbital, brains were removed quickly and the ipsilateral ischemic regions were processed for immunoblotting.

Behavioral tests

After the animal recovered from anesthesia, behavioral functional tests were performed by an observer who was masked to the experimental conditions. Neurological deficits were scored on a scale of 0 to 5 (Murakami et al, 1998): no neurological deficit (0); failure to extend the right forepaw fully (1); circling to the right (2); falling to the right (3); unable to walk spontaneously (4); and dead (5). The second test, known as the corner test, which is a sensorimotor functional assessment, was performed in ischemic animals as described previously (Zhang et al, 2002). In this test, the ischemic rat turns preferentially towards the non-impaired side. The animals that exhibited only a 1st or 2nd degree of behavioral deficit were taken in this study (Video-1)

TTC staining

After decapitation ischemic rat brains were dissected immediately and chilled in ice-cold saline for 5 min. The brain was sliced into 2mm thick slices with the help of brain matrices. The slices were then incubated in phosphate-buffered saline (pH 7.4) containing 2% TTC at 37^0C for 20 min and then stored in 10% neutral-buffered formalin (Brenden et al., 2006). Slices were photographed with the help of Nikon camera.

Cresyl Violet staining

Formalin fixed, paraffin embedded ischemic rat brain sections were deparaffinized in xylene, rehydrated in alcohol series and incubated in 0.1% Cresyl violet

Fig-10: Surgical procedure for MCA occlusion in rat. The detailed surgical procedure of MCA occlusion in rat has been photographed and incorporated. Arrows point towards the major blood vessels that were isolated, cauterized and arteriectomized to facilitate the insertion of nylon monofilament and to achieve the occlusion of middle cerebral artery. A nylon monofilament of 3-0 size was inserted through the external carotid artery and extended to a length of 17.5 to 18 mm in the internal carotid artery to achieve MCA occlusion. The filament was retained for 3 hrs and then pulled back to facilitate reperfusion. Animals showing any signs of hemorrhage evident by the efflux of blood from eyes and nose were not taken into the study. Some of the animals showing the signs of effusion but not hemorrhage were also not taken to study.

Fig-10

Surgical procudere for Middle Cerebral atrery (MCA) occlusion in rat

Anaesthetised rat
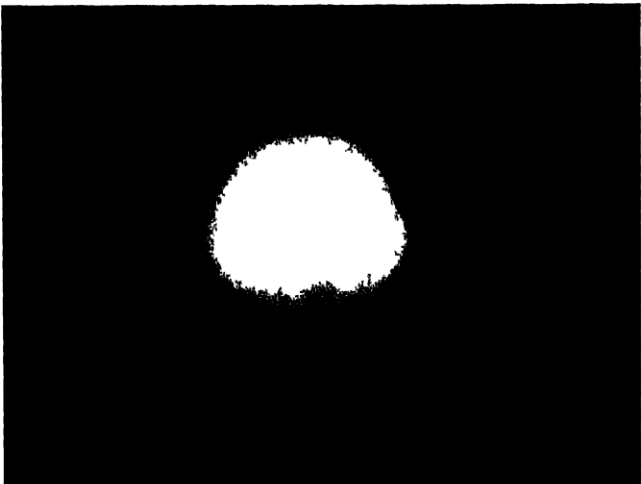
Mid-line incision on neck
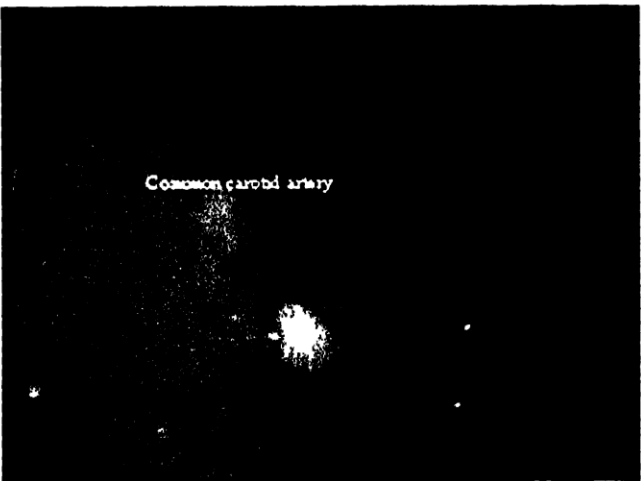
Isolation of common carotid artery

Cauterization of superior thyroid artery

Separation of vagus nerve from carotid artery

Isolation of occipital artery

Arteriectomy of external carotid artery
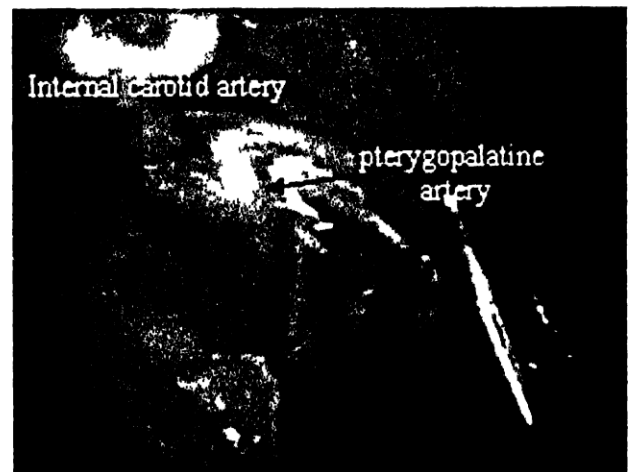
Occluding pterygopalatine artery

Insertion of nylon monofilament from arteriectomized external carotid artery
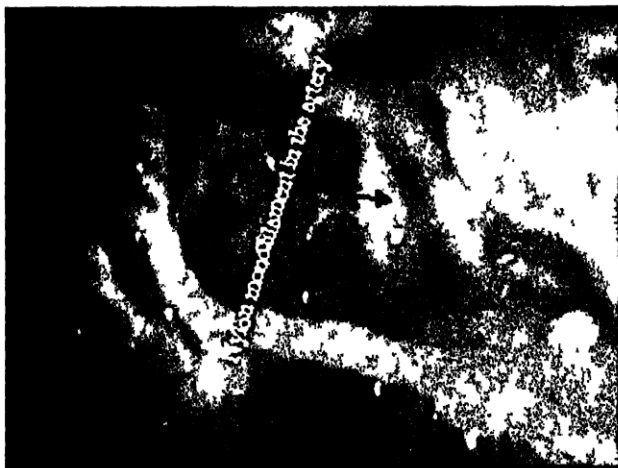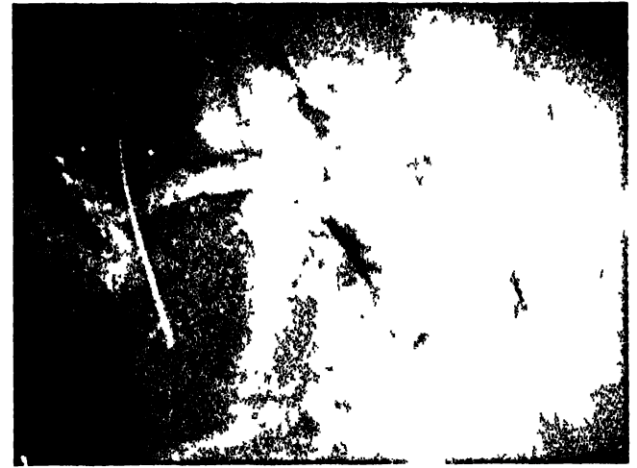
Filament removed after 3 hours

Recovery of the animal from anaesthesia

Experimental Procedure

solution for 3-5 mins. The sections were then rinsed in distilled water and differentiated in 95% alcohol, followed by dehydration in 100% alcohol. The sections were then cleared in xylene and mounted using DPX mounting medium.

Antibody dilutions

Western blot analyses for Calpain, cathepsin-b, caspase-3, α-spectrin, PSD-95, NF-κB 50, NF-κB 65, IP-10/CXCL10, IL-2, TNF-, COX-2, GFAP, Gra-b, PARP, HSP-70, and AIF were performed at a dilution of 1:1000.

Immunohistochemical analyses were performed according to the following dilutions. Calpain, cathepsin-b, caspase-3, IP-10/CXCL-10, gra-b, AIF (1:100); NF-κB 105, CD11b (1:200); IBA (1:250); CD-8 (1:50); Neu-N (1:200).

Double immunofluorescence analyses were performed according to the following dilutions. PARP (1:250), gra-b (1:100), NSE (1:200), CD-3 (1:50), TubIII (1:250), NF-kB (1:100), MAP-2 (1:300).

Western blots

Sham and ischemic rats were killed with an overdose of pentobarbital and their brains were dissected out (n=4). Contralateral and ipsilateral hemispheres were separated and immediately snap frozen in liquid nitrogen. Tissues were then homogenized in the modified radio-immunoprecipitation assay buffer containing 50 mM Tris–HCl pH 7.4, 150 mM NaCl, 1 mM EDTA, 0.4% Na deoxychlolate, 1% non-idet NP-40 containing protease inhibitor 2 mM PMSF, and the phosphatase inhibitors 10 mM β-glycerophosphate, 10 mM NaF, and 0.3 mM Na_3VO_4. The lysates were sonicated for 2 min at equal time intervals and centrifuged at 14,000g for 15 min at 4^0C. Supernatants were collected in prechilled eppendorf tubes and used as protein samples for further

Experimental Procedure

analysis. The samples were stored at -80^{0}C for further experiments. An equal amount of protein was separated using SDS-PAGE and transferred onto a nitrocellulose membrane. After blocking in non-fat milk (5%) in tris buffer saline (TBS; 10 mM Tris pH 7.5, 150 mM NaCl) for 2 hrs at room temperature, membranes were incubated for 12–14 hrs in primary antibodies at 4^{0}C over night. The membranes were subsequently washed and incubated with ALP-conjugated secondary antibodies for 2 hrs at room temperature. The blots were washed further and then developed using NBT/BCIP substrate.

Immunohistochemistry

For immunohistochemical analysis (n=3), rats after MCA occlusion were perfusion-fixed with saline and then with 4% paraformaldehyde solution by overdose of pentobarbital. Brains were removed and post fixed in the same fixative for another 24 hrs. Then each tissue block was dehydrated, embedded in paraffin, and cut into 3-4 μm thick coronal sections. Paraffin was removed from slides using xylene, followed by rehydration in an alcohol dilution series. Antigen retrieval was performed using a microwave method. Slides were incubated for 20 mins after slow boiling for 10 mins and rinsed in PBS. Slides were soaked in 0.1% Triton-X 100 in PBS for 5 mins to increase permeability of fixed tissue, followed by rinsing in 1X PBS. Endogenous peroxidase was blocked by incubation for 45 mins in methanol containing 1.5% hydrogen peroxide and blocked using 10% normal goat serum for 1 hr. The sections were then stained with monoclonal antibodies raised against calpain, cleaved caspase-3 (p-20 fragment) and cathepsin-b (diluted 1:100). Later the sections were washed and incubated for 1 hr with peroxidase goat anti-mouse and anti rabbit antibodies followed by developing with DAB complex (DAKO-kit) or AEC kit. All incubations were performed under humidified conditions,

Experimental Procedure

and slides were washed 4 times for 5 mins each in PBS between steps. After developing the sections with AEC substrate, they were counterstained with cresyl violet for immunohistochemical analysis with CD-8.

Double immunohistochemistry

For double immunohistochemical analysis similar procedure was followed, except that after developing the sections with AEC substrate for the first antibody they were further blocked for 30 min in 10% normal goat serum and then incubated in second primary antibody overnight at 4^0c. The sections were subsequently washed and then incubated in the respective secondary antibody conjugated to ALP and then developed using BCIP/NBT substrate.

Double immunofluorescence

Double immunofluorescence analysis was performed by incubating sections in a cocktail of primary antibodies overnight at 4^0C after processing as afore mentioned. The sections were washed and then incubated in cocktail of fluorochrome-conjugated secondary antibodies for 1 hr at room temperature and mounted using 90% glycerol. The immunofluorescence was visualized under Leica confocal microscope.

Co-localization of TUNEL and Gra-b

As described for immunofluorescence analysis, 3-μm-thick sections were processed for gra-b. The sections were then incubated with monoclonal antibody directed against anti-mouse gra-b (1:100 dilution) overnight at 4^0C. The sections were subsequently washed and incubated in equilibration buffer for 10 mins and processed according to the TUNEL protocol. Briefly, after incubating the sections in equilibration buffer, the sections were incubated in a mixture consisting of FITC-labeled BrdU and

Experimental Procedure

TdT enzyme in equilibration buffer for 60 min at 37^0C. Later, the reaction was stopped in stop buffer, washed, and incubated in anti-mouse TRITC secondary antibody (1:500 dilution) for 30 mins at room temperature and visualized under a Leica confocal microscope.

Co-immunoprecipitation

Co-immunoprecipitation was performed to examine protein–protein interactions between gra-b and caspase-3, Bid, and PARP using standard procedures (Cao et al, 2001). Briefly, cytosolic protein was isolated from cerebral cortices using a homogenization buffer containing 50 mM Tris–HCl pH 7.4, 150 mM NaCl, 1 mM EDTA, 0.4% Na deoxychlolate, 1% non-idet NP40 containing protease inhibitor 1 mM PMSF, and the phosphatase inhibitors 10 mM β-glycerophosphate, 10 mM NaF, and 0.3 mM Na_3Vo_4. Equal amounts of protein from each sham and 1 hr ischemic samples (250 μg per sample) was suspended in immunoprecipitation buffer consisting of 50mMTris HCl (pH 7.4), 150mM NaCl, NP40 0.25%, PMSF 2mM, and normal goat serum 2%. After pre-clearing the sample with 10μlts of protein A sepharose beads, the lysates were incubated with Gra-b (0.5 μg) antibody overnight at 4^0C. The lysate was further incubated with 25 μl of protein A sepharose beads for 60 mins. The beads were then washed 5 times with PBS (pH 7.4), boiled in 2X sample buffer, and separated on SDS-PAGE. This was followed by immunoblotting with caspase-3 (1:1000), Bid (1:1000), and PARP (1:1000), respectively.

Status of suicidal proteases mediating apoptotic and necrotic cell deaths during the pathology of cerebral ischemia

INTRODUCTION

Types of cell death

Apoptosis

Apoptosis (Greek- falling of leaves) is the most common and well-defined form of programmed cell death. It is the physiological program of cellular suicide whose role is inevitable in embryonic development, proper function of immune system and maintenance of tissue homeostasis (Kerr et al., 1972, Jacobson et al., 1997). Apoptosis in mammalian cells is regulated by a family of suicidal proteases known as caspases (cysteine activated aspartate proteases). Effector caspases (caspase-3 and 7) are initially expressed as inactive precursors. During apoptotic insults they are activated by initiator caspases such as caspase-8 and or caspase-9. Effectors cleave various cellular substrates resulting in specific well known biochemical and morphological changes (Stefan et al., 2004). Morphological features of apoptotic phenotype include cellular shrinkage, condensation and margination of chromatin, blebbing of plasma membrane, and formation of apoptotic bodies, which consist of cell organelles and or nuclear material, surrounded by intact plasma membrane (Fig-11) (Kerr et al., 1972). The most important of apoptotic cell death which renders it the most desired forms of death is the package of cellular contents into apoptotic bodies without allowing them to spill into the environment thereby resulting in the absence of inflammatory process. The apoptotic cells are finally engulfed by macrophages or surrounding cells with out eliciting inflammatory or immune response, which might be detrimental to the surrounding cells (Fadok et al., 1992).

Classically intrinsic and extrinsic pathways were known to activate caspases, which mediate apoptotic cell death. Extrinsic pathway involves the activation of Fas and Tumor Necrosis Factor (TNF) receptor by Fas and TNF ligands respectively. The binding of Fas and TNF to their receptor receptors results in the formation of Death Inducing Signaling Complex (DISC), which recruits caspase-8 and promotes the cascade of pro-caspase activation (Budihardjo et al., 1999). Mitochondria play a pivotal role in intrinsic pathway. The pathway is triggered by extra and intracellular stresses like growth factor withdrawal, hypoxia, DNA damage and oncogene induction. A series of biochemical events like translocation of Bid and Bax to the mitochondrial membrane takes place which results in the cytosolic release of cytochrome-c (Cyt-c) and other pro-apoptotic proteins like Apoptosis Inducing Factor (AIF). In the cytosol, Cyt-c and Apoptotic Protease Activating Factor-1 (APAF-1) in presence of dATP/ATP forms apoptosome complex, which activates pro-caspase-9, which further, activates pro-caspase-3 resulting in apoptosis (Kluck et al., 1999). Once Cyt-c is released the downstream of caspase cascade is irreversible. However apart from intrinsic and extrinsic cell death pathways caspase-3 can be activated directly by calpains and granzymes and indirectly by cathepsins during various cell death stimuli (Lomgren et al., 2001, Metkar et al., 2003, Yamashima 2000). The ability of these proteases to interact and activate each other has lead to the concept calpain-caspase-calpastatin-cathepsin hypothesis (Fig-12) (Rami 2003).

Necrosis

Necrotic cell death (Necros-dead in Greek) is radically different from apoptosis in most of the aspects. While necrosis results in robust immune and inflammatory

Fig-11: Morphological features of apoptosis and necrosis. Morphological features of apoptosis and necrosis were shown in the picture. Shrinkage of cell, membrane blebbing with no loss of membrane integrity, Formation of apoptotic bodies and non-random mono and oligo-nucleosomal DNA fragmentation resulting in ladder pattern on agarose gel are some of the typical features of the apoptotic cell death. Loss of membrane integrity, swelling of intracellular organelles, absence of vesicle formation and total cell lysis and shearing of DNA resulting in smear pattern on agarose gel are some of the typical features of necrotic cell death.
Image taken from 'www.imbb.forth.gr/worms/worms/newnecrosis.jpg'

Fig-12: Biochemistry of apoptotic and necrotic death. Caspases, calpains and cathepsins were known to mediate cell death independent or dependent of each other. Caspases mediate apoptotic cell death exclusively whereas calpains and cathepsins mediate both apoptotic and necrotic cell deaths. How ever the type of death they mediate depends on the type of insult and the cell type. Further they can act synergically via cross talks during various pathological conditions.

Fig-11

Morphological features of apoptosis and necrosis

NECROSIS

APOPTOSIS

Chromatin clumping
Swollen organelles
Flocculent mitochondria

Mild convolution
Chromatin compaction
and segregation
Condensation of
cytoplasm

Nuclear fragmentation
Blebbing
Apoptotic bodies

Disintegration

Phagocytosis

Apoptotic body

Release of
intracellular
contents

Phagocytic
cell
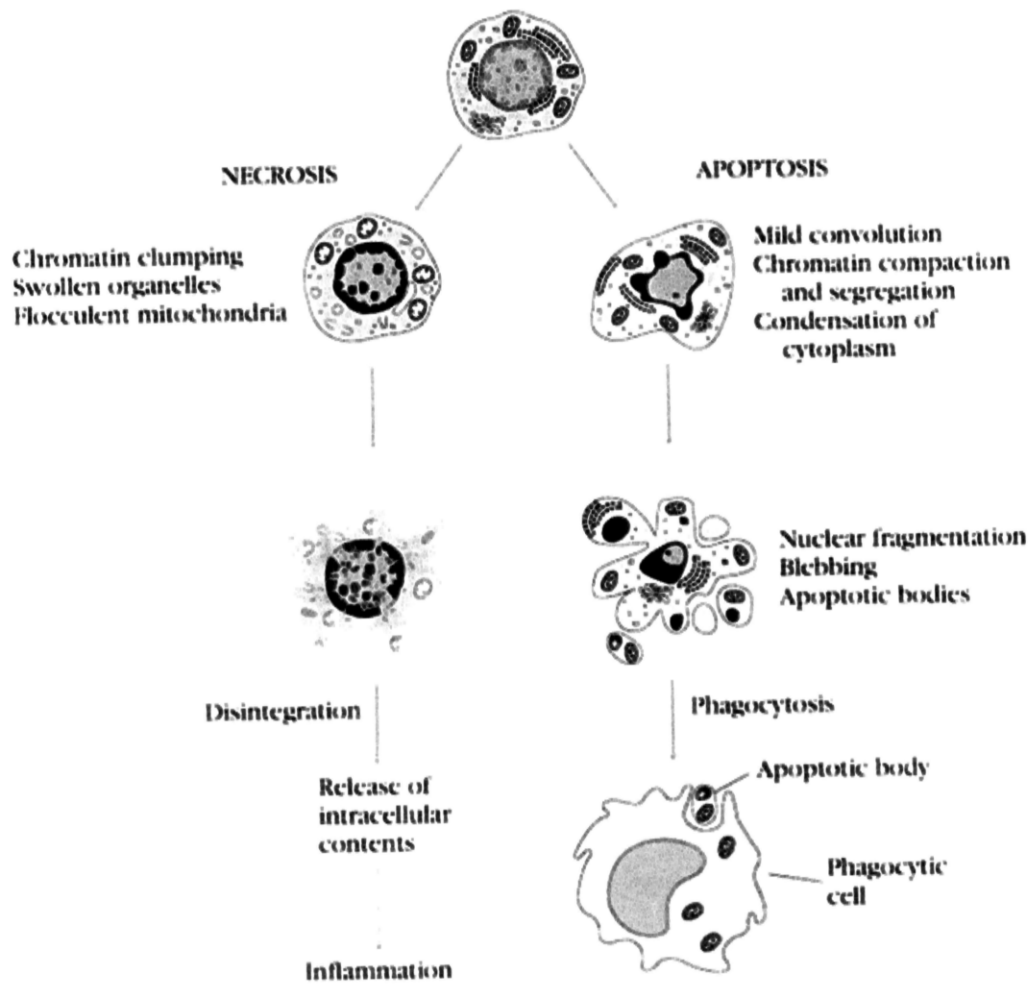
Inflammation

Fig-12

Bio-chemical features of apoptosis and necrosis

TRPM7   ASIC   NMDA   NXC   AMPA/kainate

ER

Lysosome

Mitochondrion

Calpains

Caspases

Cathepsins

H+ H+
H+
H+ H+
H+ H+

AIF   EndoG

Apoptosis   Necrosis

Ca²⁺   ★ Na⁺   ★ Reactive oxygen spieces (ROS)
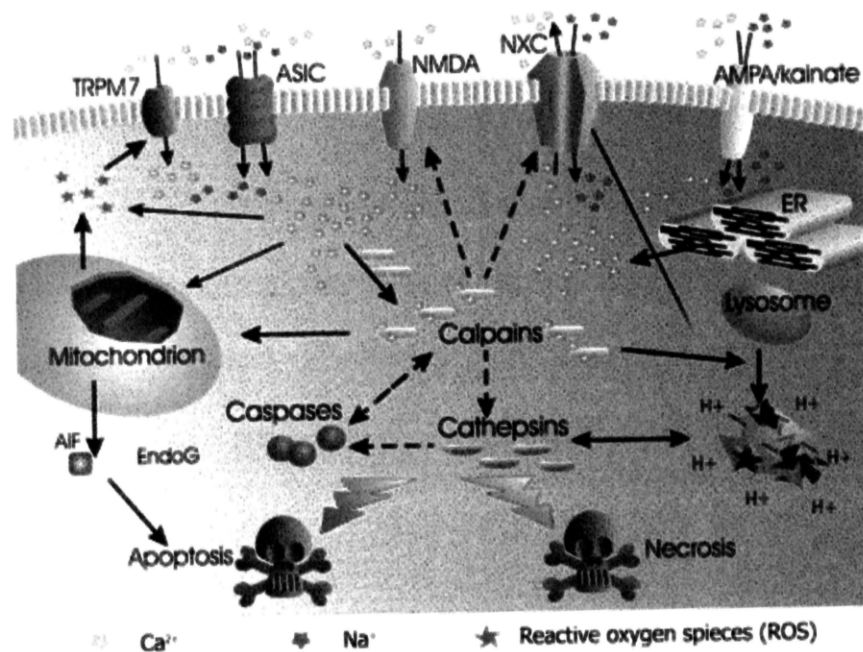
responses, apoptosis is non-immune and non-inflammatory mode of death. The previous notion that necrosis is accidental form of death is put under question in the recent days due to the involvement of specific cell death proteases mediating this form of death. Necrotic death was considered to be inexorable chaotic breakdown of cells under intolerable conditions like extreme environmental conditions and or genetically encoded insults (Syntichaki and Travernarakis 2002). Necrotic cells display morphological features that are strikingly different from those exhibited by apoptotic cells. Extensive swelling of the cell and its intracellular organelles (oncosis), occasional condensation and random fragmentation of nuclear DNA rupture or loss of membrane integrity are the usual features of necrotic cells (Syntichaki and Travernarakis 2003) (Fig-11). Necrotic cell death is further considered to be passive as it doesn't require new protein synthesis, needs only minimal energy requirements and is not regulated by homeostatic mechanism. However most of these biochemical features were not considered to be true in the recent days. It was clearly shown in the recent paper that lysosomal biogenesis and the involvement of cathepsins are required for necrotic cell death (Marta et al., 2006) (Fig-12). Further it was shown that proteases like calpains, TNF and Fas, granzymes and perforins were known to mediate necrotic cell death (Xiuli et al., 2004, Yamashima et al., 2003, Michael et al., 2008, Young et al., 2007). Due to this necrosis, that was earlier known as 'non-programmed or accidental form of death' has been shifted to programmed 'necrosis' by many authors (Sergey et al., 2003). Necrotic cell death has been observed under physiological conditions like intestinal epithelium homeostasis (Barkla and Gibson 1999) and during pathological conditions like hypoxia, ischemia, hypoglycemia, exposure to toxins extreme temperature and nutrient deprivation. However necrosis

which results in inflammation and immune responses causing damage to the surrounding cells has been chosen as preferred form of death during some physiological conditions and what precise mechanisms might be involved in controlling the extent of necrotic death without causing harm to the surrounding cells is still mystery. Contrary to the progresses in deciphering the molecular and biochemical mechanisms of apoptosis, much progress hasn't been made in necrosis. This is because of the lack of suitable and reliable animal models that reproduce the crucial aspects of necrotic death.

Pyknosis

Eukaryotic chromatin has many condensation states characteristic of its various activities. These range from the decondensed chromatin of highly active genes, to moderately condensed interphase chromatin, to much more condensed mitotic chromatin, down to the intensely condensed pyknotic state found in dying and dead cells. The most distinctive aspect of death in vertebrate cells is the physical collapse of the nucleus called "hyper-condensation of chromatin". Intense nuclear condensation with intense refractivity (pyknosis) is the ubiquitous terminus of all apoptosis and some necrosis of vertebrate cells (Fig-13). This observation of strikingly condensed nuclei with clumped, condensed chromatin (DNA complexed with proteins) as a sign of cell death phenomenon is termed 'pyknosis', which is often accompanied by 'karyorrhexis' (fragmentation of the nucleus) (Naoufal and Guido 1999).

In normal mammalian cells there appear to be two types of pyknosis. The most common, the nucleolytic pyknosis of apoptosis is usually accompanied by DNA fragmentation. The anucleolytic pyknosis of necrosis is less studied but has been observed previously and reported to precede the nucleolytic type in mammalian cells as,

for example, with a cytokine-induced death (Sun et al., 1994). Though the factors that were involved in pyknotic death were under investigation, in most instances, addition of caspase inhibitors prevents pyknosis. This indicates caspases may act upstream of other effectors, or they may act directly on nuclear proteins to dismantle the nuclear envelope and facilitate the condensation and digestion of chromatin. Further, Acinus (for 'apoptotic chromatin condensation inducer in the nucleus') is one of the factors, which was thought to be indispensable for nuclear pyknosis, in some experimental settings. Cleavage of Acinus at a specific aspartate residue (Asp 1093) by caspase-3 is necessary but not sufficient to activate the DNA-condensing activity of Acinus (Sahara et al., 1999).

Processing of Inhibitor of Caspase Activated DNAse (ICAD) by caspase-3 or 7 results in the release of CAD, which translocates to nucleus. In the nucleus it interacts with histone H1 and high-mobility-group 2 proteins, and exerts its DNase and chromatin-condensation activities (Kumiko et al., 1998). One of the proteins responsible for caspase- independent chromatin condensation is Apoptosis Inducing Factor (AIF), a flavoprotein that is normally confined to the space between the outer and inner mitochondrial membranes. During various cellular insults, AIF translocates from the mitochondrion to the nucleus, and causes partial chromatin condensation in the periphery of the nucleus, which is clearly distinct from those, induced by CAD or Acinus (Susin et al., 1999). L-DNase II is another chromatin-condensation factor, which translocates from the cytoplasm to the nucleus that may be triggered by cytosolic acidification, a metabolic change that often accompanies apoptosis and necrosis (Torriglia et al., 1998). Further another protein that might contribute to chromatin condensation and inter-nucleosomal DNA fragmentation is cathepsin B. This protein could be activated on its release from

lysosomes of the apoptotic cell. Alternatively, cathepsins might act as degradative enzymes in the phagolysosome (Vancompernolle et al., 1998) (Fig-14, Table-1).

Biochemistry of cerebral ischemia

Cerebral ischemia is the second leading cause of death and disability worldwide. Involvement of large numbers of protease families, their cross talk and heterogeneity in cell death renders pharmaceutical interventions ineffective for the pathology of cerebral ischemia (Yamashima et al., 2000, Chaitanya et al., 2008, Charriaut et al., 1996). Ischemic stroke occurs usually by mechanical occlusion of cerebral blood vessels either by thrombus (clot that develops in an artery supplying blood to the brain) or embolus (clot that forms in one area of the body and travels through the bloodstream to another place where it may lodge). As brain consumes relatively large amount of oxygen and glucose and depends exclusively on oxidative phosphorylation for energy production, any problem that results in deficient supply of oxygen and glucose results in severe damage to the organism. During moderate to severe cerebral ischemia at cerebral blood levels around 20mL/100g/min oxygen extraction becomes maximal and the cerebral metabolic rate for oxygen begins to fall (Wise et al., 1983). This results in normal neuronal function being affected and cortical electroencephalographic activity flow is restricted. At levels below 10mL/100g/min cell membranes and neuronal functions are severely affected (Hakim 1987). At this threshold lack of oxygen inhibits aerobic respiration and activates anaerobic respiration resulting in a rise of lactate accumulation leading to pH decrease and intra and extra cellular acidosis. Further with energy depletion membrane potential is lost and neurons and glia depolarize (Philip et al., 2003). Due to this energy dependent process like glutamate reuptake is impaired resulting in the accumulation of glutamate at

Fig-13: Morphological features of pyknotic cell death. Intense cellular and nuclear condensation with high refractivity is usually termed as pyknotic cell death. Arrows point towards pyknotic cells.

Fig-14: Biochemistry of pyknotic cell death. Several proteins were implicated in pyknotic cell death. Some of the proteases were also known to mediate apoptosis, necrosis and other non-apoptotic forms of cell death like caspases, cathepsins, DNAses and AIF respectively. The role of these proteins in mediating pyknotic cell death individually or by activating other target proteins were depicted in the present picture.
Zamzami N, Kroemer G, Condensed matter in cell death. Nature. 1999;401:127-128

Table-1: Various proteases that were involved in pyknotic cell death were shown in the table.

Fig-13

Morphological features of pyknosis
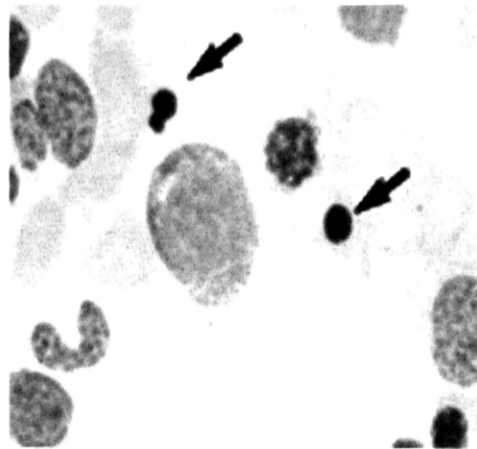
Fig-14

Biochemistry of pyknotic cell death
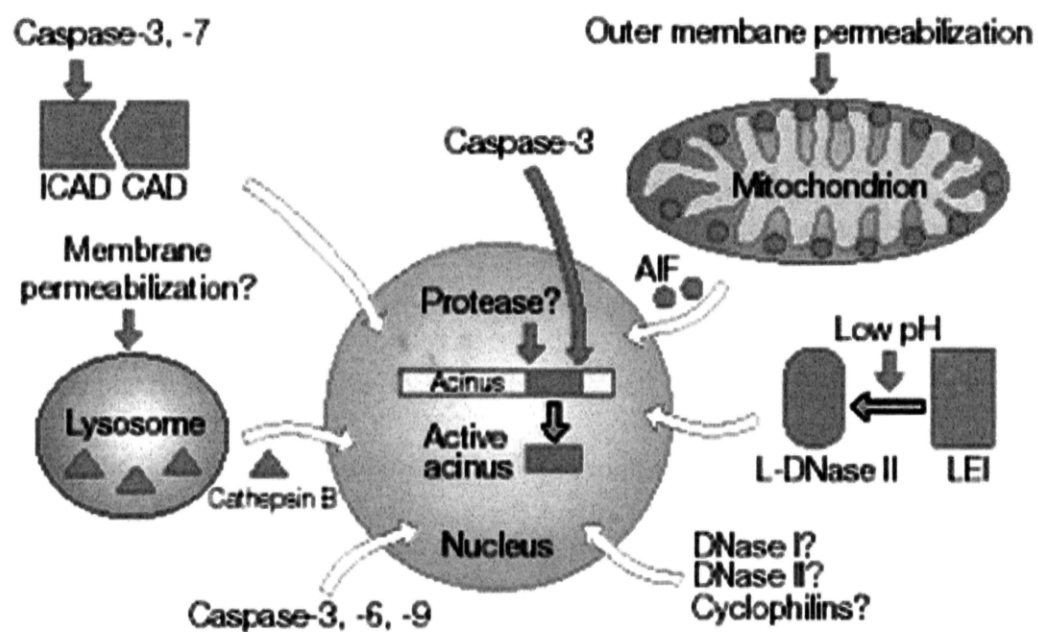
Table-1

	Acinus	CAD	AIF	L-DNase II	Cath B	DNase I	DNase II	Cyclophilin	Caspases
Type of chromatin condensation	Karyo-rrhexis	Karyo-rrhexis	Peri-pheral	Pyk-nosis	Peri-pheral	Pyk-nosis	Pyk-nosis	?	None
Type of DNA fragmentation	None	Oligos	≥50 kb	Oligos	Oligos	Oligos	≥50 kb	None	
Proteolysis	?	None	None	None	?	None	None	None	

pre-synaptic clefts resulting in increased influx of calcium into the cell by NMDA, AMPA and kainite receptors. The consequence of unregulated rise in intracellular calcium linked with glutamate excitotoxicity results in several biochemical processes like calpain activation, apoptotic and necrotic cell deaths which are detrimental to ischemic brain tissue (Fig-15).

Ischemic cell death is often considered to be chaotic due to involvement of many proteases belonging to various families and their cross talks. Ischemic brain injury after ischemia-reperfusion is modulated by at least two morphologically distinct cell death pathways, namely necrosis and apoptosis. The induction of apoptosis and necrosis is tightly regulated process by several biochemical intermediates including alterations in high-energy phosphates, intracellular calcium accumulation and reactive oxygen species etc., (Mc Conkey 1998, Haunstetter and Izumo 1998, Syntichaki and Tavernarakis 2003).

Apoptosis is an evolutionarily conserved mode of cell death characterized by a discrete set of biochemical and morphological events through the members of caspase family. Necrosis has been defined as a type of cell death that lacks the features of apoptosis and autophagy. It is considered to be uncontrolled, initiated by non-cellular mechanisms such as ischemia, trauma and thrombosis. These events ultimately lead to irreversible cell death with depletion of high energy stores and disruption of the cellular membrane involving fluid and electrolyte imbalance, cell swelling, loss of potassium and magnesium ions, accumulation of intracellular water, sodium chloride, hydrogen and calcium (Syntichaki and Tavernarakis 2003, Nicotera et al., 1998, Sapolsky et al., 1996). However, recent research suggests that its occurrence and course might be tightly regulated. The acidification of cytoplasm is required for necrotic cell death though the

reason for the acidification remains unclear (Sapolsky et al., 1996, Syntichaki et al., 2005). Investigations in both nematodes and mammals converge to implicate specific calpain and lysosomal proteases (cathepsins) in the execution of necrotic cell death (Xiuliet al., 2004, Marta et al., 2006).

Caspases belong to the cysteine protease family, which were specifically activated during apoptotic stimuli. Caspase-activated and caspase-mediated cell death is marked by the fragmentation of nuclear DNA and the generation of inter-nucleosomal fragments (mono- and/or oligomers of 200 bp, DNA ladders), whereas DNA degradation in necrosis is random and nonspecific). While caspase activation is specific to apoptosis, calpains and cathepsin-b activation occurs during both apoptosis and necrosis. Recent data suggest that necrosis rather than apoptosis appear to be the crucial component of the damage to the nervous system during human ischemic injuries and neurodegenerative diseases (Syntichaki and Tavernarakis 2003).

Studies in primates indicate that damage to the lysosomal membrane is inflicted enzymatically by activated calpains, which localize to lysosomal membranes after the onset of ischemic episodes, with subsequent spillage of cathepsins into the cytoplasm. This observation led to the formulation of the "Calpain–Cathepsin hypothesis" whereby the calcium-mediated activation of calpains results in the rupture of lysosomes and leakage of killer cathepsins that eventually dismantle the cell (Fig-16) (Yamashima 2003). The relative role of these proteases, which mediate necrosis and apoptosis, remains unclear in transient fore brain ischemia. Determining the relative roles of calpains, caspases and cathepsins in post ischemic neuronal death is further complicated by potential cross talk between these proteolytic systems. Calpains and caspases cleave

Fig-15
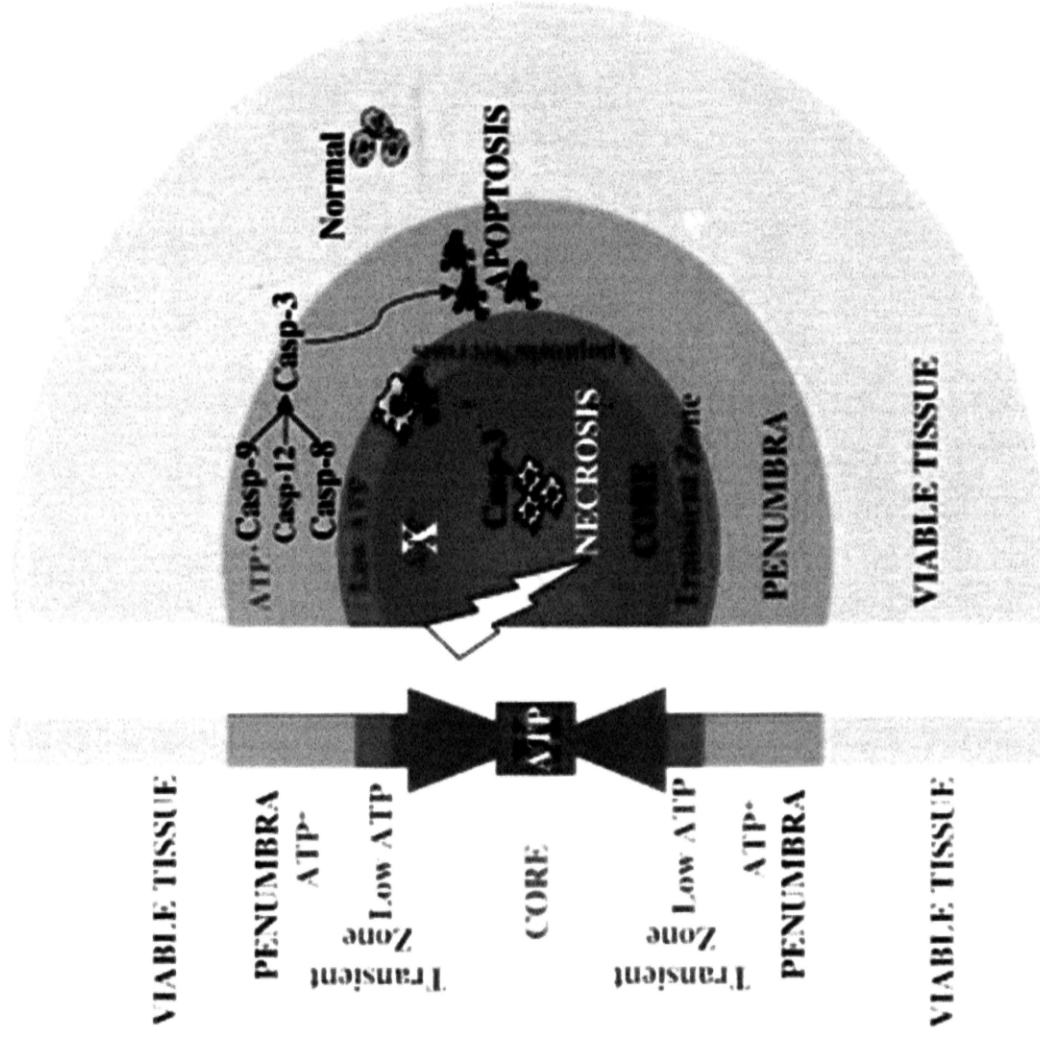
A prototype brain damage during cerebral ischemia: core, a region where cells undergo necrosis. The region surrounding the core is called ischemic penumbra, a site of delayed mode of cell death (apoptosis) due to availability of ATP. Further, a transient zone in-between the core and penumbra is likely to merge to the core if the CBF is not restored early. The penumbral region is surrounded by a region of viable tissue

Ram Raghubir et al., *Brain Research Reviews April 2007*

Fig-16: Cross talk between calpain and cathepsin proteolytic systems. Various cellular insults like ischemia results in activation of calpains via the elevation of calcium levels. Activated calpains interact with lysosomal membranes resulting in the spillage of cathepsins. These proteases can mediate either apoptotic or necrotic cell death independent of each other or synergically. Further calpains were known to activate caspases and caspases can activate calpains via the cleavage of calpastatin which is an endogenous inhibitor of calpains. Moreover cathepsins were also known to activate caspases. These interactions result in further amplification of cell death processes. However these interactions are mostly dependent on the intensity of insult and the type of death chosen by the cell.

Fig-16

Cross-talk between calpain and cathepsin proteolytic systems
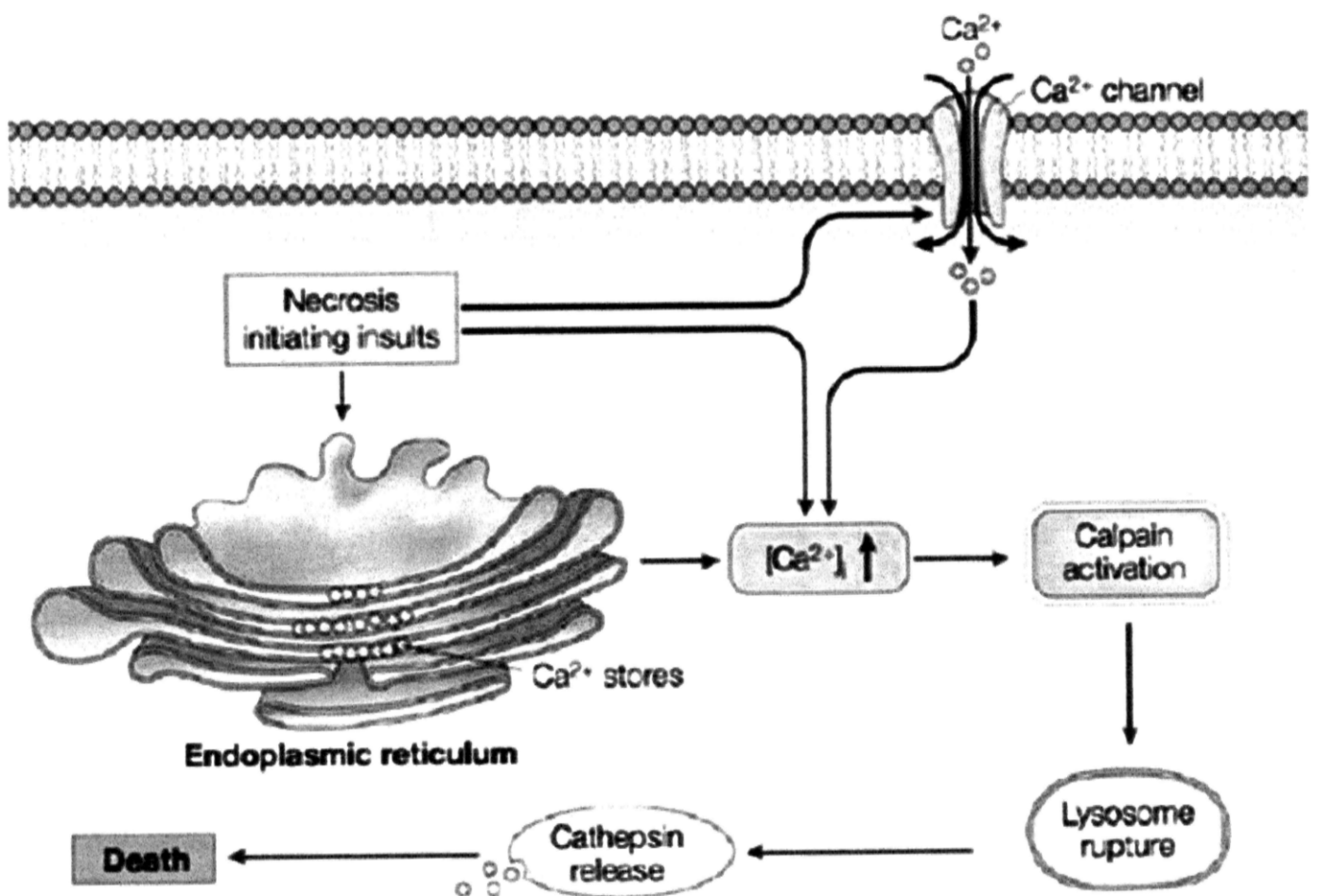
many common substrates including cytoskeletal and regulatory proteins (Wang 2000). In addition, these protease systems appear to modulate each other via calpain-mediated cleavage of caspases 3, 7, 8, 9, cathepsin (Wang 2000, Lomgren et al., 2001) and caspase-3-mediated cleavage of calpastatin (Kato 2000), which is an endogenous inhibitor of calpain, there by activating calpain. These potential interactions amplify the importance of understanding the spatio-temporal distribution of calpain, caspase and cathepsin-b in the post ischemic brain. In the present study we compared the relative activity, localization, and time course of calpain, active caspase-3 and cathepsin-b and proteolysis mediated by them on various substrates in the adult rat brain following middle cerebral artery occlusion in rat.

RESULTS

Elevation of calpain and cathepsin-b levels

The intensity of the calpain levels evident by the western blot analysis showed a significant increase from 0 hr reperfusion till the third day (Fig-17). However a maximal increase was observed during 1hr and 12hr indicating the contribution of reperfusion injury in the pathology of cerebral ischemia at these time points. Serial sections probed with calpain in order to check its localization in the brain during ischemia revealed a significant increase and localization in the striatum of the infarct in the ipsilateral hemisphere of the rat brain (Fig-18) compared with the contralateral hemisphere.

The intensity of the cathepsin-b levels was maximal at 1hr and 12-hr reperfusion time periods correlating with the elevated levels of calpains (Fig-19). However a maximal increase was observed during 1hr and 12hr indicating the contribution of reperfusion injury in the pathology of cerebral ischemia at these time points.

Immunohistochemical analysis on serial sections with cathepsin-b revealed a significant increase and localization of cathepsin-b in the striatum and cortical region of the infarct in the ipsilateral hemisphere over the contra lateral hemisphere, which correlated with the localization of calpains (Fig-20). Immunohistochemical analysis was performed on 1hr reperfused brain samples. However, during later time periods, correlating with the activation of caspases the presence or localization of calpains and cathepsins varied due to the decrease in the intensity of insult.

Elevation of cleaved caspase-3 levels

Apoptosis is a highly regulated programmed cell death mediated by activated caspases. We observed a significant increase in the cleaved active form of caspase-3 from 1 hr of reperfusion till the 3 day, 1day and 3 day time periods being the maximal intensity observed (Fig-21).

Further, in order to check the localization of active caspase-3 in the tissue section we performed immunohistochemical analysis. We observed a significant increase in the active caspase-3 immunoreactivity around the infarct maximum in the cortical region compared to striatum (Fig-22). We didn't observe any significant increase in the contralateral hemisphere. Though we observed some immunoreactivity in the striatum, it might be due to some of the cells, which might have undergone secondary necrosis failing to execute the apoptotic program.

Differential breakdown of Spectrin by caspases and calpains

α-Spectrin is cyto-skeletal protein, which is known to produce signature fragments of 145, 150 kDa and 120 kDa upon cleavage by calpain and caspase-3 respectively. Consistent with other reports we observed significant increase in the

Fig-17: Western blot and densitometric analysis of calpain levels during cerebral ischemia in rat brain. A significant increase in the calpain levels were observed in ischemic samples over the sham operated samples starting from the permanent occlusion for 3 hrs time period till the third day of reperfusion. SI (Sham ischemic), 0I (0 hr ischemic), 1HI (1hr ischemic), 12HI (12 hr ischemic), 1 DI (1 day ischemic), 3DI (3 days ischemic) reperfused ischemic ipsilateral samples respectively after 3 hrs occlusion. P >0.05.

Fig-18: Immunohistochemical localization of calpain in the ischemic rat brain. A significant increase in the localization of calpain in the ipsilateral cortex than contralateral is visible. Images were taken under a magnification of 12.5x and 1000x to have a clear view of regional and cellular localization of calpains in the infarct. Pyknotic cells and few shrunken cells resembling apoptotic cells stained positive for calpain in striatum and cortex respectively. White arrows point the less immunoreactive cells and black arrows point the degenerating cells, which were highly immunoreactive for calpain. Photographs were taken with Nikon Alphaphot YS2 microscope.

Fig-17

Western blot analysis of calpain

94 kDa
84 kDa

30 kDa

SI   0I   1HI   12HI   1DI   3DI

Densitometric analysis of calpain

Arbitray Units

35
30
25
20
15
10
5
0

SI   0I   1HI   12HI   1DI   3DI

Ischemic brain samples

Fig-18

Immunohistochemistry of calpain

Contralateral cortex 1000x

Contralateral striatum 1000x

Ipsilateral 12.5x

Contralateral 12.5x

Ipsilateral cortex 1000x

Ipsilateral striatum 1000x
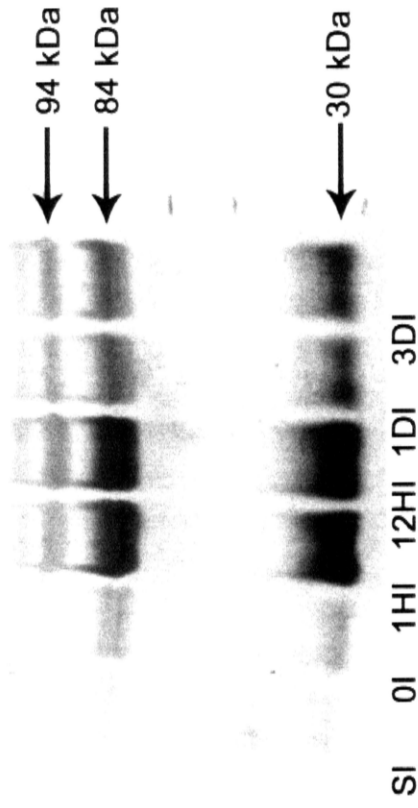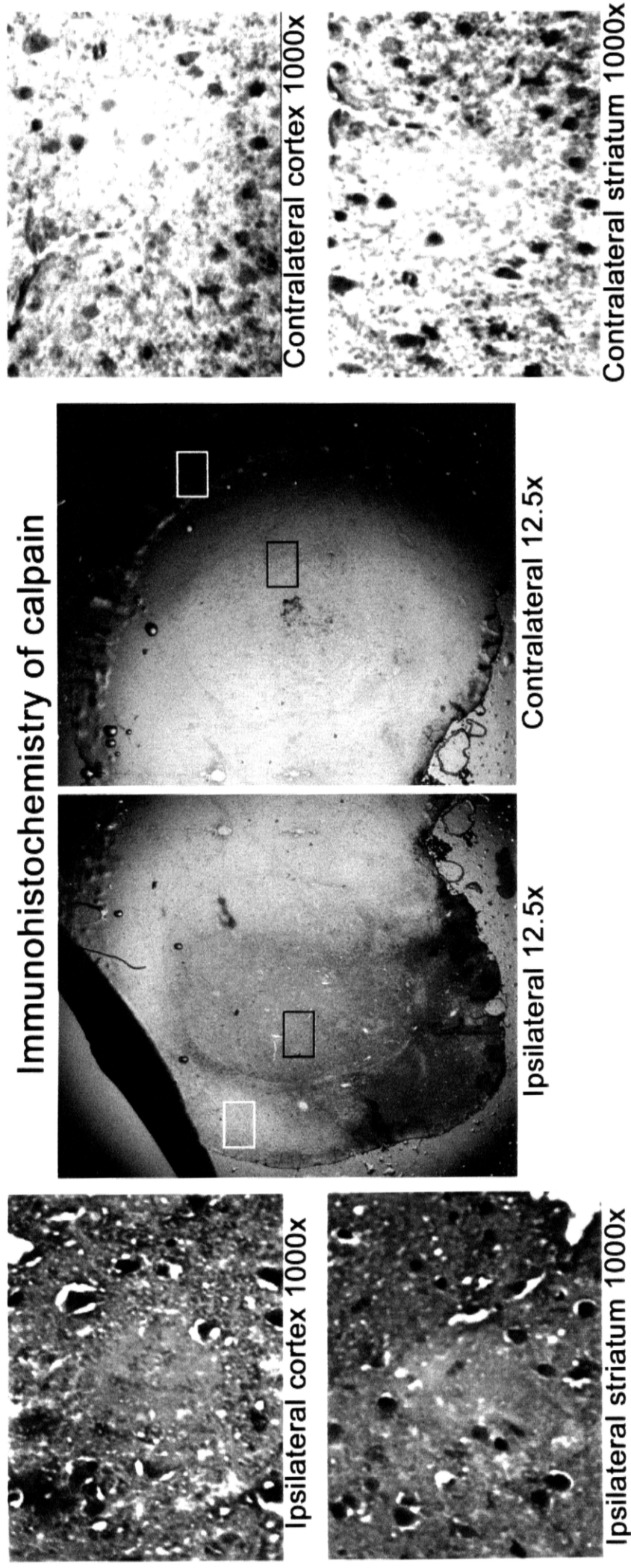
Fig-19: Western blot and densitometric analysis of cathepsin-b levels during cerebral ischemia in rat brain. A significant increase in the cathepsin-b levels was observed in ischemic samples over the sham operated, starting from 1 hour reperfused time period till the third day of reperfusion. SI (Sham ischemic), 0I (0 hr ischemic), 1HI (1hr ischemic), 12HI (12 hr ischemic), 1DI (1 day ischemic), 3DI (3 days ischemic) reperfused ischemic ipsilateral samples respectively after 3 hrs of occlusion. P >0.05

Fig-20: Immunohistochemical localization of cathepsin-b in the ischemic rat brain. A significant increase in the localization of cathepsin-b in the ipsilateral cortex than contralateral is visible. Black arrows point the degenerating cells, which were highly immunoreactive for cathepsin-b. Images were taken under a magnification of 12.5x and 1000x to have a clear view of regional and cellular localization of calpains in the infarct. Bright field Images were taken with Olympus UCTR30-2 fluorescent microscope.

Fig-19

Western blot analysis of cathepsin-b

32 kDa
Cathepsin-b

SI   OI   1HI   12HI   1DI   3DI

Densitometric analysis of cathepsin-b

Arbitrary Units

SI   OI   1HI   12HI   1DI   3DI
Ischemic brain samples

Fig-20

Immunohistochemistry of cathepsin-b

Contralateral cortex 1000x

Contralateal striatum 1000x

Ipsilateral 12.5x

Contralateral 12.5x

Ipsilateral cortex 1000x
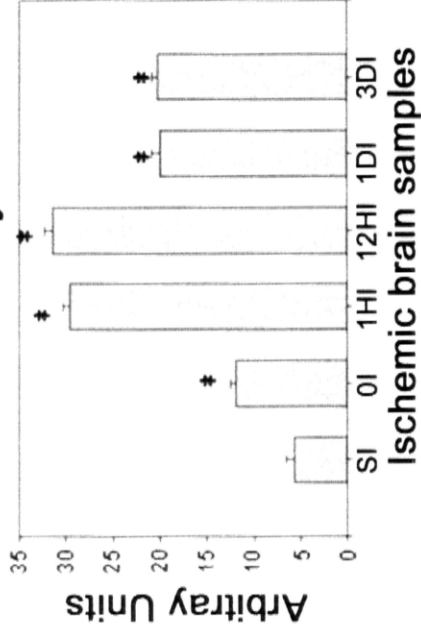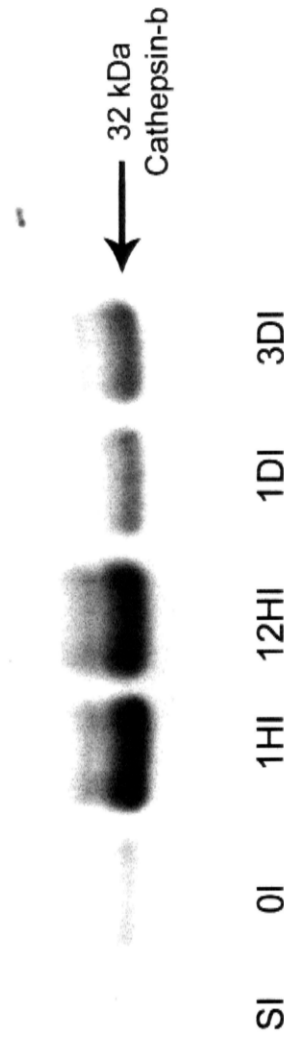
Ipsilateral striatum 1000x

Fig-21: Western blot and densitometric analysis of cleaved caspase-3 levels during cerebral ischemia in rat brain. A significant increase in the cleaved caspase levels were observed in ischemic samples over the sham operated, starting from 1 hour reperfused time period till the third day of reperfusion. However there was a significant increase in the levels of active caspase-3 starting from 1-day reperfusion time period till 3 day indicating the contribution of apoptotic cell death from these time periods. SI (Sham ischemic), 0I (0 hr ischemic), 1HI (1 hr ischemic), 12HI (12 hr ischemic), 1DI (1 day ischemic), 3DI (3 days ischemic) reperfused ischemic ipsilateral samples respectively after 3 hrs of occlusion. p>or = 0.05

Fig-22: Immunohistochemical localization of cleaved caspase-3 in the ischemic rat brain. A significant increase in the localization of active caspase-3 in the ipsilateral cortex than contralateral is visible. However increase in the immunoreactivity is mostly confined to apoptotic cells in the cortex than the pyknotic cells in the striatum. White arrows point the less immunoreactive cells and black arrows point the degenerating cells, which were highly immunoreactive for cleaved caspse-3. Images were taken under a magnification of 12.5x and 1000x to have a clear view of regional and cellular localization of active caspase-3 in the infarct. Bright field Images were taken with Olympus UCTR30-2 fluorescent microscope.

Fig-21

Western blot analysis of caspase-3

Pro-caspase 3

Active caspase-3

SI | 0I | 1HI | 12HI | 1DI | 3DI

Densitometric analysis of active caspase-3

Arbitrary Units

SI | 0I | 1HI | 12HI | 1DI | 3DI
Ischemic brain samples
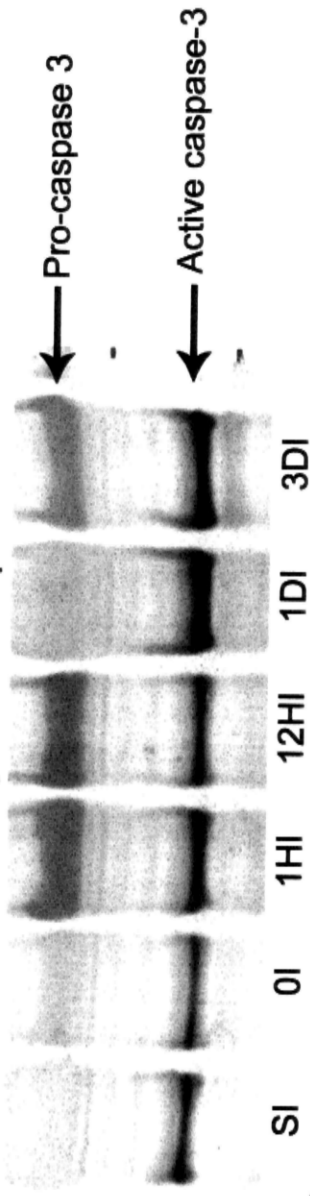
Fig-22

Immunohistochemistry of active caspase-3

Contralateral cortex 1000x

Contralateral striatum 1000x

Contralateral 12.5x

Ipsilateral 12.5x

Ipsilateral cortex 1000x

Ipsilateral striatum 1000x
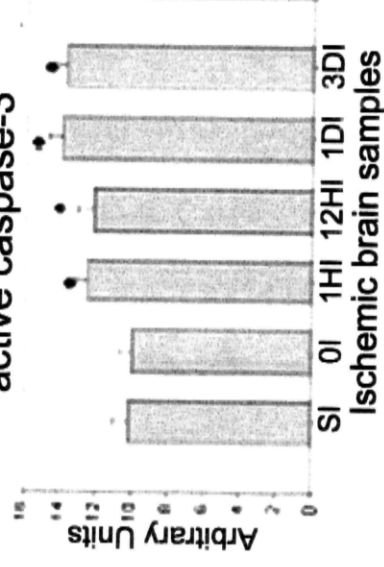
breakdown products of α-spectrin to 150, 145 kDa signature fragments produced by calpains and 120 kDa signature fragment produced by caspase-3 during cerebral ischemia (Fig-23). The intensity of the SBDP (Spectrin Break Down Products) significantly increased during the reperfusion period, indicating the involvement of both proteases in the ischemic injury and also the impact of reperfusion injury during cerebral ischemia.

Cleavage of PSD-95 by calpains

PSD-95 belongs to MAGUK (Membrane Associated Guanylate Kinase) family. Alterations in the calcium concentration, plays an important role in the activation of calpains thereby acting upon many of its substrates of which PSD-95 is one. We observed two truncated products migrating at 50 and 36 kDa respectively generated from PSD-95 (Fig-24) during cerebral ischemia. The intensity of cleaved products was almost in a similar manner with that of the elevated levels of calpain. We observed a significant increase in the intensity of the cleaved PSD-95 starting from 0 hr till the 3rd day, of which 1 hr and 12 hr reperfusion samples being the maximum intensity over the sham operated ischemic brain region.

DISCUSSION

Cerebral ischemia results in an infarct comprising of central necrotic core and a physiologically ill penumbra, which gradually merges into the core. Calpains and cathepsin-b are known to mediate necrotic cell death and apoptotic cell death independent or dependent of caspases (Lankiewicz et al., 2000, Xiuli et al., 2004, Stefan and Yigong 2004). Even though substantial amount of literature is available on the involvement of various proteases and cell death mechanisms during cerebral ischemia their time periods of activation, regional localization and their cross talks are sparse. Therefore in the

present study, we investigated the role of these protease systems during middle cerebral artery occlusion.

Focal cerebral ischemia model has been standardized for 3 hr occlusion in rat model and studied reperfusion induced cell death at different time periods and localization of the proteases in and around the infarct as well as the status of some of their substrates like PSD 95 and α-Spectrin during the reperfusion period of cerebral ischemia. We observed a significant increase in the levels of calpains, cathepsin-b and cleaved caspase-3 respectively. Disturbances in the cellular calcium levels results in a fast and transient over activation of calpains. The time course of their activation mainly depends on the intensity of the insult. We observed a significant increase in calpain levels starting from 0 hr reperfusion period, which peaked by 1 hr. Over activation of calpains might be the key and first step in the cell death during cerebral ischemia. Cathepsin-b levels were also significantly increased by 1 hr reperfusion period. Over production of free radicals might damage the lysosomal membrane there by contributing to the spillage of cathepsins during the reperfusion phase of cerebral ischemia. Moreover, interaction of calpains with the lysosomal membranes also exacerbates this process (Marta et al., 2006). The elevation and activation of calpains and cathepsin-b provides clear information about their crucial role in mediating necrosis during the initial hours of the insult. However, the extent they mediate the necrotic cell death independently, during cerebral ischemia needs to be elucidated.

Cell death in penumbra is known to be apoptotic, mediated by caspases (Charriaut et al., 1996). Though we observed an increase in the levels of active caspase-3 from 1hr reperfusion period, its intensity was at peak only from 1 day after reperfusion indicating

Fig-23: Western blot and densitometric analysis of spectrin cleavage pattern during cerebral ischemia in rat brain. A Differential cleavage pattern of spectrin is observed in the form of 150,145 and 120 kDa produced by calpains and active caspase-3 respectively. Significant increase in the 150,145 kDa fragment levels were observed in ischemic samples over the sham operated, starting from 0 hr reperfused time period till the third day of reperfusion. However 120kDa fragment showed an increase starting from 1 hr reperfusion time period. SI (Sham ischemic), 0I (0 hr ischemic), 1HI (1hr ischemic), 12HI (12 hr ischemic), 1DI (1 day ischemic), 3DI (3 days ischemic) reperfused ischemic ipsilateral samples respectively after 3 hrs of occlusion.

Fig-24: Western blot and densitometric analysis of PSD-95 levels during cerebral ischemia in rat brain. A significant increase in the cleavage of PSD-95 was observed in ischemic samples over the sham operated, starting from permanent occlusion for 3 hrs time period till the 3rd day of reperfusion. We observed the cleavage products 50 kDa and 36 kDa produced by the action of calpains. SI (Sham ischemic), 0I (0 hr ischemic), 1HI (1hr ischemic), 12HI (12 hr ischemic), 1DI (1 day ischemic), 3DI (3 days ischemic) reperfused ischemic ipsilateral samples respectively after 3 hrs of occlusion. Western blot analysis of β-actin levels during cerebral ischemia in rat brain on SI (Sham ischemic), 0I (0 hr ischemic), 1HI (1hr ischemic), 12HI (12 hr ischemic), 1DI (1 day ischemic), 3DI (3 days ischemic) reperfused ischemic ipsilateral samples respectively after 3 hrs of occlusion showed equal loading of protein into the gels.

Fig-23

Western blot analysis of alfa- spectrin

150 kDa
145 kDa
120 kDa

SI   0I   1HI   12HI   1DI   3DI
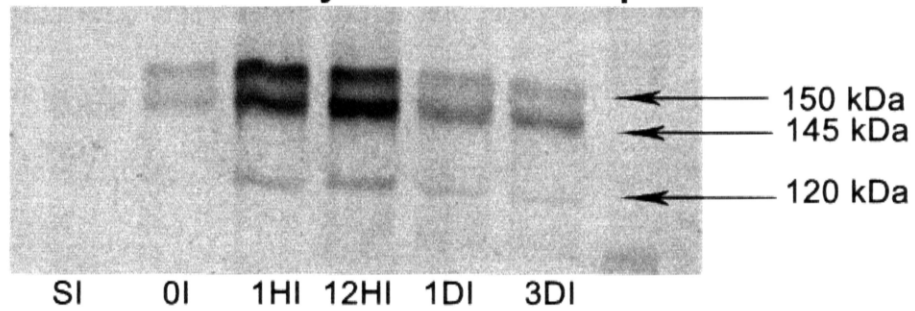
Densitometric analysis of alfa-spectrin
120, 145 kDa fragments
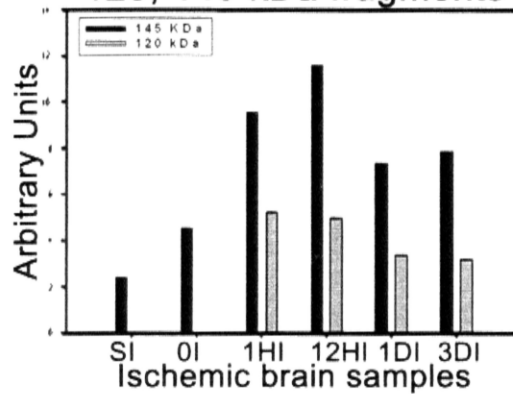
Fig-24

Western blot analysis of PSD-95
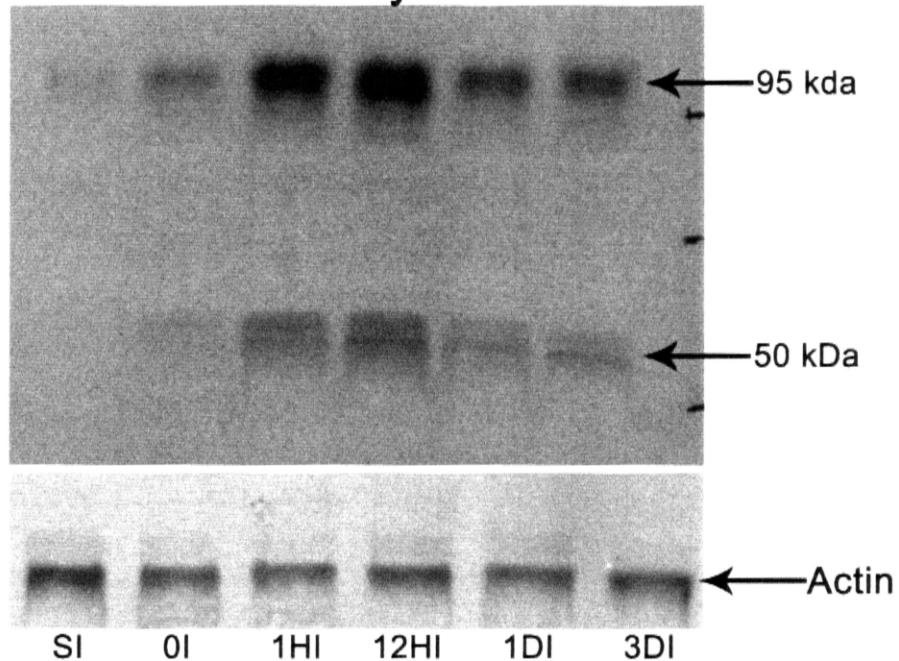
95 kda

50 kDa

Actin

SI   0I   1HI   12HI   1DI   3DI

Densitometric analysis of PSD-95
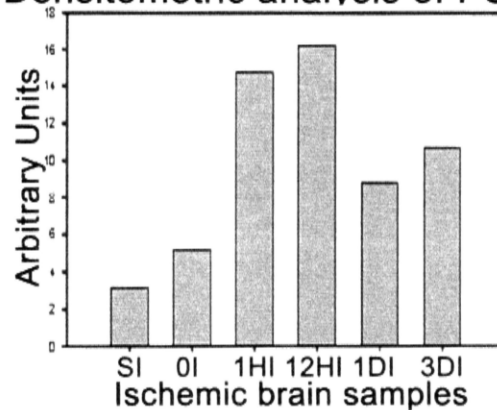
that apoptosis might be a late event in the pathology of cerebral ischemia (Cheng et al., 1996). We observed a clear presence of calpains and cathepsins in the infarct presumably in the necrotic core during the initial hourrs. However, caspase activation was mainly confined to the periphery presumably penumbra, though a small increase in its intensity in core is observed. Caspases are not implicated in necrotic cell death and are strict regulators of apoptosis. The presence of caspase activity amidst necrotic cells might be due to the execution of both apoptotic and necrotic cell death mechanisms in the same cell. Further apoptosis of immune cells infiltrating the infarct also might contribute to the caspase positivity in the necrotic core of the infarct (Unal and Dalkara 2003, Unal et al., 2004). Further the cell death morphology observed by staining the sections with cresyl violet showed necrotizing and pyknotic cells in striatum and apoptotic cells in the cortical region (Fig-25), correlating with the increase immunoreactivity of calpains and cathepsins in striatum and active caspase-3 in cortex respectively. Moreover calpain and cathepsin-b immunostaining correlated with the white colored region of the TTC stained ischemic rat brain and active caspase-3 immunostaining correlated with the red colored region (Fig-26).

Activation of these proteases brings about the breakdown of wide range of substrates like PARP, which is a substrate of caspases, calpains, cathepsins and granzymes, spectrin a substrate for calpains and caspases and PSD-95 a substrate for calpain alone. PARP generates an array of signature fragments of 89 and 21 kDa, 72, 64 kDa and 50 kDa when acted upon by caspases, granzymes and cathepsins respectively (Wang 2000, Gobeil et al., 2001). We observed a significant increase in the break down products of spectrin to 150, 145 kDa belonging to calpain and 120 kDa belonging to

caspases respectively. However, the intensity of calpain-derived fragments over the caspase-derived fragment was significantly high implicating a prominent role of calpains during cerebral ischemia. It has been observed that PSD-95 is cleaved by calpains to 50 kDa and 30 kDa during developing and adult rat brain (Xiao et al., 2000). We observed a significant increase in the 50 kDa and 30 kDa-truncated products generated by calpain during middle cerebral artery occluded rat model. While 150,145 kDa spectrin fragments were increased from 0 hr reperfusion period correlating with the increase of calpains, 120 kDa fragment was observed only after the reperfusion has started even the intensity is low indicating that the calpains might be the first proteases to be activated in the molecular events leading to cellular demise in cerebral ischemia.

Cell death in cerebral ischemia is extremely complex and is disordered, due to the involvement of large number of proteases (Yamashima 2000, Robert et al., 2003). The nature of these proteases in mediating cell death individually and in synergic manner with proteases of other families makes the understanding of the molecular and biochemical events extremely difficult. The time dependent elevation and activation of these proteases makes pharmaceutical intervention in cerebral ischemia extremely difficult. A combination of drugs aimed at suitable time periods depending on activation time periods of these proteases might be of potential use. However, studies in this direction to elucidate the molecular events during focal cerebral ischemia are necessary.

Fig-25: Cresyl violet stained rat brain sections. Cresyl violet stains the nissil granules of the neurons and renders purple colour to neurons a) necrotizing neurons in the striatum of ipsilateral hemisphere. b) Pyknotic cells in the striatum of ipsilateral hemisphere. c) Apoptotic neurons in the cortex of the ipsilateral hemisphere. d, e, f) Normal neurons in the striatum and cortex of contralateral hemisphere. Bright field Images were taken with Olympus UCTR30-2 fluorescent microscope.

Fig-25

Cresyl violet staining of ischemic brain sections
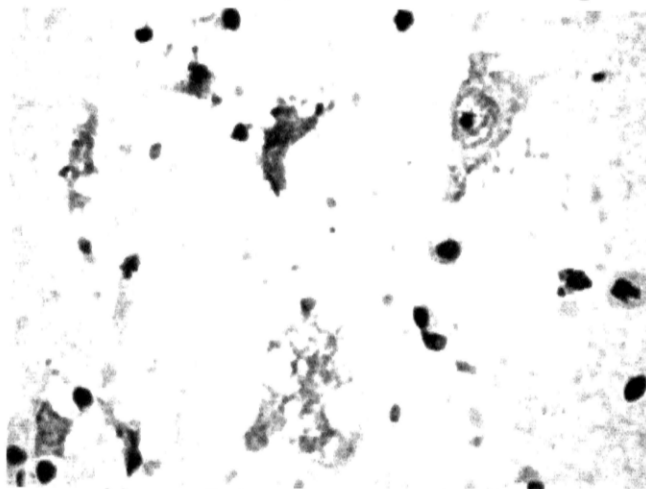
Necrotizing neurons in the
ispilateral striatum 1000x
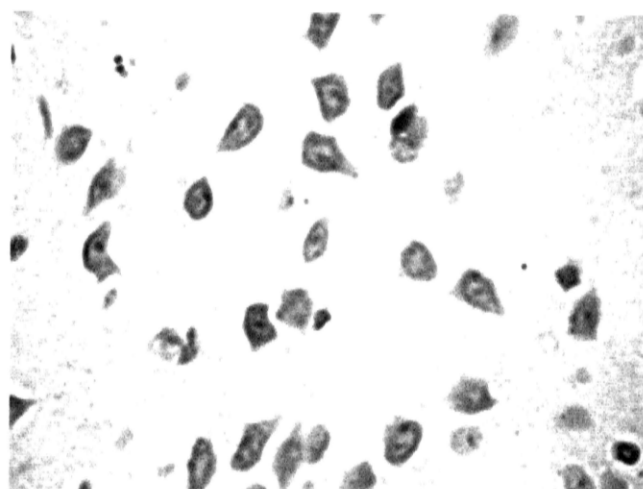
Neurons in the contralateral striatum
1000x

Pyknotic neurons in ipsilateral striatum
1000x
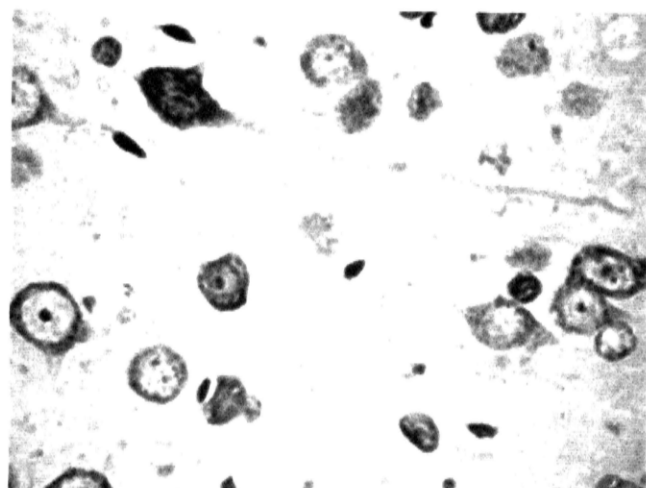
Neurons in the contralateral striatum
1000x
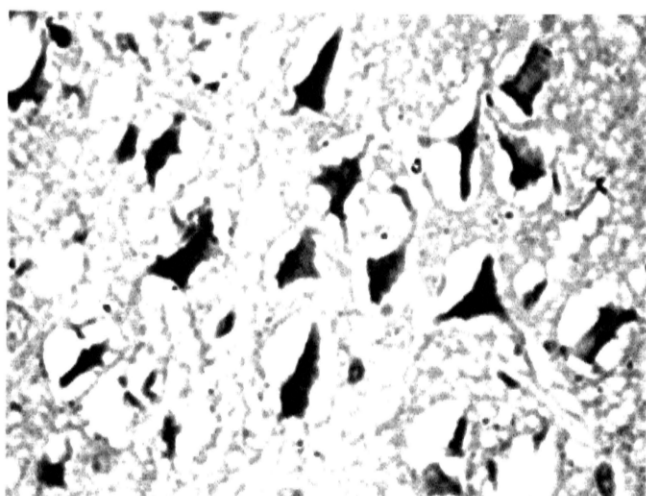
Apoptotic neurons in the
ipsilateral cortex 1000x
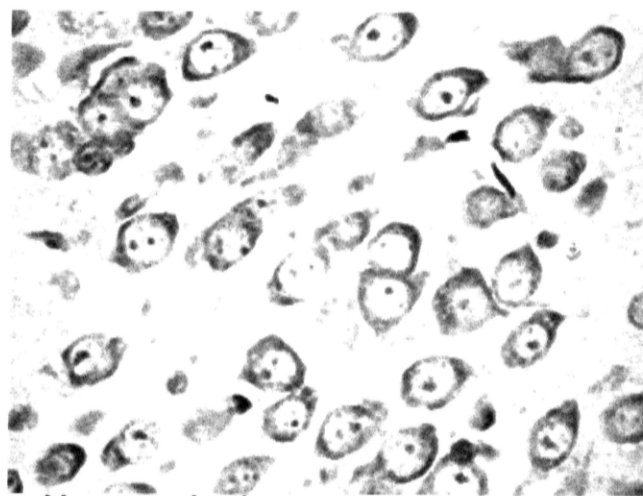
Neurons in the contralateral cortex
1000x

Fig-26: Comparision of cresyl violet, Tetrazolium Tri Chloride (TTC) staining and Immunohistochemistry of calpain, cathepsin and active caspase-3 on ischemic brain slices and sections. TTC staining on rat brain sections was performed by cutting ischemic rat brain 2mm thick slices and incubated in TTC solution for15-20 min at 37^0c. Ischemic regions appeared white in color and non-ischemic region red in color. Immunohistochemical analysis was performed on other ischemic rat brain sections correlating with the encircled TTC stained ischemic brain slices. Necrotic cells and pyknotic cells were present mostly in the striatum where we observed significant increase in calpain and cathepsin-b immunoreactivity. Localization of calpains, cathepsin-b, necrotic and pyknotic cells were confined to white colored region in TTC staining. Apoptotic cells were present mostly in cortex where we observed significant increase in active caspase-3 immunoreactivity and was confined to red colored region in TTC staining.

Fig-26
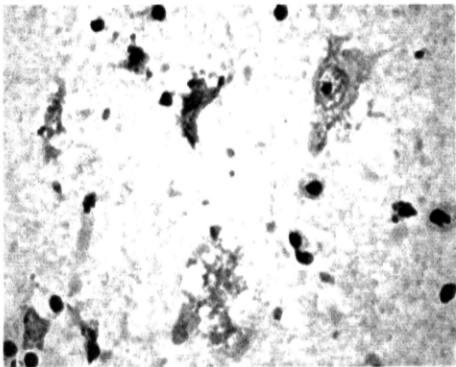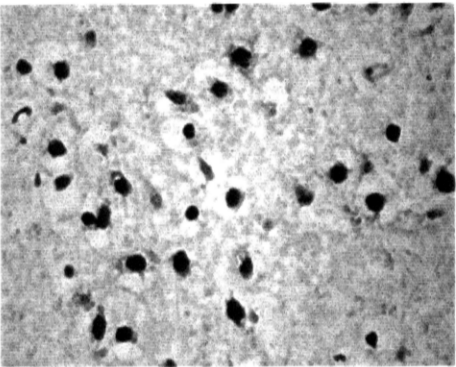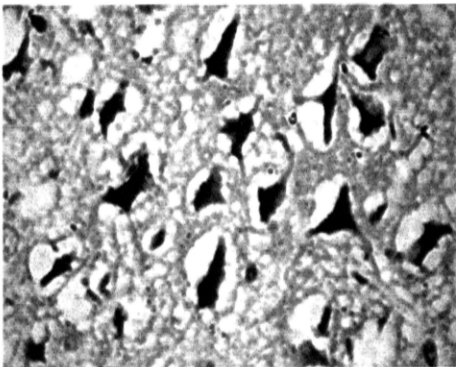
Cresyl violet staining	TTC staining	Immunohistochemistry

Necrotic neurons in
ipsilateral striatum 1000x

Pyknotic neurons in
ipsilateral striatum 1000x

Apoptotic neurons in
ipsilateral cortex 1000x
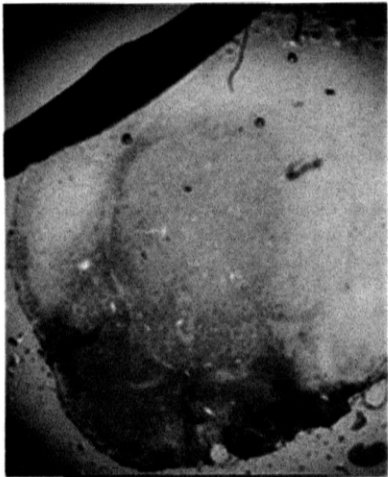
Calpain
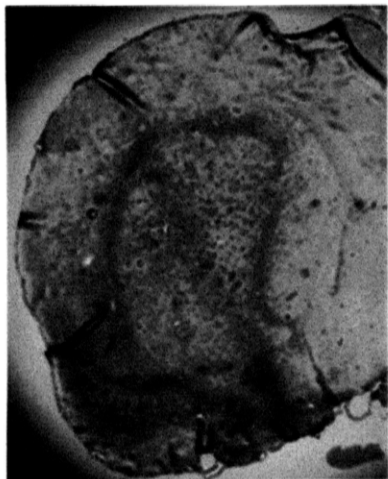
Cathepsin-b
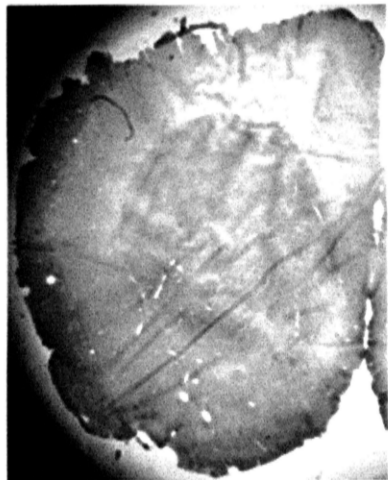
Cleaved Caspase-3

Role of NF-kB, chemokines and blood brain barrier in facilitating the infiltration of immune cells during focal cerebral ischemia.

INTRODUCTION

The paradox of life is that it cannot continue without death. The most preferred and favorite fate of dying cells is phagocytosis by professional phagocytes or neighboring cells as it prevents the release of cytotoxic substances by the cell corpse, which can damage the neighboring cells. Phagocytosis of apoptotic cells with their content being isolated helps in attenuating any inflammatory or immune responses during cell death. This is one of the main discriminating features of apoptotic and necrotic cell deaths, which plays a main role during various pathological conditions (Majno and Joris 1995). Necrotizing cells elicit a robust inflammatory and immunogenic stimulus due to release of intracellular contents and later cell remnants, which are a source of endogenous adjuvants, intracellular antigens, chemoattractants, activators of neutrophils, dendritic cells and PCD initiating factors (Shacter et al., 2000). Though previously this deleterious necrotic cell death was believed to be accidental and non-programmed, recent reports have shed more light indicating that necrosis similar to apoptosis is controlled and genetically programmed (Sergey et al., 2003). Further similar to apoptosis, necrotic cell death is accompanied by the appearance of specific markers, chemokines and phagocytosis promoters that modulates phagocytosis and immunogenic reactions (Vercammen et al., 1998).

Cerebral ischemia is known to result in robust inflammatory and immune responses. Immune response during cerebral ischemia is accompanied by the infiltration of immune cells like neutrophils, monocytes, and T cells (Schroeter et al., 1994). This is due to the involvement of necrotic cell death, elevation of chemokines and disruption of blood-brain-barrier. CNS is usually thought to be impermeable to immune cells because

of the presence of blood brain barrier, lack of conventional lymphatics, lack of MHC expression. However breakdown of blood brain barrier during cerebral ischemia, which has been shown in previous experiments, was known to facilitate the entry of immune cells into the ischemic infarct (Fig-27) (Neumann et al., 2002). Apart from the break down of blood brain barrier, elevated levels of chemokines and cytokines which functions as the major signaling molecules in directing the immune cells into the damaged region is of crucial importance. Further glial cells which are known to be the immune cells of the brain were known to regulate the path of immune cells preferably leukocytes into the injured area in a mice model of axonal injury caused by entorhinodentate lesions (Aloisi et al., 2000, Babcock et al., 2003). The role of glial cells in modulating immune responses gains more importance when their role in functioning as dendritic cells in presenting antigens to the immune cells is considered. However the controversy 'whether the dendritic cells seen in the brain of ischemic regions are resident glial cells which have attained dendritic morphology or they are migrated bone marrow cells which function as dendritic cells' exists (McMohan et al., 2006).

Rel/NF-κB family is comprised of c-Rel, Rel-A, Rel-B, p105/NF-κB1 and p100/NF-κB2. It is one of the most important transcription factors, which plays a prominent role in regulating inflammatory and immune responses, development, cellular growth and repair process, oncogenesis and cell death. Its role in diverse functions, which are often contradictory, makes it very difficult to ascertain a specific functional role during neurodegenerative disorders like cerebral ischemia (Youssef and Steinman 2006). NF-κB either promotes harmful inflammation or guides the regeneration required to repair the inflamed tissue (Sha 1998). Molecules like TNF, which can activate NF-κB

Fig-27: Extravasation of evans blue dye. Extravasation of evans blue dye into the brains is one of the marked features of blood brain barrier damage. 200μl of 2mg/ml of evans blue in PBS was injected into the ischemic rat tail vein 1 hr before sacrifice. The dye was allowed to circulate in the blood for 1 hr. Later the rat was sacrificed in excess of diethyl ether and perfused with ice cold PBS. The brain of the ischemic rat was taken out and 3mm thick slices were cut and photographed. Blue arrow points toward the extravasated dye in the ipsilateral hemisphere of ischemic brain.

Fig-27

Extravasation of evans blue dye

Ischemic region →

Contralateral region ←
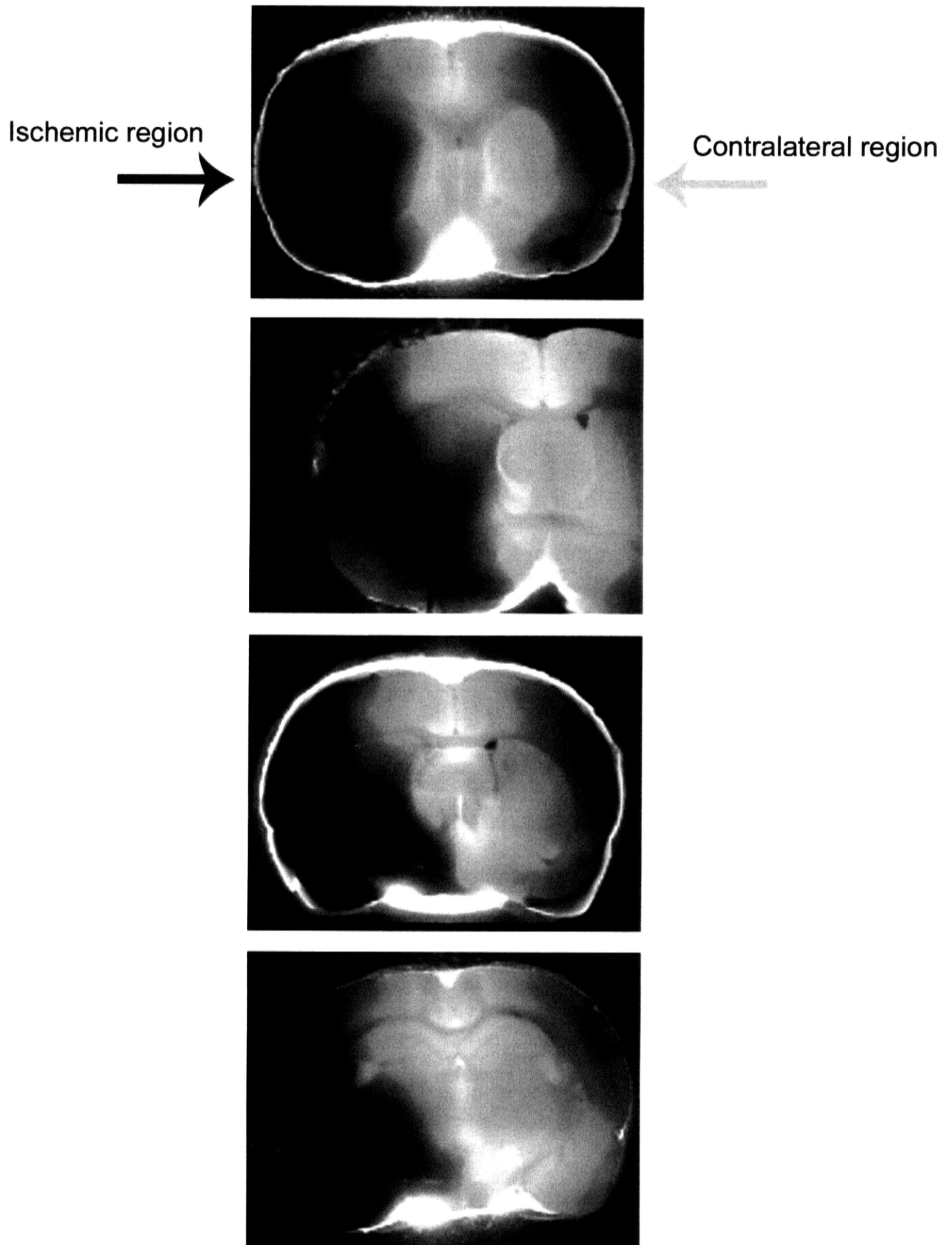
also, have a similar role i.e. it can promote harmful inflammation or regeneration. The best example that one can cite in this respect is that the NF-κB knockouts were shown to be protective as well as detrimental in the pathology of cerebral ischemia (Zhang et al., 2005, Duckworth et al., 2006, Nijboer et al., 2008). NF-κB resides in the cytosol in an inactive form bound to Iκ-B an inhibitor of NF-κB. NF-κB is activated by either NF-κB1 canonical pathway or NF-κB2 alternate pathway (Beinke and Ley 2004).

Canonically, phosphorylation of IκBα is critical for activation of NF-κB. A cascade of kinases, including a complex consisting of IKK1 (IKKα), IKK2 (IKKβ) and NEMO (IKKγ), orchestrates this canonical pathway (Ghosh and Karin 2002). This pathway is activated under various stimuli like microbial lipopolysaccharide and cytokines such as tumor necrosis factor and interleukin1. Alternate pathway of NF-κB activation depends on the stimuli such as lymphotoxin-β, CD-40 ligand and B-cell stimulating factor (Ishimaru et al., 2006). This alternate pathway is usually involved in the development of secondary organs, B cell maturation and adaptive immune responses. In the alternate pathway NF-κB1 inducing kinase plays a major role. NF-κB kinase activates IKK1-IKK1 complex resulting partial degradation of NF-κB2 (p-100-RelB) and activation of NF-κB2 (p-52-RelB) (Ghosh and Karin 2002). Activated NF-κB translocates into the nucleus and form homo or hetero dimers which form complex with DNA and helps in the transcription of the down stream targets (Fig-28). NF-κB controls the transcription of multiple genes involved in many aspects of the inflammatory and immunological responses (Soren and Steven 2004). Some of the pro-inflammatory cytokines and chemokines are TNF-α, IL-6 and IL-1; colony-stimulating factors; chemokines as IL-8, monocyte chemoattractant peptide-1 (MCP-1), IP-10/CXCL10 and

RANTES; adhesion molecules such as vascular cell adhesion molecule-1 (VCAM-1), intracellular cell adhesion molecule-1 (ICAM-1); MHC class I and II; acute-phase proteins such as serum amyloid A and enzymes such as the iNOS and cyclooxygenase and the anti-oxidant defense enzyme Mn-superoxide dismutase (SOD) (May and Ghosh 1998, O'Neill and Kaltschmidt 1997). Some of the down stream targets of NF-κB, which play a major role in immune responses, are listed in (Table-2).

Chemokines (chemotactic cytokines) are very important mediators in immune cell trafficking during diseased and health conditions (Bajetto et al., 2002). Of the various cytokines and chemokines, which regulate the inflammation and immune responses cyclooxygenase-2 (Cox-2), interleukin-2 (IL-2), interferon-γ inducible protein-10 (IP-10/CXCL10) and tumor necrosis factor-α (TNF-α) are some, which play a major role. The IL-2/IL-2R (Il-2 receptor) interaction plays a prominent role in activation and proliferation of NK cells and CTLs. It stimulates the differentiation and survival of antigen-selected cytotoxic T cells by activating the expression of specific genes and stimulates increased production of granule contents (Beadling and Smith 2002). Further modulation of NK cell mediated apoptotic and necrotic death has been shown to be modulated by IL-2 (Blom et al., 1998, Gardiner and Reen 1998).

Interferon-γ inducible protein-10 (IP-10/CXCL10) is a 10 kDa CXC-chemokine that acts on its receptor; CXCR3, to attract activated T cells, NK cells and blood monocytes, and appears to be an important participant in a variety of inflammatory conditions (Dai et al., 1997). It was first identified as the product of an early response gene to IFN-γ and is known to be produced by a variety of cells like T cells, macrophages, endothelial cells and astrocytes. It has been shown that T cell responses

Fig-28: Activation of NF-κB during various cellular insults. Vaious cellular insults like ischemia, toxin exposure, growth factors, lipopolysaccharides were known to activate NF-κB. Inactive NF-κB residing in the cytosol bound to IκB will be activated by IKK by cleaving IκB. Free NF-κB translocates into the nucleus and modulates the transcription of several genes that were responsible for the inflammation, immune responses, cell death and survival depending on the type of cellular insult.

Table-2: Some of the target genes which play a prominent role in immune responses were depicted in the table along with references. The highlighted in red were taken into our study.

Fig-28

Activation of NF-kB pathway during various cellular insults

Bacteria
Bacterial products
Viruses
Inflammatory cytokines

Physiological Stress
Physical Stress
Oxidative Stress
Chemicals

Mitogens
Growth Factors
Hormones

IKK

IkB
NF-kB

IkB^{PP}
NF-kB → Proteasome

NF-kB   Nucleus
Transcription

Immune Responses

Stress Responses

Cell Survival
Development
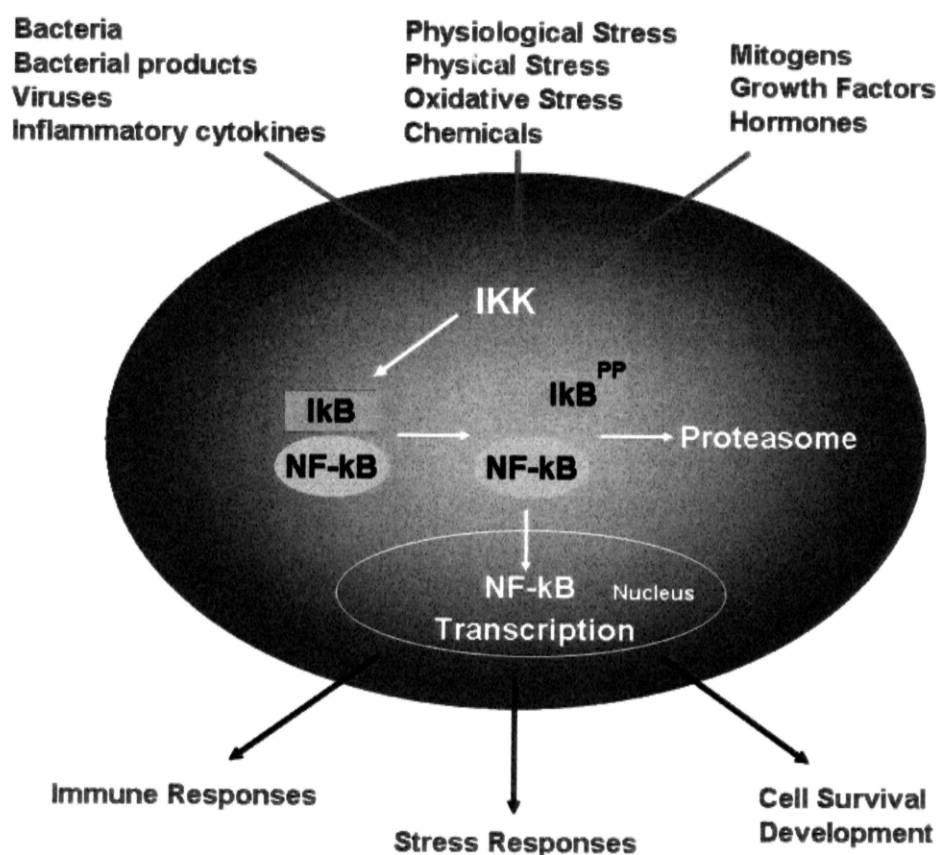
Table-2

Some of the target genes of NF-kB playing prominent role in Chemo-attraction of immune cells

Gene		Reference
IL-2	Interlukin-2	*Serfling et al.,1989; Hoyos et al., 1989; Lai et al.,1995*
IP-10	Interferon γ inducible protein 10	*Ohmori and Hamilton 1993*
TNF-α	Tumor necrosis Factor	*Shakov et al., 1990; Collart et al., 1990*
MHC class1	Mouse histocompatibility antigen	*Israel et al., 1989*
MIP-1α	Macrophage inflammatory protein	*Grove and plumbi 1993; widmer et al., 1993*
MCP-1	Macrophage chemotactic protein	*Udea et al., 1994*
COX-2	Cyclo-oxygenase-2	*Yamamoto et al., 1995*

were greatly reduced in IP-10 knock out mice indicating its crucial role in employing T-cells at the injured area during neurodegenerative disorders like spinal cord injury, ischemia (Dufour et al., 2002).

TNF-α is prominent among pro-inflammatory cytokines known to be associated with neuropathological effects underlying several neurodegenerative disorders (Fillit et al., 1991, Merrill 1992). TNF-α mediates its biological effects via its receptors, TNFRSF1A (TNFR1; p55) and TNFRSF1B (TNFR2; p75). TNF-alpha has been demonstrated to cause expression of pro-adhesive molecules on the endothelium, which results in extravasation of neutrophils, lymphocytes, monocytes and leukocyte accumulation by enhancing the adherence and migration from capillaries into the brain. It also affects immune responses by controlling T cell activation (Pimentel-Muiños et al., 1994), stimulating the cell surface expression of major histocompatibility complex (MHC) class I and class II molecules on a variety of cell types usually in synergy with IFN-γ as well as by inducing the synthesis of numerous cytokines like IL-1, IL-6, colony-stimulating factors and TNF-α, through auto-feedback pathways (Wallach 1996). Furthermore, TNF-alpha activates glial cells, thereby regulating tissue remodeling, gliosis and scar formation. In experimental autoimmune encephalomyelitis (EAE) the pro-inflammatory cytokines interferon (IFN)-gamma, tumor necrosis factor (TNF)-alpha, interleukin (IL)-1beta, IL-6, IL-12 and IL-18 are critically involved in the initiation and amplification of the local immune response in the CNS. Further IP-10 mediated phenotype maturation of langerhans cells was shown to be dependent of TNF-α (Berthier et al., 2005). Moreover TNF-α can induce both apoptosis and necrosis via intracellular signaling (Morgan et al., 2008).

COX exists in 2 isoforms, COX-1 and COX-2 encoded by distinct genes. COX-1 is expressed in almost all tissue in basal condition implicating its crucial role in synthesis of prostaglandin precursors; However COX-2 is mainly an inducible enzyme during inflammatory conditions. Cytokines like IL-1, TNF-α, platelet derived growth factor (PDGF), epidermal growth factor (EGF), fibroblast growth factor (FGF) were shown to induce COX-2 expression during various conditions (Diaz et al., 1998, Goppelt-Struebe et al., 2003). Further COX-2 expression gains more importance when increase in Th-2 responses upon COX-2 is taken into consideration. This clearly points out that elevated levels of COX-2 during inflammatory conditions dampen Th-2 responses thereby resulting in enhancement of systemic Th-1 responses (Laouini et al., 2005).

Healthy CNS is immunologically quiescent, presumably due to the presence of the blood-brain barrier, lack of conventional lymphatics, lack of intraparenchymal leukocytes, low T-cell trafficking and low MHC expression (Fabry et al., 1994). However, it is becoming clear that immune and inflammatory reactions do occur in the CNS, where they appear to originate either intrinsically or in the peripheral tissues and are then imported by competent immune cells into the CNS (acquired immunity) (Kato et al., 1996). Furthermore, brain-derived antigens that develop during various pathological conditions can induce strong immune responses that may contribute to disease. A delicate balance between inflammatory and anti-inflammatory states is maintained by the innate (nonspecific) and adaptive immune systems when the immune system becomes activated. The adaptive immune system is characterized by its ability to alter receptor expression and cellular functions upon encountering new antigens, self or foreign; functions include cell-mediated immunity, humoral immunity, immune response regulation, memory, and

immunological tolerance (Baird 2006). Cells of the adaptive immune system include T-cell lymphocytes (helper T cells (generally CD-4^{+}) and cytotoxic T cells (generally CD-8^{+}), natural killer cells, and B-cell lymphocytes. After antigenic activation, CD-4^{+} T cells can be differentiated into at least 3 subsets:

Th1: which are involved in cell-mediated immunity and secrete pro-inflammatory cytokines such as interferon gamma (IFN-γ), interleukin (IL)-2, and lymphotoxin,

Th2: which promote humoral immunity and secrete anti-inflammatory cytokines such as IL-4 and IL-10), and

Regulatory T cells (CD-4^{+} CD-25^{+}) which secrete transforming growth factor-β (TGF-β) and IL-10. (Baird 2006)

Surveillance mechanisms in the CNS are unique in that only activated CTLs (cytotoxic T lymphocytes) are allowed to patrol there and in that the CNS has the lowest number of CTLs per gram tissue when compared with any other tissue (Yeager et al., 2000). However, the number of CD-8^{+} CTLs is greatly increased in various neurodegenerative disorders such as Alzheimer's disease and traumatic and ischemic brain lesions and these cells are enriched at the site of actively demyelinating lesions (Robinson et al., 2001, Patricia et al., 2007). Moreover, T-cell invasion of the spinal cord in amyotrophic lateral sclerosis is associated with motor neuron damage (Engelhardt et al., 1993). The pathology of cerebral ischemia goes hand in hand with robust immune responses, inflammation, and cell death (Kriz 2006). After ischemic reperfusion neutrophils are known to infiltrate the ischemic brain, which is followed by monocytic and T lymphocytic infiltration. Though immune responses occur during cerebral ischemia, the role of CTLs and the toxic mediators in promoting cell death has not been

elucidated yet. Information on whether and how T cells may kill neurons is limited. Conflicting data in the literature point to perforin and/or Fas-mediated cell death of the neuronal population, released by CTLs (Rensing et al., 1996, Isabelle et al., 2000) and the susceptibility of neurons to cell death-mediated CTLs in a contact-dependent manner (Giuliani et al., 2003, Nitsch et al., 2004).

The interplay between glial cells, infiltrating immune cells including lymphocytes and induced cytokines leading to CNS pathology is complex and incompletely understood. Further assessment of the functional contribution of cytokines critically depends on the elucidation of downstream secondary signaling mechanisms. Because immune cells involving T-cell migration, activation, and function are controlled by chemokines and cytokines, and the cells that secrete them, we compared levels of select chemokines and cytokines, activation status of glial ells and the status of upstream NF-κB during ischemic and reperfusion in rat model.

RESULTS

Translocation of NF-κB into neuronal nucleus during ischemia/reperfusion

NF-κB is one of the crucial transcription factors whose nuclear presence is considered to be one of the markers for NF-κB activation. Western blot analysis revealed elevated levels of NF-κB at 1 hr and 12 hrs reperfusion time periods in nuclear fractions correlating with the elevated levels of calpains and cathepsin-b (Fig-29). Further immunohistochemistry for NF-κB using NF-κB antibody which recognizes both active and inactive forms clearly showed nuclear presence of active NF-κB in ipsilateral hemisphere where as inactive NF-κB was localized in cytosol of contralateral hemisphere (Fig-30). Some of the cells showing nuclear NF-κB were found to be neuronal due to

Fig-29: Western blot analysis of nuclear NF-κB 50 and NF-κB 65 during cerebral ischemia in rat brain. Maximal increase in the NF-κB 50 and NF-κB 65 kDa levels were observed in nuclear ischemic samples over the sham operated at 1HI (1 hr ischemic) and 12HI (12 hr ischemic) reperfusion time periods after 3 hrs of occlusion.

Fig-30: Immunohistochemistry of NF-κB 105. Immunohistochemistry with NF-κB 105 which recognizes both active and inactive forms of NF-κB revealed the presence of inactive NF-κB mostly in the cytosol in contralateral hemisphere, whereas active NF-κB was present in the nucleus of ipsilateral hemisphere. It was well known that inactive NF-κB will be localized in the cytosol whereas only active NF-κB can translocate into the nucleus. Hence our result demonstrating the presence of active NF-κB in the nuclei of ipsilateral hemisphere indicates the activation of NF-κB during cerebral ischemia. Images were taken at 1000x magnification with olympus fluorescent microscope attached with a digital camera.

Fig-29

Western blot analysis of NF-kB 50

←——— NF-kB 50
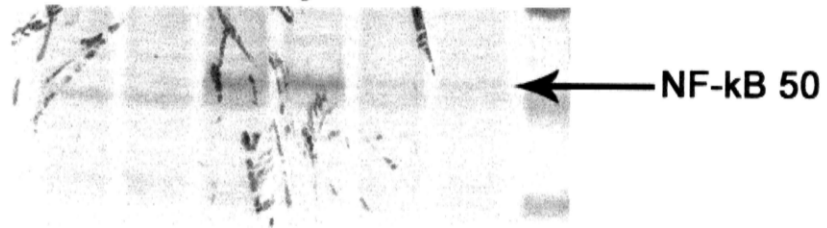
Western blot analysis of NF-kB 65

←——— NF-kB 65
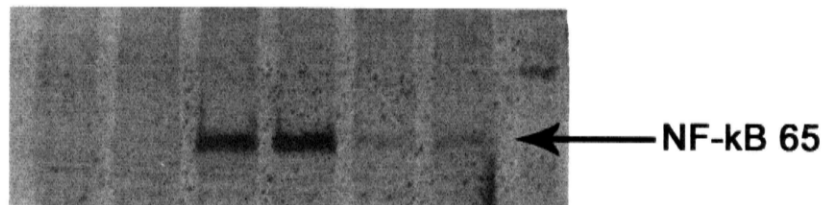
Fig-30

Immunohistochemistry of NF-kB 105
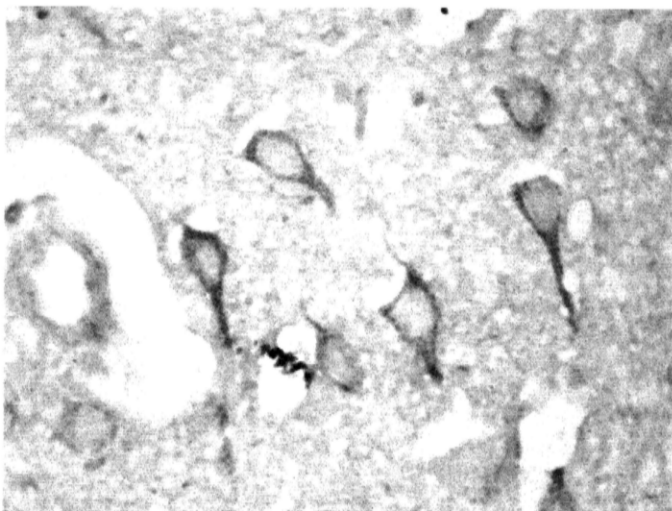
Contralateral hemisphere 1000x
Localization of inactive NFkB in
the cytosol
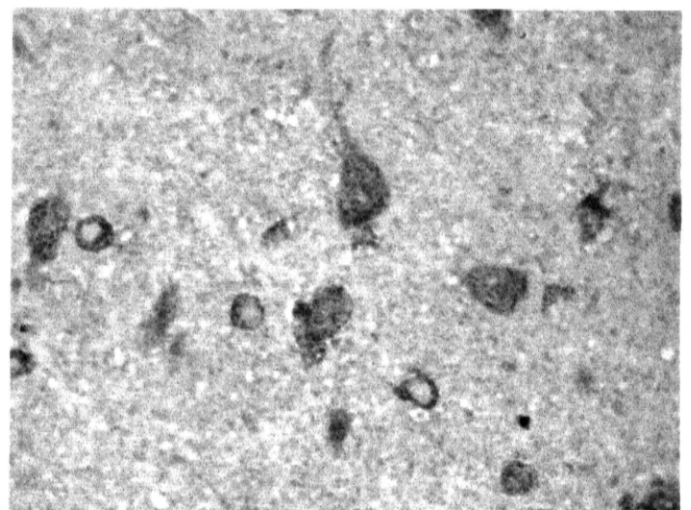
Ipsialateral hemisphere 1000x
Localization of active NFkB in
the nucleus

their appearance and presence of axonal structures. In order to check the status of NF-κB in neurons, we performed double immunofluorescence analysis for NF-κB (antibody recognizes active form only and MAP-2 (Microtubule associated protein–2) a neuronal marker. Double immuno fluorescence analysis revealed nuclear presence of NF-κB in neurons of ischemic infarct where as activated NF-κB was not found in the contralateral hemisphere (Fig-31).

Elevation of TNF- α, IL-2, IP-10/CXCL10 and Cox-2 levels in the ischemic infarct.

Unlike apoptotic cells, necrotic cells stimulate dendritic cell maturation and the production of inflammatory cytokines. Western blot analysis revealed a significant increase in the levels of the cytokines IP-10/CXCL10 (Fig-32), IL-2 (Fig-33), TNF-α (fig-34) and COX-2 (Fig-35), which are known to be some of the important cytokines and chemokines responsible for inflammation, infiltration of CTLs and for increasing gra-b activity. These cytokines reached a maximal level after a reperfusion time of 1 hr. Immunohistochemical analysis revealed a significant increase in the neuronal production of IP-10/CXCL10 in the ischemic infarct. In degenerating apoptotic and necrotic neurons IP-10/CXCL10 production was clearly higher than the production of neurons in the contralateral hemisphere (Fig-36). The increase in the levels of these cytokines paralleled or preceded the infiltration of CTLs and the increase in gra-b levels in the ischemic hemisphere.

Presence of CD-11b⁺ macrophage like cells

CD-11b is one of the markers that are known to be expressed by macrophages. Immunohistochemistry with CD-11b antibody (raised against CD-11b of peripheral macrophages) revealed the presence of CD-11b⁺ cells, which displayed macrophage like

appearance (Fig-37). Though microglia were also known to express CD-11b, the structure of CD-11b$^+$ cells was very distinct from microglial morphology. Immunohistochemistry was performed on 1hr reperfusion samples. Presence of CD11b$^+$ cells by 1 hr of reperfusion indicates the intensity of chemokines and immune responses that were occurring in the ischemic brain during initial reperfusion time periods.

Elevation of reactive microglia in infarct.

Ionized calcium-binding adaptor molecule 1 (IBA-1) is one of the markers for microglial cells. Immunohistochemistry with IBA-1 revealed elevated number of reactive microglia some with amoeboid in shape and some with more number of ramifications around ischemic infarct (Fig-38). Elevated number of reactive microglia gives a clear indication of inflammatory responses occurring in the infarct of the ipsilateral

hemisphere. Further, western blot analysis revealed an increase in the levels of Glial Fibrillary Acidic protein (GFAP) indicating the elevated levels of reactive astrocytes in the ischemic samples over the control (Fig-39). Elevated levels of reactive microglia and reactive astrocytes induce the expression of cytokines and chemokines, which might parallel or precede the immune cell infiltration into the ischemic infarct during cerebral ischemia.

Infiltration of CD-8$^+$ CTLs

CTLs kill their target cells either in a contact dependent manner or by releasing granzymes, perforins or Fas-L or TNF into the vicinity of the target cell (Fig-40). Infiltration of CTLs was previously reported in Alzheimer's disease, multiple sclerosis, and spinal cord injury. Although CTLs are known to mediate axonal damage by myelin sheath degradation, their role in mediating neuronal death during cerebral ischemia is not

Fig-31: Double immunofluorescence of NF-κB and Micro tubule Associated Protein -2 (MAP-2). Alex flour-488 was conjugated to MAP-2 primary antibody and TRITC was conjugated to secondary antibody specific for NF-κB 65 primary antibody. Antibody for NF-κB 65 recognizes only active NF-κB 65 but not inactive NF-κB. Immunofluorescence of MAP-2 was depicted in green, immunofluorescence of NF-κB was depicted in red and merged images shows the co-localization of both proteins. We hadn't observed any immunofluorescence of active NF-κB 65 in contralateral hemisphere whereas active NF-κB immunofluorescence was found in the neuronal nucleus of the ipsilateral hemisphere. Images were obtained by using leica confocal microscope.

Fig-31

Double immunmofluorescence analysis of NF-kB 65 and MAP-2

Contralateral hemisphere

Ipsilateral hemisphere
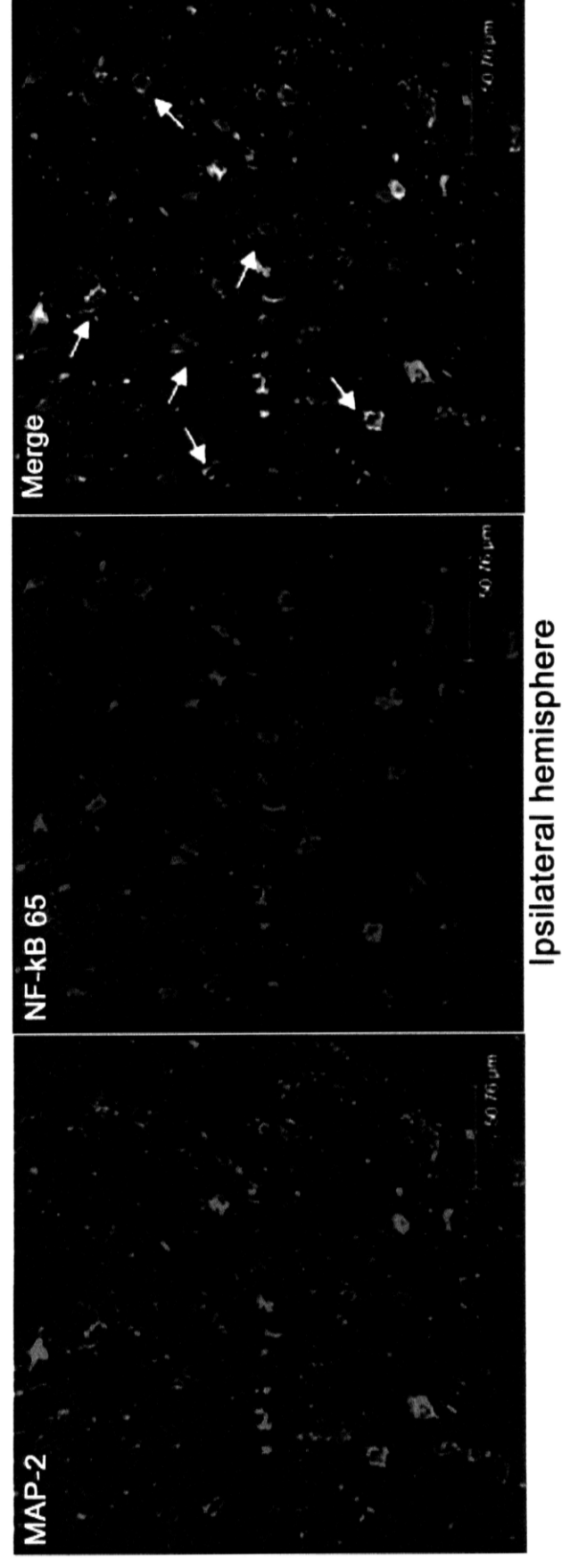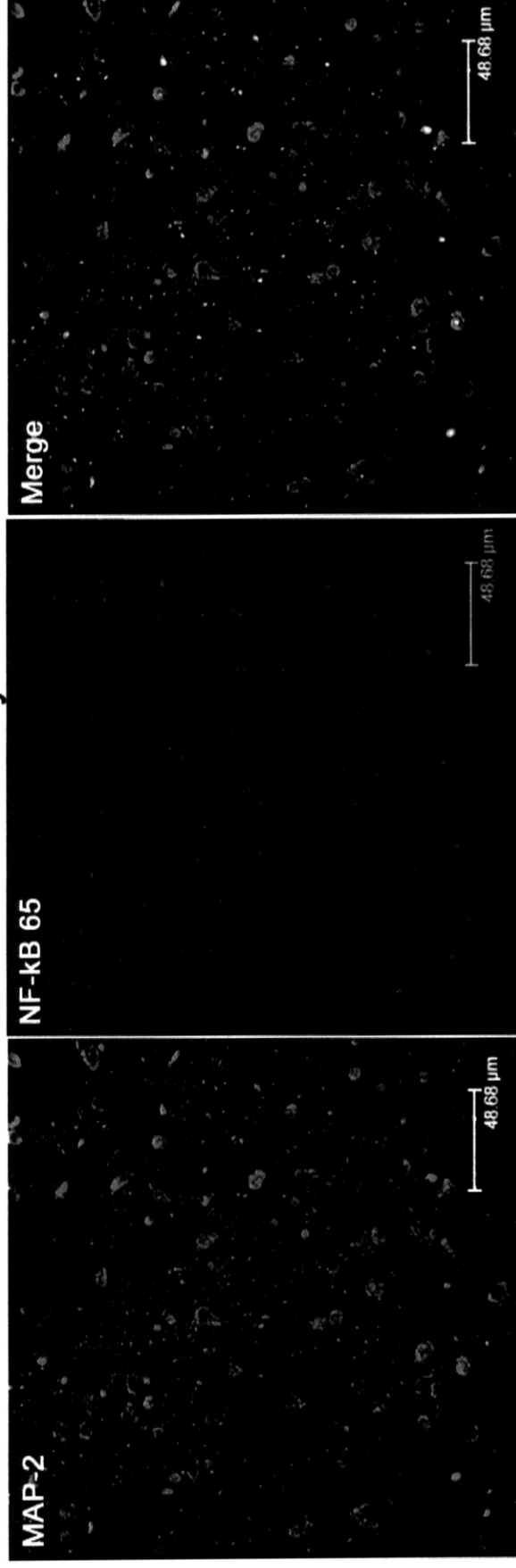
Fig-32: Western blot analysis of IP-10/CXCL10 levels in ischemic rat brain. Representative Western blot from 4 individual IP-10/CXCL10 blots. A significant increase in the IP-10/CXCL10 level was observed in ischemic samples compared to the sham-operated samples starting from the permanent occlusion for 3 hrs until the third day of reperfusion. SI (Sham ischemic), 0I (0 hr ischemic), 1HI (1hr ischemic), 12HI (12 hr ischemic), 1DI (1 day ischemic), 3DI (3 days ischemic) reperfused ischemic ipsilateral samples, respectively, after 3 hrs of occlusion. Densitometric analysis was performed using NIH image analysis software.

Fig-33: Western blot analysis of IL-2 levels in ischemic rat brain. Representative blot of 4 individual western blots of IL-2. A significant increase in the IL-2 level was observed in ischemic samples as compared to the sham-operated samples starting from the permanent occlusion for 3 hrs until the third day of reperfusion. SI (Sham ischemic), 0I (0 hr ischemic), 1HI (1hr ischemic), 12HI (12 hr ischemic), 1DI (1 day ischemic), 3DI (3 days ischemic) reperfused ischemic ipsilateral samples, respectively, after 3 hrs of occlusion. Densitometric analysis was performed using NIH image analysis software.

Fig-34: Western blot analysis of TNF-α levels in ischemic rat brain. Representative blot of 4 individual western blots of TNF-α. A significant increase in the TNF-α level was observed in ischemic samples as compared to the sham-operated samples starting from the permanent occlusion for 3 hrs until the third day of reperfusion. SI (Sham ischemic), 0I (0 hr ischemic), 1HI (1hr ischemic), 12HI (12 hr ischemic), 1DI (1 day ischemic), 3DI (3 days ischemic) reperfused ischemic ipsilateral samples, respectively, after 3 hrs of occlusion. Densitometric analysis was performed using NIH image analysis software.

Fig-35: Western blot analysis of COX-2 levels in ischemic rat brain. Representative blot of 4 individual western blots of COX-2. A significant increase in the COX-2 level was observed in ischemic samples as compared to the sham-operated samples starting from the 1 hr reperfusion till the third day of reperfusion. SI (Sham ischemic), 0I (0 hr ischemic), 1HI (1hr ischemic), 12HI (12 hr ischemic), 1DI (1 day ischemic), 3DI (3 days ischemic) reperfused ischemic ipsilateral samples, respectively, after 3 hrs of occlusion. Densitometric analysis was performed using NIH image analysis software.

Fig-32

Western blot analysis of IP10/CXCL10
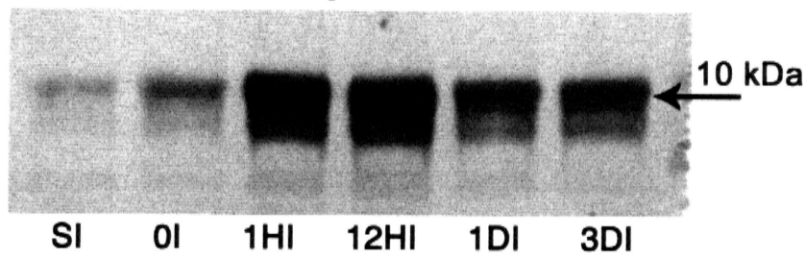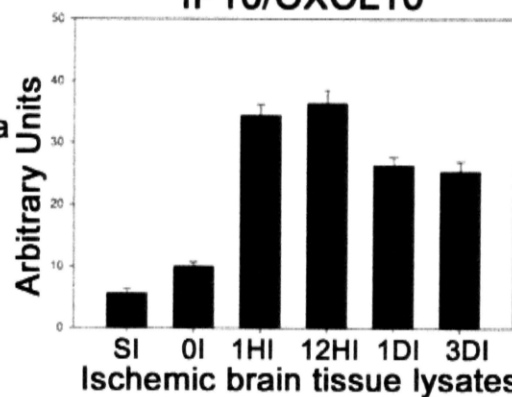
10 kDa

SI   0I   1HI   12HI   1DI   3DI

Densitometric analysis of IP10/CXCL10

Ischemic brain tissue lysates

Fig-33

Western blot analysis of IL-2

17 kDa

SI   0I   1HI   12HI   1DI   3DI

Densitometric analysis of IL-2

Ischemic brain tissue lysates

Fig-34

Western blot analysis of TNF-α

17 kDa

SI   0I   1HI   12HI   1DI   3DI

Densitometric analysis of TNF_α

Ischemic brain tissue lysates

Fig-35

Western blot analysis of COX-2

72 kDa

Actin

SI   0I   1HI   12HI   1DI   3DI

Densitometric analysis of COX-2

Ischemic brain tissue lysates
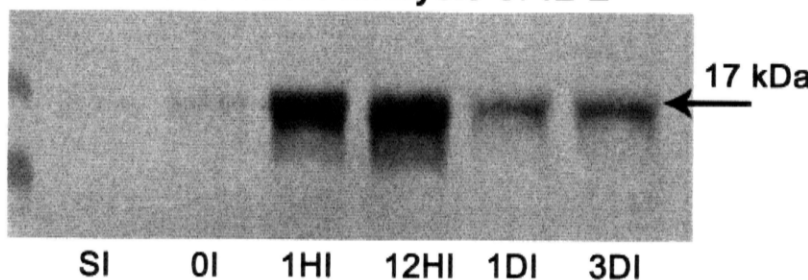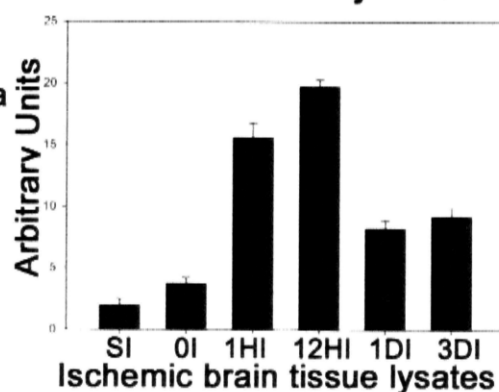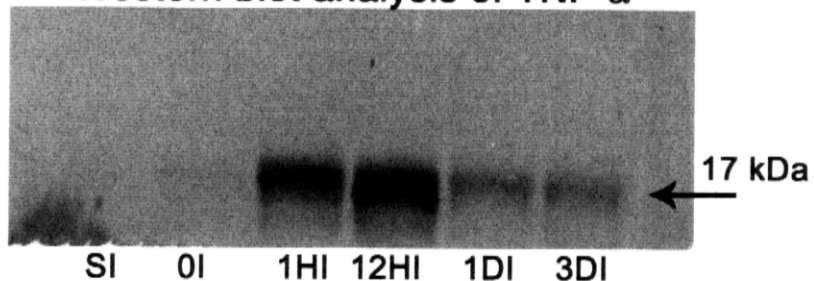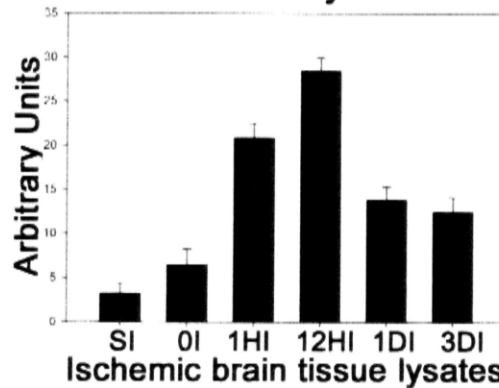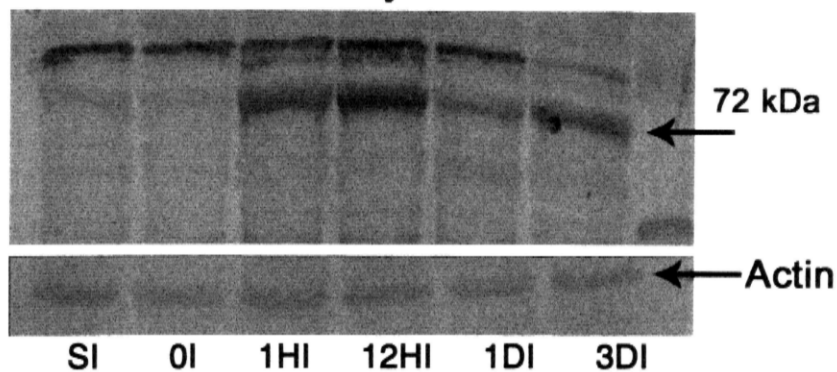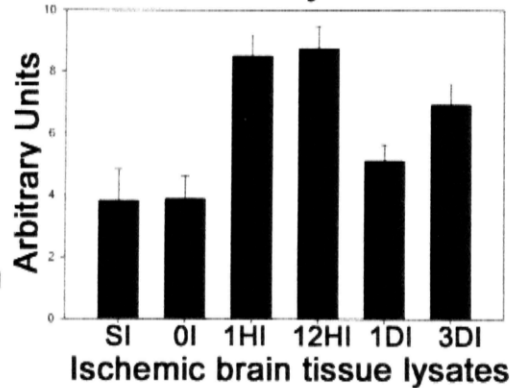
Fig-36: Double immunohistochemical analysis of IP-10/CXCL10 and Neu-N. Neu-N was immunostained using AEC substrate and IP-10/CXCL10 using NBT/BCIP substrate. a) Neurons of the contralateral hemisphere at 1000x magnification. b) Ischemic neurons stained red expressing IP-10/CXCL10 stained blue at 400x magnification. c) Degenerating neurons in the ipsilateral hemisphere with apoptotic morphology expressing IP-10/CXCL10 at 1000x magnification. Yellow arrows point to the apoptotic neurons expressing IP-10/CXCL10. d) Degenerating neurons in the ipsilateral hemisphere with necrotic morphology expressing IP-10/CXCL10 at 1000x magnification. Arrows point to the necrotizing neurons expressing IP-10/CXCL10.

Fig-36

Double immunohistochemistry of IP-10/CXCL10 and Neu-N

Contralateral 1000x

Ipsilateral 100x

Ipsilateral 1000x

Ipsilateral 1000x
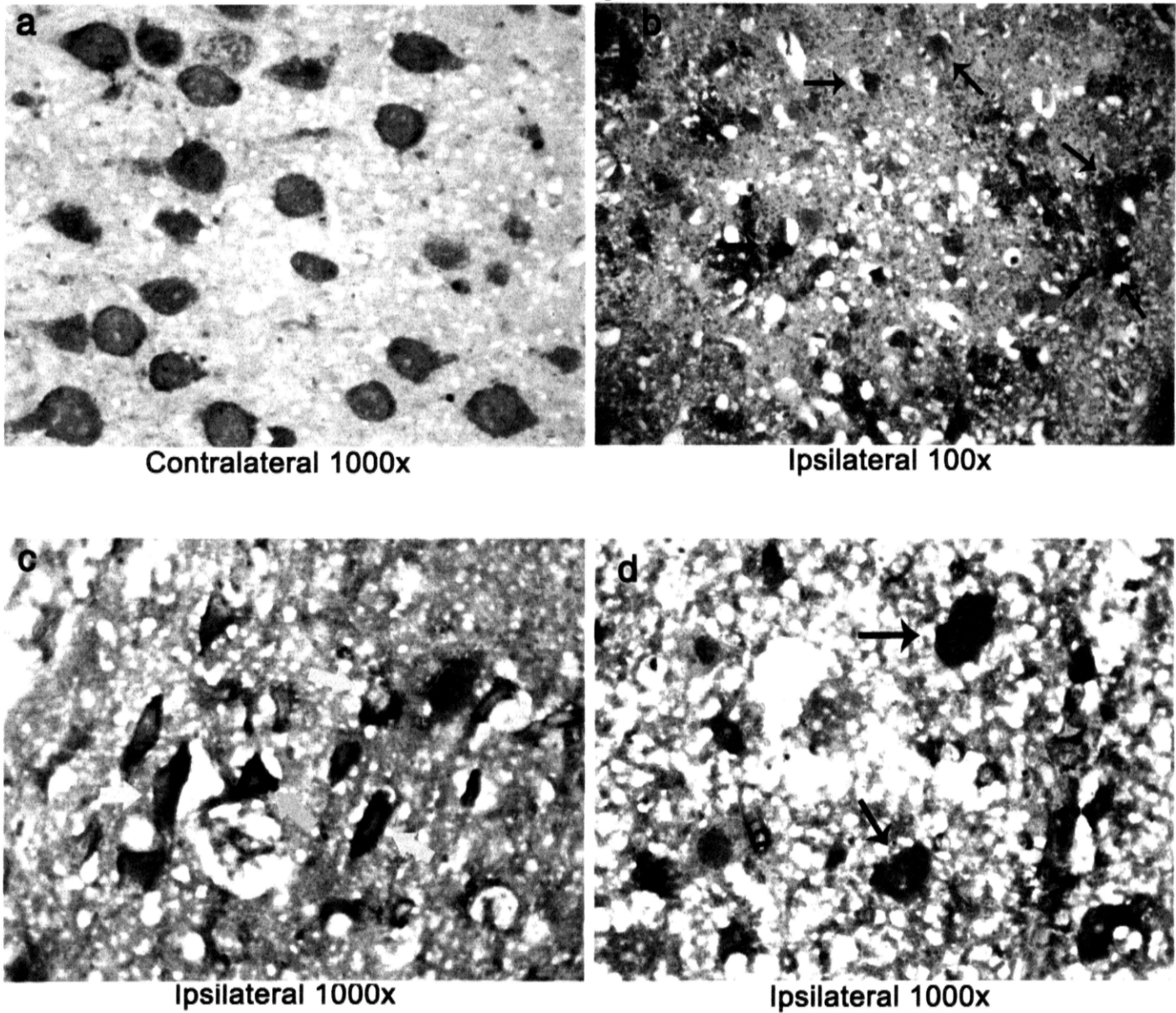
Fig-37: Immunohistochemistry of CD-11b. CD11b is one of the markers used to detect the macrophages. Immunohistochemical analysis with CD-11b antibody which was raised against macrophages revealed the presence of infiltrating macrophages in the ischemic infarct. CD-11b positive cells were mostly present in the ipsilateral striatum which was shown to be undergoing necrotic cell death and was treated as ischemic core. We hadn't found any CD-11b positive macrophages in the contralateral hemisphere. Images were taken at 100x and 400x magnifications. The presence of CD-11b positive macrophages correlated with the observations from other reports.

Fig-38: Immunohistochemistry of Ionized calcium binding adaptor molecule (IBA). IBA is one of the markers for microglial cells. Resting microglial cells were usually small with fewer ramifications. During various neuropathological events they become large in size and attain amoeboid shape and some of them contain increased ramifications. We observed both amoeboid and heavily ramified microglia which increased in size in the ipsilateral hemisphere over the contralateral hemisphere. Small round and less ramified microglia were present in the contralateral hemisphere. Images were taken at 400x magnification at 2 different locations.

Fig-39: Western blot analysis of Glial Fibrillary Acidic Protein (GFAP) during cerebral ischemia in rat brain. Maximal increase in the GFAP levels were observed in ischemic samples over the sham operated starting from permanent occlusion (0I) till 3rd day of reperfusion (3DI) after 3 hrs of occlusion.

Fig-37

Immunohistochemistry of CD-11b
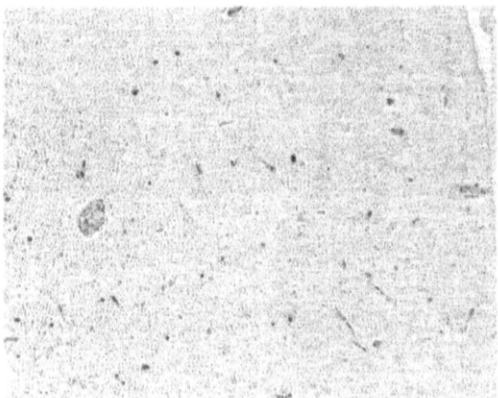
Contralateral region 100x
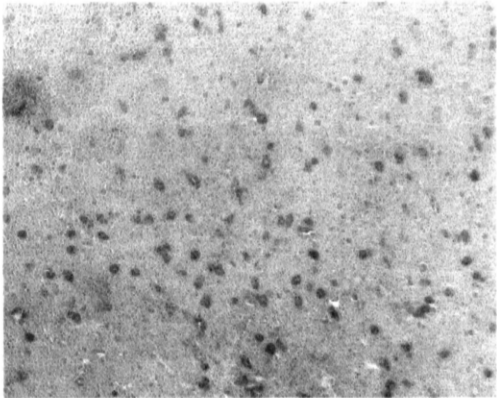
Ipsilateral region 100x
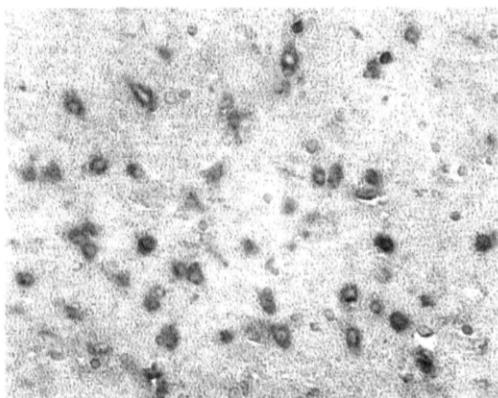
Ipsilateral region 400x
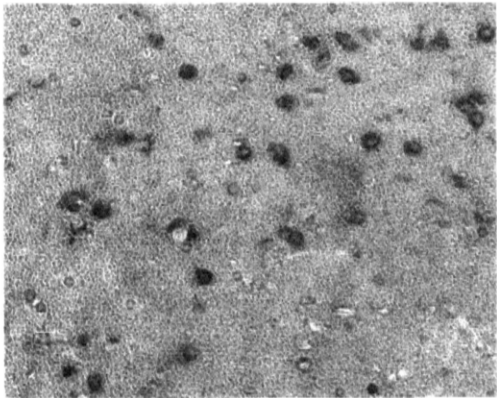
Ipsilateral region 400x

Fig-38

Immunohistochemistry of IBA
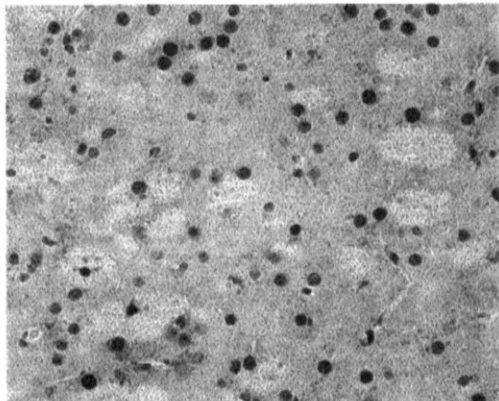
Contralateral region 400x
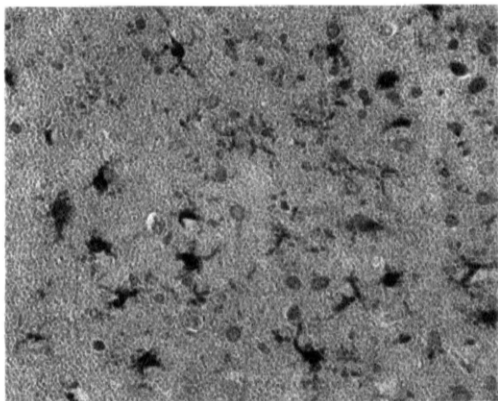
Ipsilateral region 400x
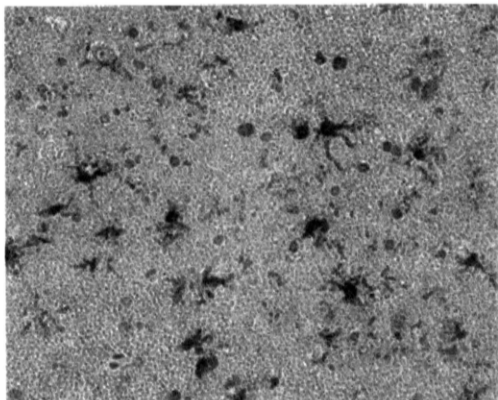
Ipsilateral region 400x

Fig-39

Western blot analysis of GFAP

50 kDa
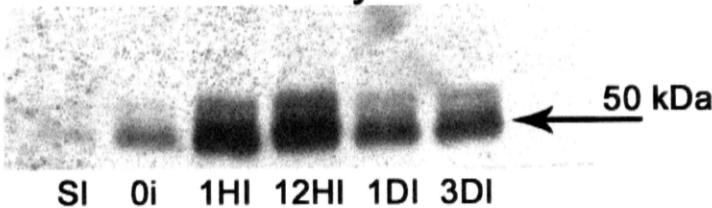
SI   0i   1HI   12HI   1DI   3DI

Fig- 40

Cytotoxic T Lymphocyte mediated cell death
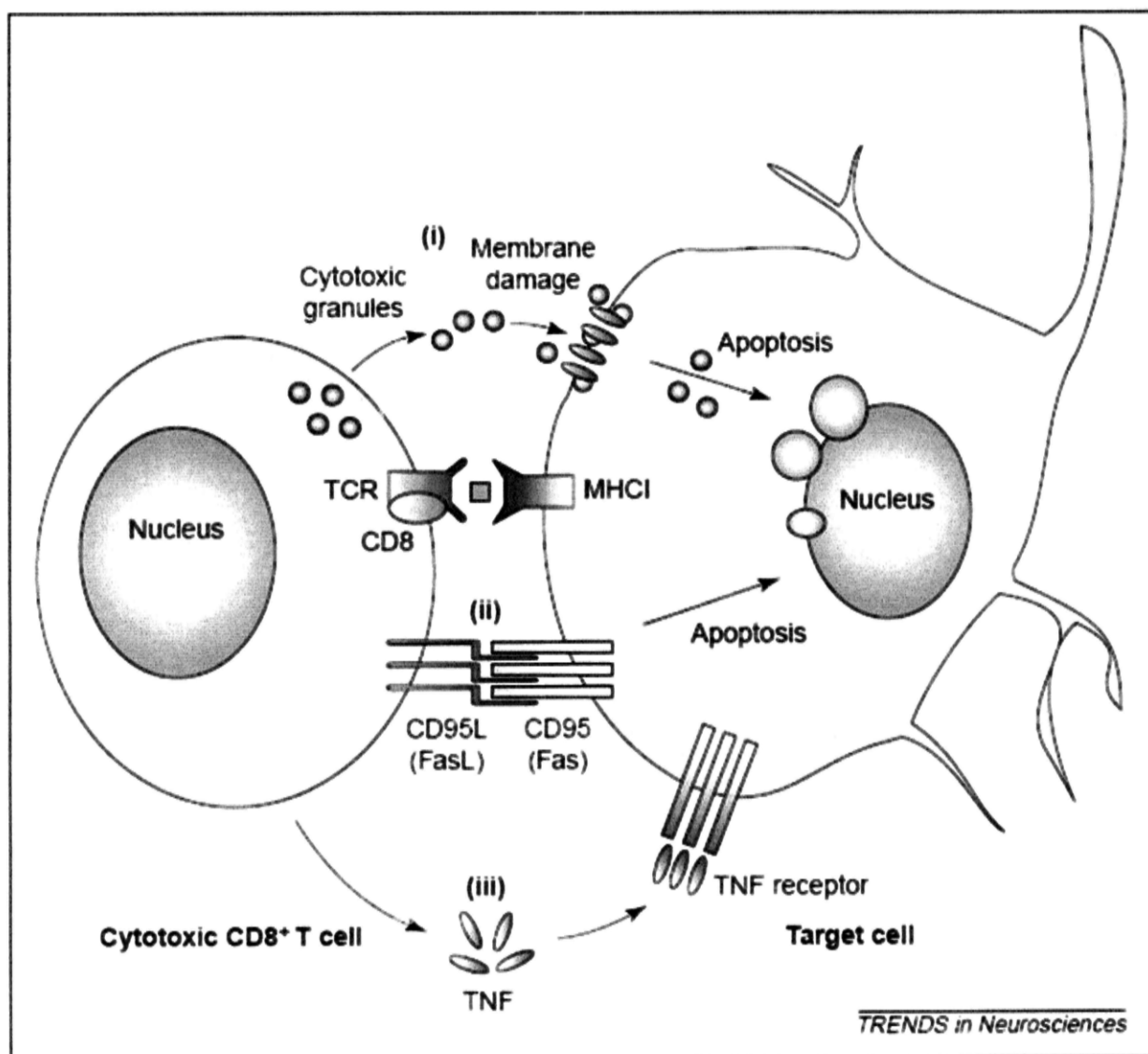
Fig. 1. Three different, although not mutually exclusive, pathways used by cytotoxic T cells (CTLs) to destroy target cells. A CD8⁺ CTL recognizes a target cell by binding of its T-cell receptor (TCR) to the appropriate combination of major histocompatability complex I (MHC I) and peptide (square). Destruction of the target cell can be performed by: (i) secretion of cytotoxic granules resulting in disintegration of the cell membrane and induction of apoptosis; (ii) activation of Fas/CD95 receptors by Fas ligand/CD95 ligand (FasL) inducing apoptosis; and (iii) release of cytokines, such as tumor necrosis factor-α (TNF).

Fig-41: Double immunofluorescence analysis of CD-3 lymphocytes and TubIII. Alexa-488 was conjugated to secondary antibody specific for CD3 primary antibody and Cy-3 was conjugated to secondary antibody specific for TubIII. Sections were counterstained with DAPI a nuclear marker. Immunofluorescence of CD-3 was depicted in green, immunofluorescence of TubIII was depicted in red, DAPI was depicted in blue, merged images shows the co-localization of these 2 proteins. Arrows point towards CD-3-positive T lymphocytes found in close proximity to TubIII-positive neurons in the ipsilateral hemisphere peripheral to the necrotic striatum. Merge images show CD-3 positive cells in white color due to the combination of DAPI (blue) and CD-3 (green) colors. Images were taken under a Leica confocal microscope.

Fig-41

Double immunofluorescence of CD-3 and TUB III

DAPI	CD-3	TUB III	Merge
75 µm	75 µm	75 µm	75 µm

Contralateral hemisphere

DAPI	CD-3	TUB III	Merge
27 85 µm	27 85 µm	27 85 µm	27 85 µm
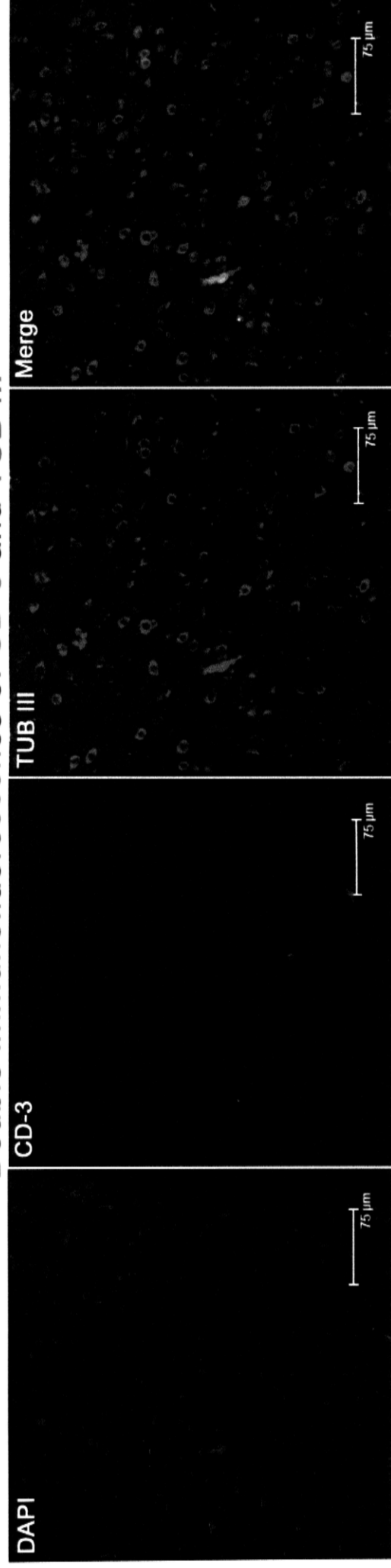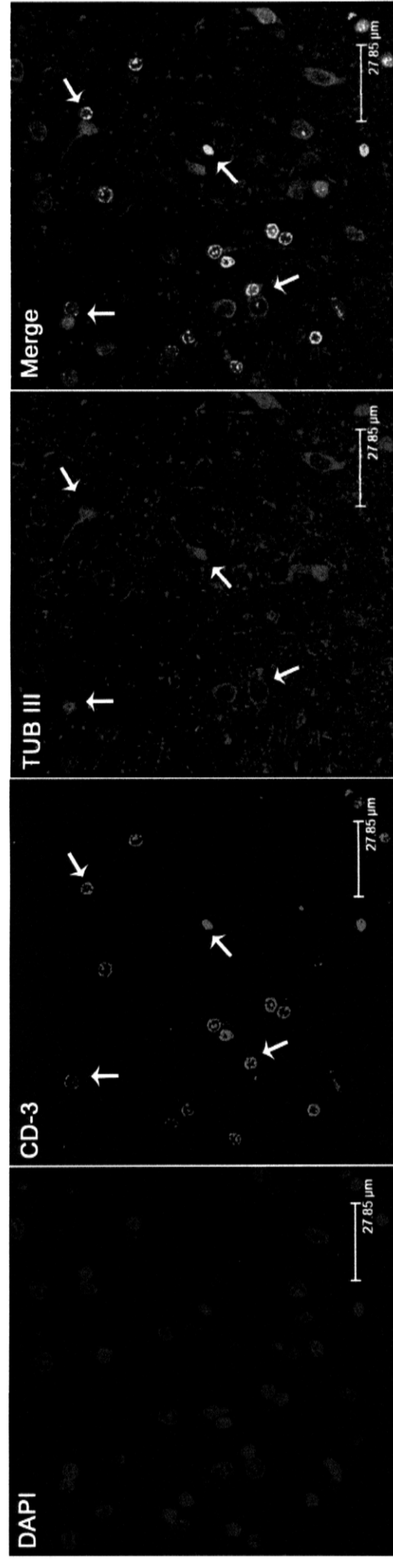
Ipsilateral hemisphere

Fig-42: Infiltration of CD-8-positive CTLs into the ischemic infarct. CD8 was immunostained using DAB substrate. Infiltration of CD-8-positive CTLs in the ischemic infarct of the ipsilateral hemisphere was observed. CD8-positive cells were not found in the contralateral hemisphere. Images were taken at 100x magnification.

Fig-43: Immunohistochemistry of CD-8 positive cells in close proximity to neurons. CD-8-positive cells were immunostained using AEC substrate and then counterstained with cresyl violet. a) Arrows point to CTLs in close proximity to neurons; b, c) Some of the degenerating neurons (violet color) were in close proximity to the CD-8-positive cytotoxic T lymphocytes (red color). Arrows point to the CTLs in the close vicinity of degenerating neurons; d) Arrows point to the CTLs undergoing cell death in the ischemic infarct (red colored cells).

Fig- 42

Immunohistochemistry of CD-8
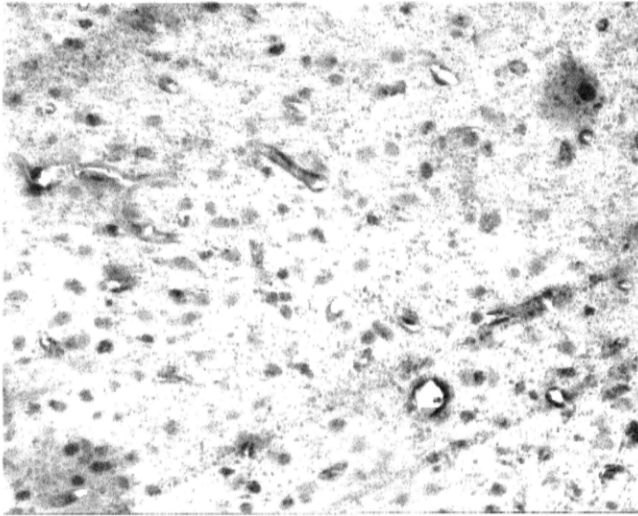
Contralateral hemisphere 100x
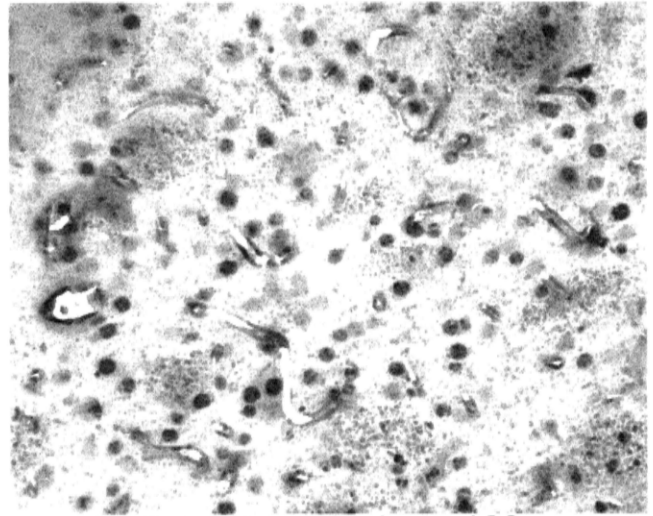
Ipsilateral hemisphere 100x

Fig- 43

Immunohistochemistry of CD-8 counterstained with cresyl violet
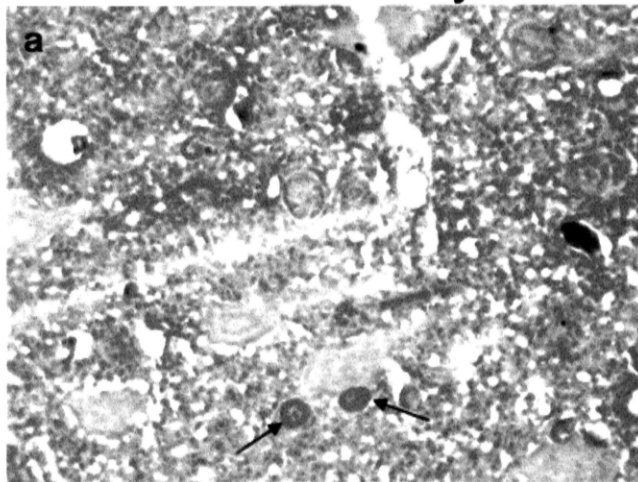
Close apposition of CTLs with neurons
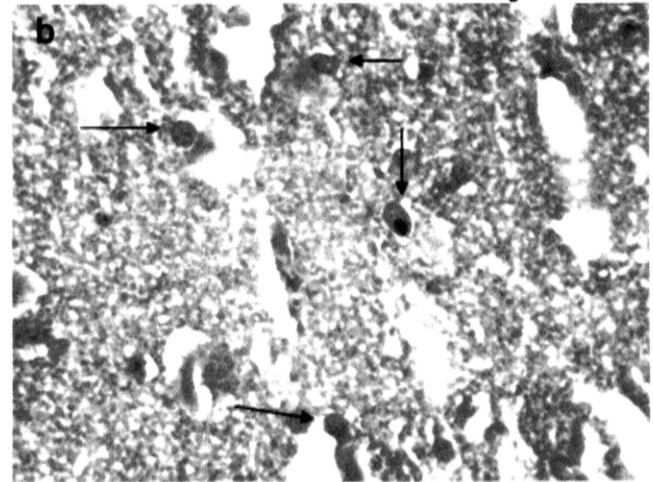
Apposition of CTLs with degenerating neurons
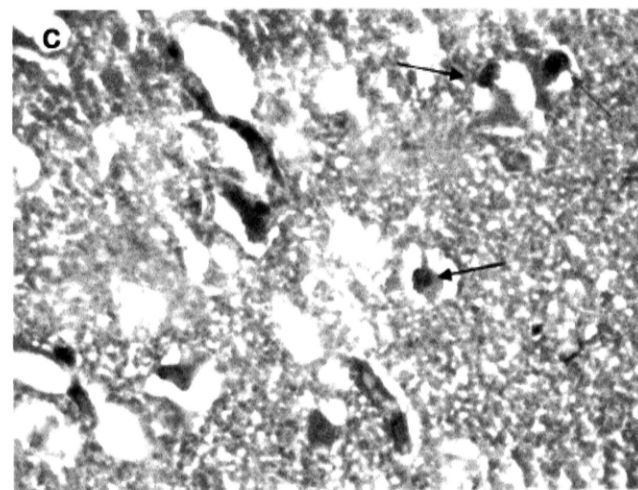
Apposition of CTLs with degenerating neurons
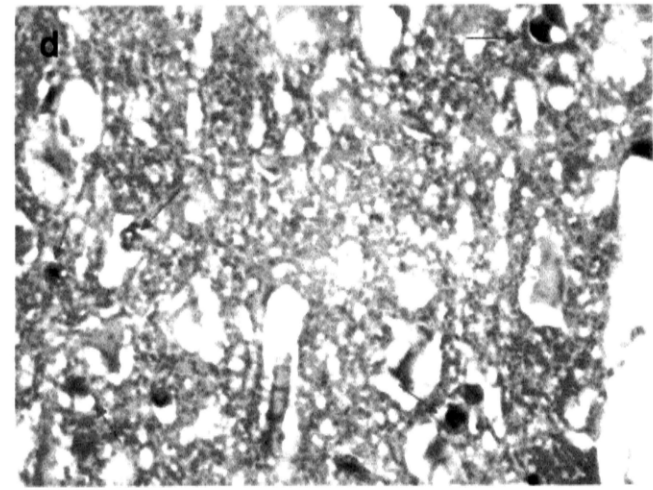
known. Double immunofluorescence analysis revealed the presence of CD-3 (T- cell marker) with Tub III (Tubulin III, neuronal marker) revealed T-cells in the close vicinity of neurons (Fig-41). We identified a significant increase in CD-8$^+$ CTL infiltration (Fig-42) in the ischemic hemisphere after a 1 hr reperfusion period. Furthermore, immunohistochemical analysis with CD-8 antibody counter stained with cresyl violet showed CTLs to be in close proximity to the degenerating neurons (Fig-43). Some of the CD-8$^+$ cells were found to be undergoing cell death according to their morphological appearance (fig-43d).

DISCUSSION

Within the first few hours after onset, cerebral ischemia is complicated by the involvement of a large number of pro-apoptotic proteins and associated cross talks, inflammatory mechanisms including the influx of monocytes/macrophages, and the activation of resident microglia and astrocytes (Chaitanya and Prakash 2008, Yamashima 2000, Giulian et al., 1993). The temporal association of chemokine expression and immune cell influx with secondary degeneration has been suggested to have a detrimental role in the immune response in CNS degenerative disorders such as traumatic spinal cord injury, multiple sclerosis, and Alzheimer's disease (Popovich et al., 2001). In addition, the release of neurotoxins, lytic enzymes, reactive oxygen, and nitrogen intermediates by leukocytes and mononuclear phagocytes activated after traumatic CNS injury exacerbates the damage greatly (Giulian et al., 1993).

Elevation of Chemokine and cytokine levels by translocated nuclear NF-κB and reactive astrocytes and microglia.

We found elevated levels of nuclear NF-κB at 1 and 12-hr reperfusion time

periods. The elevated levels of translocated nuclear NF-κB at 1 and 12 hrs reperfusion time periods is interesting in view of elevated necrotic proteases (cathepsin-b and calpains) and low levels of apoptotic protease (caspase-3) at that time period. This result points out towards the importance of NF-κB in necrotic death, which has to be addressed further. Nuclear translocation of NF-κB results in the induction of various cytokines and chemokines like IP-10/CXCL10, TNF-α, IL-2 and COX-2, which might play a major role in inflammation, and infiltration of T-Cells. Further we found elevated levels of reactive microglia and reactive astrocytes in the ischemic region over the contralateral. Reactive microglia and reactive astrocytes were known to induce the expression of cytokines and chemokines thereby modulating inflammatory and immune responses (Tanuma et al., 2006, Falsig et al., 2006). Chemokines that were expressed by glial cells was shown to direct the path of leukocytes to the damages area (Babcock et al., 2003). Chemokine expression by glial cells is not very new, but expression of IP-10/CXCL10 by neurons is interesting and the role of neuronal participation in inflammatory conditions needs to be further exploited. Though inflammatory responses are very beneficial, unrestrained inflammatory responses is detrimental causing to sever alteration in cellular functions and leading to cell death. Moreover, it is known that reactive microglia and astrocytes function as Antigen Presenting Cells (APC) during various neuro-inflammatory conditions (Beauvillain et al., 2008, Constantinescu et al., 2005) indicating their potential role in modulating immune responses involving T cells during the pathology of cerebral ischemia (Cash and Rott 1994). Further presence of CD-11b$^+$ macrophages in the ischemic hemisphere is interesting and raises further question that whether resident microglial cells have attained the macrophage morphology or peripheral macrophages

have infiltrated the ischemic infarct due to the elevated levels of chemokines and blood brain barrier disruption. However due to the reports which have shown using tracking studies that peripheral macrophages enter brain during inflammatory conditions (Kleinschnitz et al., 2003) and microglial cells have the ability to attain macrophage morphology (Denker et al., 2007), both of them have equal chances to occur during cerebral ischemia (Zhang et al., 2005).

Recruitment of CD-8^{+} CTLs via the elevation of IP-10/CXCL10, IL-2 and TNF-α

Cytokines play an important role in regulating cytotoxicity by activated CTLs. Chemokine induction has been described in many neurodegenerative disorders of the CNS within hours of injury (Masabumi et al., 2006, Mc Tigue et al., 1998). Cerebral ischemia provokes the expression of, for example, IL-2, IP-10/CXCL10, and TNF-α, indicating an important role of these cytokines in the chemoattraction of T cells towards the injured cells of the infarct. We observed a significant increase in the levels of IP-10/CXCL10, which belongs to the CXC family of chemokines and which is known to be a potent chemoattractant for T cells. Besides functioning as a chemoattractant, it also promotes T-cell proliferation and cytokine production and has a role in generating antigen-specific T cells (Dufour et al., 2002). Immunoblot analysis revealed a significant upregulation in the expression of IP-10/CXCL10 from 1 hr reperfused animals compared to the sham-operated animals. Double immunohistochemical analysis showed the increased production of IP-10/CXCL10 by apoptotic and necrotizing neurons, contributing to the chemoattraction of CTLs in their vicinity. In the present study, increased IP-10/CXCL10 expression preceded or paralleled T-cell influx after cerebral ischemia. We observed a significant increase in the infiltration of CTLs, as shown by the

presence of CD-3^{+} and CD-8^{+} in the immunohistochemical and immunofluorescence analysis. The larger number and rapid appearance of T cells in the infarcted area of ischemic rat brain is related to the magnitude of chemokines and the cytokine environment that develops at the injury site. Thus, chemokines expressed in the infarcted tissue of MCA-occluded rats would serve diverse roles, including enhancement of T-cell recruitment, activation, and effector potential (Gardiner et al., 1998, Stoll 2002). Once they are activated, CTLs exert a pathological effect by liberating granzymes or via a contact-dependent mechanism. Immunoblot analysis revealed a significant increase in IL-2 and TNF-α levels, providing a signal strong enough to induce NK cell proliferation and stimulate an increase in granule content. In addition, it has been shown that IL-2 induces higher gra-b activity (Bloom et al., 1999, Berthier et al., 2005).

Neuronal death mediated by CTLs

Activated T cells are known to cause axonal damage and motor neuron death in various pathological conditions (Neumann et al., 2002, Yilmaz et al 2006). However, their role in mediating neuronal death in the pathology of cerebral ischemia has not yet been elucidated. CTLs require MHC I expression on target cells to exert their cytotoxic effects. However, recent reports indicate that neurons are susceptible to cell death mediated by T cells accumulating in diseased CNS in Antigen-independent, non-MHC I mechanism. As neurons are known to express MHC I during pathological conditions, it is important to determine whether the cell death mediated by CTLs is MHC I dependent or independent of neuronal expression during cerebral ischemia (Jane et al., 2002, Isabelle et al., 2001). We observed CD-3^{+} and CD-8^{+} CTLs to be in close proximity to neuronal bodies and peritoneal macrophages infiltrating the infarct starting after 1 hr of

reperfusion. Immunohistochemical analysis for CD-8 clearly showed the presence of CD-8^+ cells in close proximity to degenerating neurons. The mode of neuronal death in the presence of CTLs appeared to be apoptotic according to their morphological appearance. Cytotoxicity mediated by CD-8^+ cells happens to be mediated by both cell-cell contact and by the release of gra-b. In support of a contact-mediated cell death mechanism, our results demonstrating the presence of CTLs in close proximity to degenerating neurons provides further evidence for the detrimental effects of T cells activated during cerebral ischemia. We further observed that some of the T cells in the infarct appeared to be dead. This finding is in line with the results reported by the group of Guiliani and with the concept that neurons can evoke T-cell death (Guiliani et al., 2003, Neumann et al., 2002). However, significant damage might have already occurred even before they are eliminated. This study highlights the importance of T cells in mediating neuronal death via both a contact-dependent mechanism and by secreting granzymes into the vicinity of the target cell.

Role of gra-b in mediating cell death during the pathology of cerebral ischemia

INTRODUCTION

CTLs and NK cells kill target cells either in contact dependent manner or by releasing granzymes into the vicinity of the target cell. Granzymes comprise about 90% of the cytolytic granules stored in the secretory lysosomes of CTLs (Jenne and Tschopp 1988). Among the granzymes, granzyme-b (gra-b) is considered to be the most powerful pro-apoptotic member. Gra-b is released through exocytosis of CTL secretory granule contents into a transient, diffusion-limited synapse formed between the killer cell and its target (Barry and Bleackley 2002, Trapani and Smyth 2002). The expression of granzymes is restricted to activated T lymphocytes, immature T cells in the thymus (thymocytes), T cells (a small population of specialized T cells mainly found in the gut) and NK cells. Naive T cells do not express granzymes, but most CD-8$^+$ and a smaller proportion of CD-4$^+$ T cells sensitized *in vitro* by antigen or lectin or following other types of stimulation express granzymes and perforin. However, the kinetics and expression level of the individual granzymes and perforin vary in different clonal populations *in vitro* and *in vivo* and depend on how they are activated (Garcia-Sanz et al., 1990, Ebnet et al., 1991). Granzymes are synthesized as zymogens that are processed at the time of packaging into cytolytic granules. Cleavage of the leader peptide leaves two amino acids attached at the mature amino terminus, which are then clipped off by dipeptidyl peptidase I (DPPI, also called cathepsin C), a peptidase constitutively expressed in lysosomes (McGuire et al., 1993). Granzymes become enzymatically active once the amino-terminal dipeptide is cleaved. As the pH optimum of granzymes is approximately 7.5, they are maximally active following release from the secretory granules into the cytoplasm (pH around 7) (McGuire et al., 1993).

There are five human granzymes (A, B) and ten mouse granzymes (A, B, C, D, E, F, G, H, J, M), expressed from three gene clusters. Granzyme A and Granzyme B (gra-a, gra-b) are the most abundant granzymes. Though perforin and granzyme genes are induced during T cell activation the only signal shown to upregulate gra-a, gra-b and perforin consistently is IL-2 (Liu et al., 1989). However, a recent study in mice showed that IL-2 regulates perforin and granzyme expression directly and independently of its effect on CD-8$^+$ T cell survival and proliferation (Janas et al., 2005). An extensive array of intracellular substrates associated with cell death is good substrates for granzyme B. Once it is liberated from CTLs it mediates cell death either independently of the caspases or by activating caspases or by interacting and activating other pro-apoptotic proteins such as Bid to tBid (Sutton et al., 2000, Barry et al., 2000). As the substrate specificity of gra-b is similar to that of the caspases, it is an important protease for mediating cell death. Thus, depending on the cellular context, it is feasible that granzyme B might kill a cell in diverse ways, such as by activating caspases directly, inducing DNA fragmentation through de-repressing CAD (Sharif-Askari et al., 2001, Thomas et al., 2000) or cleaving key structural proteins in the nuclear membrane or cytoskeleton (Zhang et al., 2001, Browne et al., 2000) (Fig-44). Among the well-known gra-b substrates HSP-70, Bid, Caspase-3, and PARP were checked to study their interaction with gra-b during cerebral ischemia.

Bid plays a crucial role in intrinsic cell death pathway. One of the preferred pathways by which gra-b chooses to execute cell death is by cleaving and activating Bid to tBid, which initiates apoptosis through activating Bax and/or Bak and promoting their oligomerization within the mitochondrial outer membrane. Oligomerization of Bax/Bak

Fig-44: Physiological substrates of gra-b. Gra-b shares similar substrate specificity with caspase-3. Hence most of the substrates cleaved by caspase-3 will also be acted upon by gra-b. Further the ability of gra-b to activate caspase-3 and induce cell death independent of caspase-3 makes it crucial protease in cell death scenario. Some of the physiological substrates upon which gra-b can act during cell death were shown in the picture.

Fig- 44

Physiological substrates of gra-b
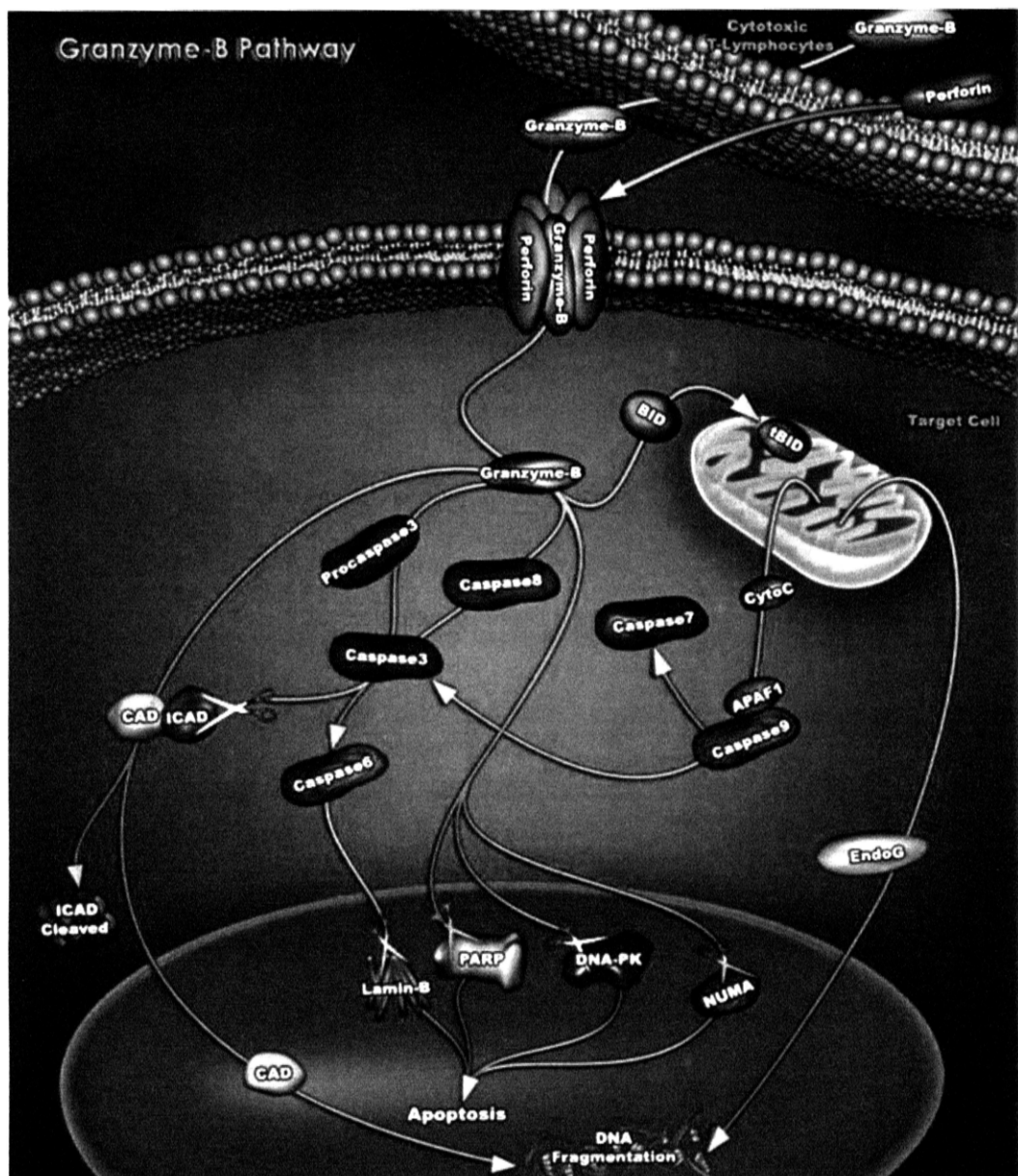
results in mitochondrial membrane permeabilization and facilitates the release of inter-membrane space proteins such as cytochrome c into cytosol (Kuwana et al., 2002, Waterhouse et al., 2005). Cytosolic release of Cyt-c helps in the formation of apoptosoome complex, which activates executioner caspases and leads to cell death (Slee et al., 1999). Though Bid has been shown to be one of the preferred targets for gra-b recent reports have shown that human and mouse granzymes differ in their substrate preference and Bid is not a favorite substrate for mouse gra-b when compared to human gra-b (Cullen et al., 2007). However the substrate specificity of Bid for mouse gra-b still exists. Caspase-3, executioner caspase of the caspase family has been shown to be one among the substrates for granzymes. The activation of caspases by granzymes directly leads to apoptotic cell in a classical phenomenon by cleaving various cellular substrates (Metkar et al., 2003). However recent reports has shown that granzymes can mediate cell death dependent or independent of caspases and mostly rely on mitochondrial permeability in mediating cell death (Pinkoski et al., 2001). PARP is a DNA repair enzyme whose conventional role is to repair DNA breaks during various cellular insults. However its role in necrotic and apoptotic cell death has changed its status dramatically. Over activation of PARP has been shown to mediate necrosis by consuming ATP drastically. Further failure of caspases to breakdown PARP during cell death was shown to shift apoptotic cell death to necrotic death (Moroni et al., 2001). Apart from these roles, PARP is one of the favorite substrates for a variety of suicidal proteases like caspases, calpains, cathepsins and granzymes (Gobeil et al., 2001, Froelich et al., 1996, Wang 2000). Moreover, each of this protease liberates specific signature fragments of PARP there by allowing us to know the protease involved by monitoring the signature

fragments during cell death.

Heat Shock Protein-70 (HSP-70) is a 72 kDa heat shock protein, which is highly stress inducible member of chaperone family (Mayer and Bukau 2005). Though the precise mechanism by which HSP-70 exerts its protective efficacy is not clearly known, it has been attributed to its chaperone function, which prevents the protein aggregation, restoring the structure and function of denatured proteins and via anti-apoptotic mechanisms (Giffard et al., 2004, Matsumori et al., 2005). Further recent work indicates that HSP-70 is also capable of modulating inflammatory and immune responses either promoting or attenuating them during various pathological conditions (Radons and Multhoff 2005, Basu et al., 2000). Various cellular stresses like cerebral ischemia leads to the induction of HSP-70 in the ischemic brain. Over expression of HSP-70 during cerebral ischemia was shown to provide protection from ischemic brain injury (Fig-45). The proposed mechanism by which HSP-70 over expression can protect ischemic injury is by reducing the cytosolic release of cytochrome-c from mitochondria thereby reducing the DNA fragmentation and reducing the nuclear translocation of AIF from mitochondrial membrane (Matsumori et al., 2005, Tsuchiya et al., 2003).

AIF is a 67-kDa flavoprotein located in the inner mitochondrial inter-membranous space that upon translocation to the nucleus during various cellular insults results in large scale DNA fragmentation (Susin et al., 1999). Though the exact stimuli required for the release of AIF from the mitochondria is not clearly known, interaction of suicidal proteases like calpains, cathepsins, Bid and PARP with mitochondrial membrane was thought to mediate the cytosolic release of AIF (Moubarak et al., 2005, Culmsee et al., 2005). The released AIF translocates to nucleus and mediates chromatin condensation or

Fig-45: Anti apoptotic role of HSP-70 during cell death. HSP-70 is one of the anti-apoptotic proteins which act on JNK, lysosomal proteases, mitochondrial permeabilization, apoptosome complex and AIF trying to attenuate the execution of cell death. The role of HSP-70 trying to attenuate AIF from translocation to nucleus was shown encircled in the picture.

Garrido C, et al., Mechanisms of cytochrome *c* release from mitochondria. Cell Death and Differentiation. 2006;13:1423–1433.

Fig-45

Anti-apoptotic function of HSP-70
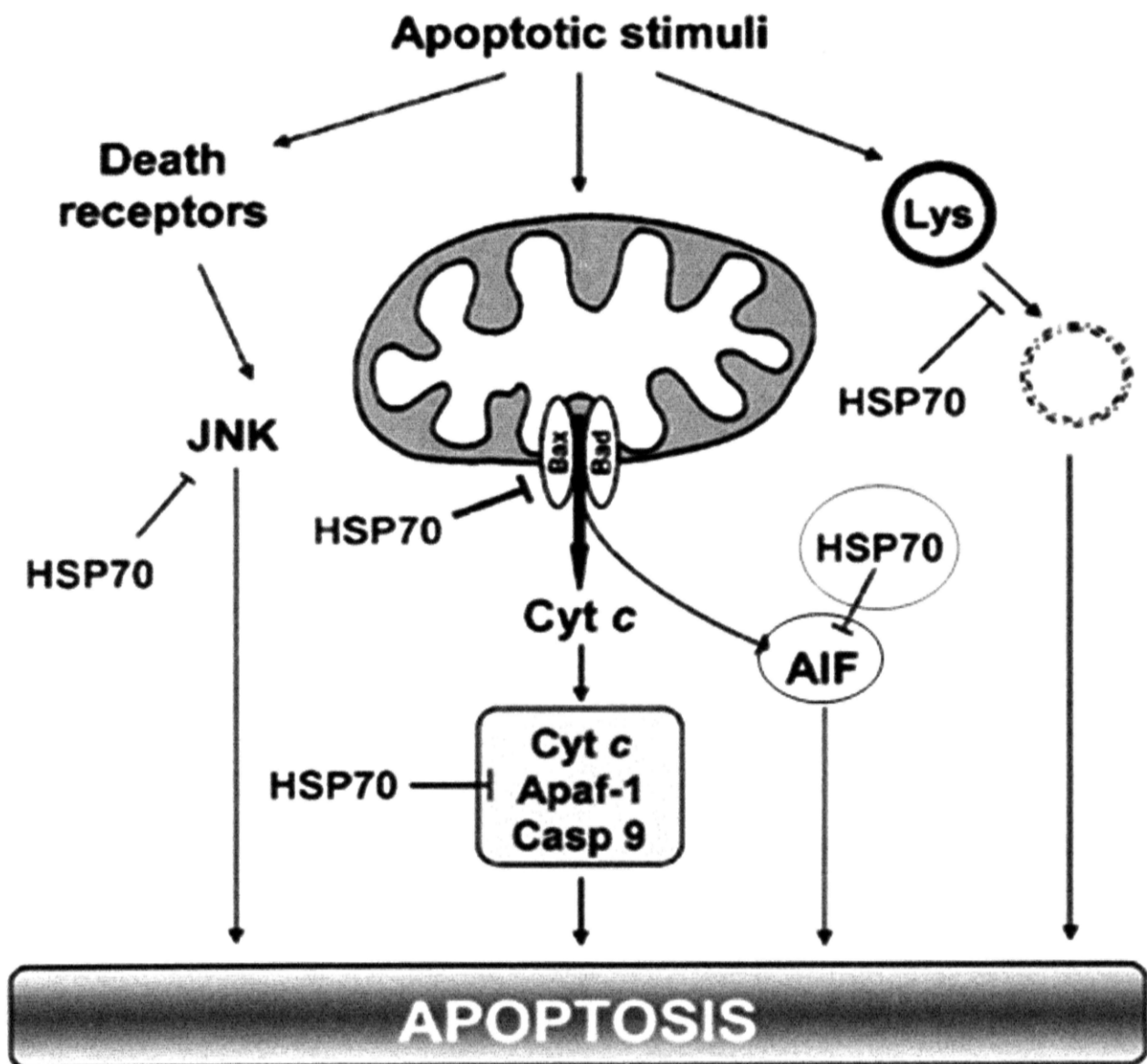
fragmentation. The nuclear translocation of AIF was shown in various animal models like Parkinson's disease, perinatal hypoxia and brain trauma (Wang et al., 2003, Zhu et al., 2004, Zhang et al., 2002). The nuclear translocation of AIF has shown to be retarded by HSP-70.

Though HSP-70 is induced during cerebral ischemia the reason why it couldn't inhibit nuclear translocation of AIF in wild type rats is not understood. One of the explanations is that the elevated levels might not suffice to inhibit the nuclear translocation of AIF. However the involvement of a large number of suicidal protease families poses a question on their involvement in nuclear translocation of AIF during cerebral ischemia. Hence in the present study we used a rat model of transient focal cerebral ischemia to investigate 1) the role of gra-b liberated by CTLs in mediating neuronal death, 2) the interactions of gra-b in with other proapoptotic proteins such as Bid, caspase-3, PARP, HSP-70 and 3) the role of gra-b in AIF mediated cell death in ischemic rat brain infarction.

RESULTS

Elevation of CTLs and gra-b levels in the ischemic infarct

Ischemia results in an increase in cytokines and chemokines, which results in increased inflammatory and immune responses in the ischemic region. Immunohistochemical analysis with CD-8 antibody revealed an increase in the levels of Cytotoxic T Lymphocyte population infiltrating the ischemic infarct of rat over the contralateral region. Cytotoxic T Cells were known to kill the target cells either in contact dependent manner or by releasing secretory proteases like granzymes and perforins into the vicinity of the target cells.

Gra-b belongs to the serine protease family and is mainly secreted from NK cells and CTLs as a 32 kDa protein. Western blot analysis revealed a significant increase in gra-b levels in the ischemic hemisphere as compared to the sham-operated animals after a 1 hr reperfusion period (Fig-46). There was a maximal increase after 1 hr of reperfusion up to the 3rd day that correlated with an increase in cytokine levels and the infiltration of CTLs. To provide more information on the localization of the gra-b, immunohistochemical analysis was performed. The intensity of the immunoreactivity in the ischemic region was significantly higher than in the contralateral hemisphere. Immunoreactivity was localized in the ischemic striatum and cortical region (Fig-47). To determine the presence of gra-b in the neuronal population in the ischemic infarct, we performed double immunostaining for neuronal-specific enolase and gra-b. Gra-b was co-localized in the cells that stained positive for neuron-specific enolase, indicating the presence of gra-b in the neurons (Fig-48).

Gra-b interacts with caspase-3, PARP, Bid and HSP-70 in the ischemic infarct.

The substrate specificity of gra-b is similar to that of caspase-3. Among the various known gra-b substrates, we investigated gra-b interaction with PARP, Bid, and caspase-3. PARP is one of the DNA repair enzymes whose cleavage is considered to be a hallmark of cells undergoing cell death. Its role in necrotic and apoptotic cell death has been widely reported (Gobeil et al 2001, Froelich et al., 1996). It is also a substrate for a variety of proteases such as caspases, calpains, and granzymes. PARP is known to produce specific signature fragments of 72, 64 kDa by gra-b, apart from the 89 and 21 kDa fragments mediated by activated caspase-3 and the 50 kDa fragment by cathepsin-b (Fig-49). Western blot analysis revealed a significant increase in the 64 kDa fragment in

Fig-46: Western blot analysis of gra-b levels in ischemic rat brain. Representative blot of 4 individual western blots of gra-b. A significant increase in the gra-b level was observed in ischemic samples as compared to the sham-operated samples starting from the permanent occlusion for 3 hrs until the third day of reperfusion. SI (Sham ischemic), 0I (0 hr ischemic), 1HI (1hr ischemic), 12HI (12 hr ischemic), 1DI (1 day ischemic), 3DI (3 days ischemic) reperfused ischemic ipsilateral samples, respectively, after 3 hrs of occlusion and GBM (human glioma tissue lysate as positive control). Densitometric analysis was performed using NIH image analysis software.

Fig-47: Immunohistochemical localization of gra-b in the ischemic rat brain. A significant increase in the localization of gra-b in the ipsilateral hemisphere compared to the contralateral hemisphere is visible. a) Arrows point to the degenerating cells, which were highly immunoreactive for gra-b. b) Immunoreactivity was not found in the cells of the contralateral hemisphere. Images were taken under a magnification of 1.25X and 100X to give a clear view of regional and cellular localization of gra-b in the infarct. Bright field images were taken with an Olympus UCTR30-2 fluorescent microscope.

Fig- 46

Western blot anlalysis of gra-b

SI   0I   1HI   12HI   1DI   3DI   GBM

← 32 kDa

Densitometric analysis of gra-b

Arbitrary Units

SI 0I 1HI 12HI 1DI 3DI GBM

Ischemic brain samples
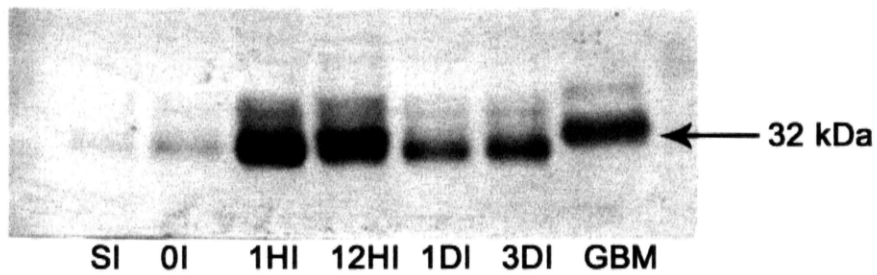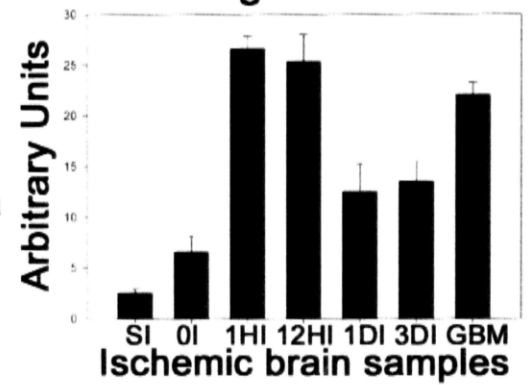
Fig- 47

Immunohistochemistry of gra-b
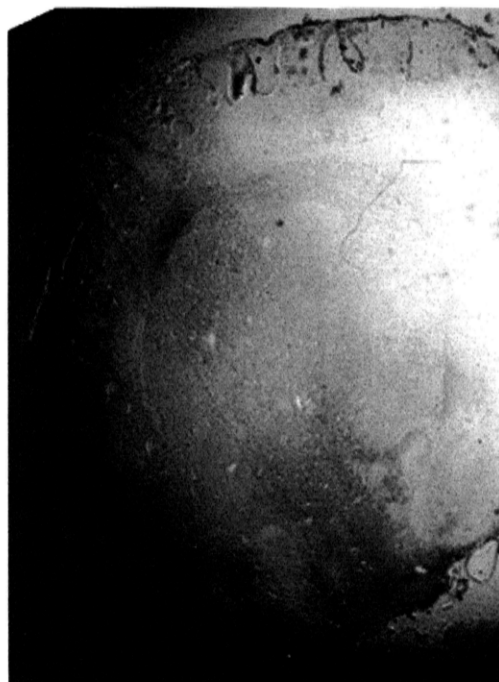
Ipsilateral hemisphere
12.5x
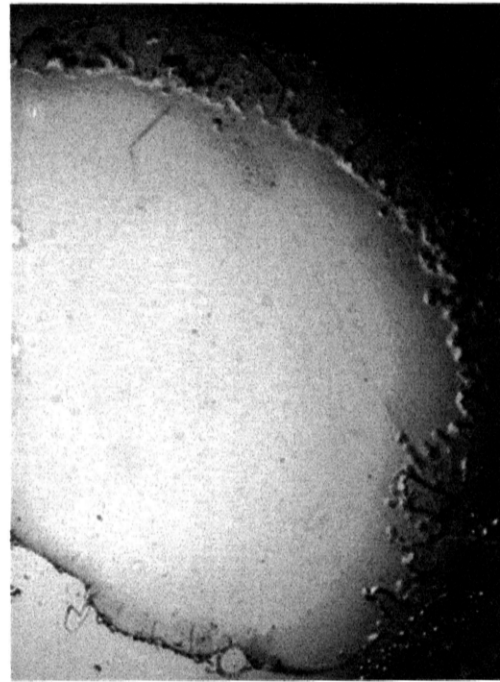
Contralateral hemisphere
12.5x
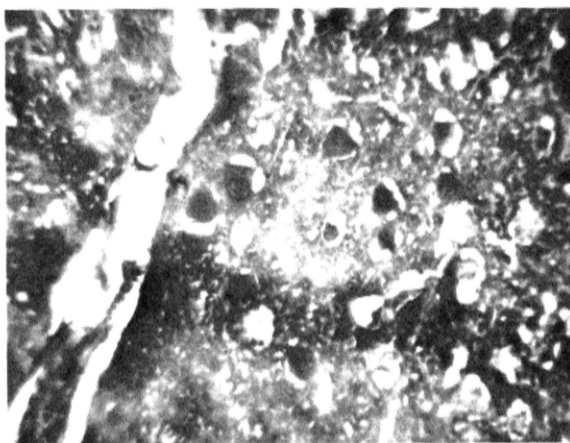
Ipsilateral hemisphere 1000x
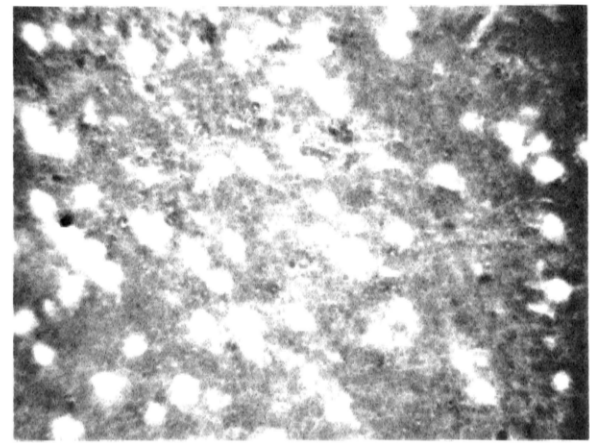
Contralateral hemisphere 1000x

Fig-48: Double immunofluorescence of gra-b and neuron-specific enolase. FITC was conjugated to secondary antibody specific to gra-b primary antibody and TRITC was conjugated to secondary antibody specific to NSE. Immunofluorescence of gra-b was depicted in green, immunofluorescence of NSE was depicted in red, merged image showing presence of gra-b in neuronal population of the ischemic infarct. We hadn't found immunofluorescence of gra-b in the contralateral hemisphere, merged image of NSE and gra-b with the bright field image showed the absence of gra-b in the neurons of the contralateral hemisphere.

Fig-48

Double immunofluorescence analysis of gra-b and Neuron specific enolase

Ipsilateral hemisphere

Contralateral hemisphere
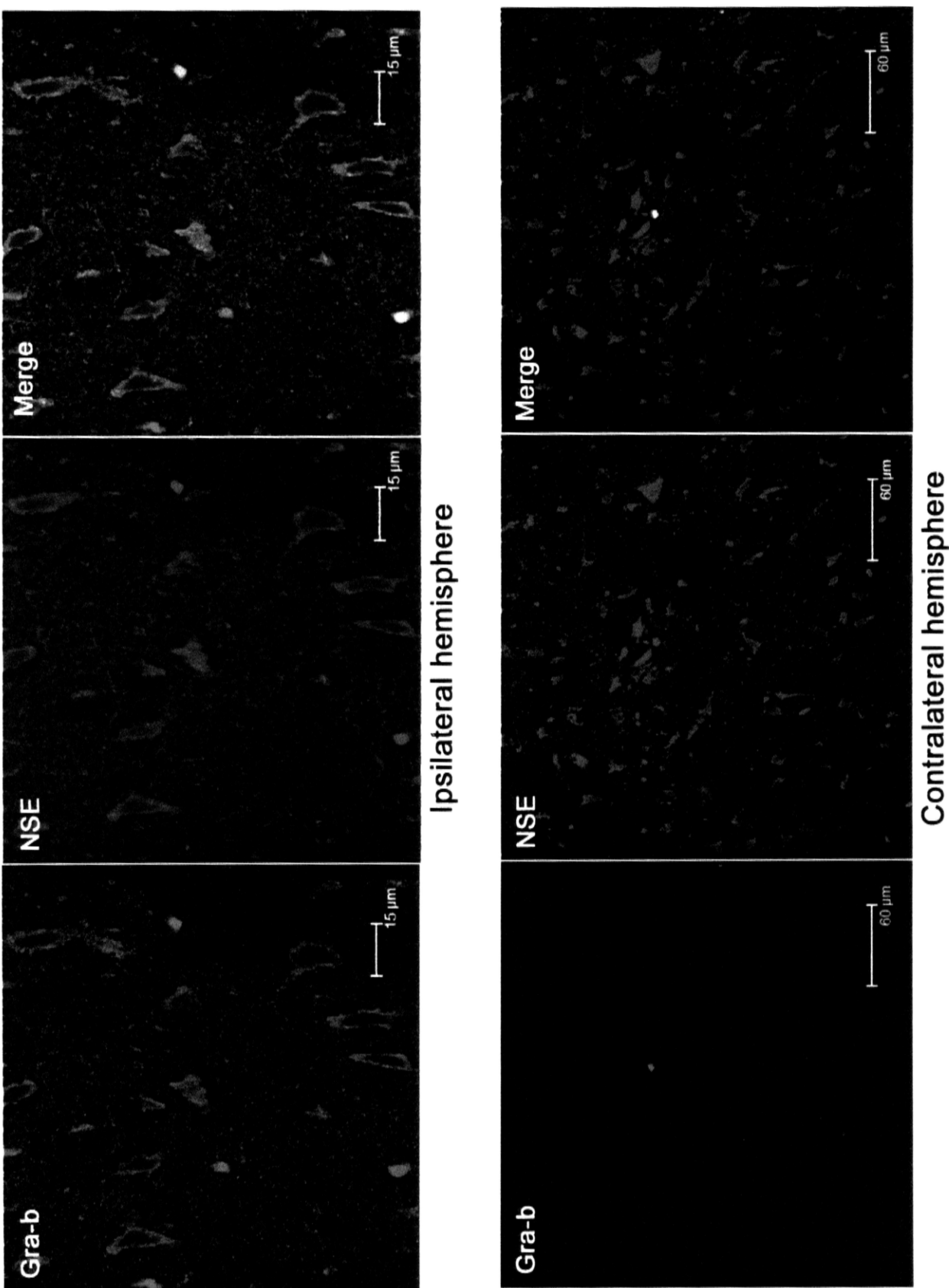
addition to 89 kDa fragment (Fig-50). The increase in the 89 kDa fragment over the 64 kDa fragment might be due to the higher affinity of caspase-3 for PARP over gra-b (Quan et al., 1996). Double immunofluorescence analysis with PARP and gra-b revealed a clear co-localization of gra-b with PARP in the ischemic infarct (Fig-51). Furthermore, co-immunoprecipitation using gra-b revealed that gra-b interacted with PARP (fig-52), Bid (Fig-53), and caspase-3 (Fig-54) in the ischemic samples.

Cleavage of HSP-70 in the ischemic infarct

Co-immunoprecipitation experiments revealed the interaction of HSP-70 with gra-b in the ischemic samples over the sham operated correlating with the breakdown of HSP-70 to 40 kDa fragment (Fig-55). Western blot analysis revealed a significant elevation in the levels of HSP-70 reaching maximal levels by 1hr and 12 hr correlating with increased levels of gra-b. Further we observed cleavage of HSP-70 to 40 kDa fragment, which was known to be the fragment liberated by the action of gra-b on HSP-70 (Fig-56). This cleavage pattern of HSP-70 was in correlation with the work done from the laboratory of Loeb et al., who showed that the 40 kDa fragment was the result of gra-b action on HSP-70 (Loeb et al., 2006).

Nuclear translocation of AIF

Western blot analysis of the nuclear fraction of ischemic and sham operated brain samples revealed a significant elevation of translocated nuclear AIF levels at 1 hr and 12 hr correlating an increase in the break down levels of HSP-70 during cerebral ischemia (Fig-57). Further immunohistochemical analysis revealed mitochondrial localization of this protein in the contralateral hemisphere, whereas its presence was largely confined to the nucleus in the ischemic region (Fig-58). Some of the cells that were undergoing cell

death evident by their nuclear morphology were seen to be positive for the nuclear presence of this protein indicating its role in mediating cell death upon translation to nucleus during cerebral ischemia.

Gra-b colocalizes with TUNEL positive cells.

Gra-b induces a caspase-independent and dependent form of cell death in the target cell after it is secreted from NK or CTLs. To establish whether gra-b positive cells were undergoing cell death, we determined gra-b immunoreactivity in the tissue sections after TUNEL labeling. Gra-b immunoreactivity was found in the same cells that contained DNA breaks as shown by Brdu-FITC fluorescence. Many gra-b positive cells (TRITC Fluorescence) were found to be TUNEL positive (FITC), indicating that gra-b was involved in mediating cell death in the ischemic hemisphere (Fig-59). Further, we observed the presence of this protein in both apoptotic and non-apoptotic cells identified by the TUNEL staining pattern in the degenerating cells. We also found a few cells that showed diffused cytosolic TUNEL staining, indicating non-apoptotic cell death (Gao et al., 2005), which also stained positive for gra-b. Cells that were undergoing cell death as shown by TUNEL positivity and gra-b positivity appeared to be neuronal.

DISCUSSION

Gra-b induces neuronal death in the infarct of ischemic rat.

Cerebral ischemia results in robust inflammatory and immune responses, which greatly contribute to the outcome. Though the precise role of these responses was under debate, it was largely accepted that acute inflammatory and immune responses pose a great threat during the pathology of cerebral ischemia. Activated CTLs infiltrating the ischemic infarct mediate cell death either in a contact dependent manner or by secreting

Fig-49: Differential cleavage of PARP by various suicidal proteases. PARP is one of the favorite substrate for various suicidal proteases. The signature fragments obtained upon cleavage by various suicidal proteases were shown in the picture.

Fig-50: Western blot analysis of PARP in ischemic rat brain. Representative blot of 3 individual western blots of PARP. A significant increase in the 89 and 64-kDa fragments was observed in ischemic samples as compared to the sham-operated samples starting from the permanent occlusion for 3 hrs until the third day of reperfusion. SI (Sham ischemic), 0I (0 hr ischemic), 1HI (1hr ischemic), 12HI (12 hr ischemic), 1DI (1 day ischemic), 3DI (3 days ischemic) reperfused ischemic ipsilateral samples, respectively, after 3 hrs of occlusion. Densitometric analysis was performed on 89 and 64-kDa fragments using NIH image analysis software.

Fig-49

Differential cleavage of PARP by various suicidal proteases

Poly ADP Ribose Polymerase (PARP)
DNA repair enzyme

Cleaved by Caspase-3 producing **89, 21 kDa** (Apoptotic) signature fragments

Cleaved by Calpain producing **45 kDa** signature fragment

Cleaved by Granzyme-b producing **72, 64 kDa** signature fragment

Cleaved by Cathepsin- b producing **50 kDa** necrotic fragment

Fig-50

Western blot analysis of PARP

← 115 kDa

← 98 kDa
— 89 kDa fragment

— 64 kDa fragment

← 51 kDa

← 37 kDa

— 21 kDa fragment

SI   0I   1HI   12HI   1DI   3DI
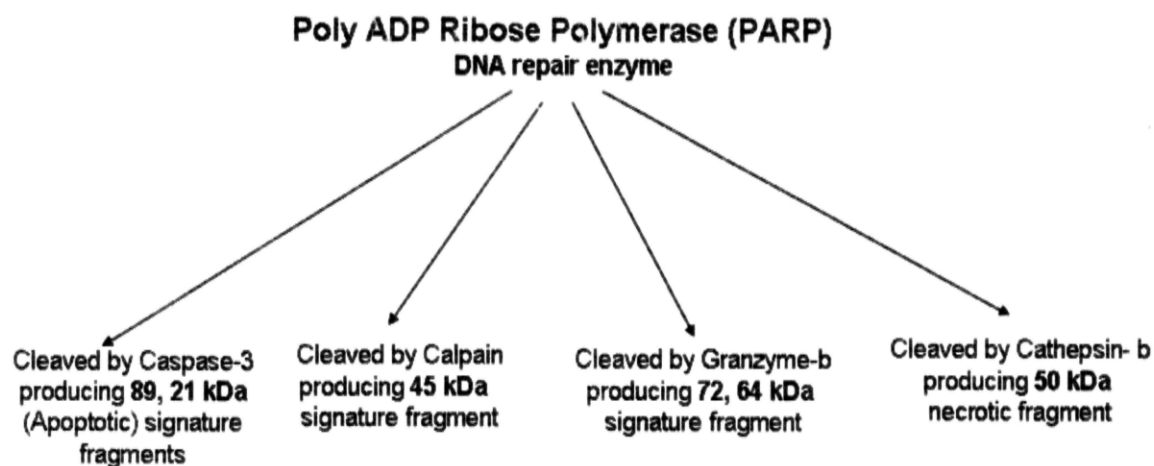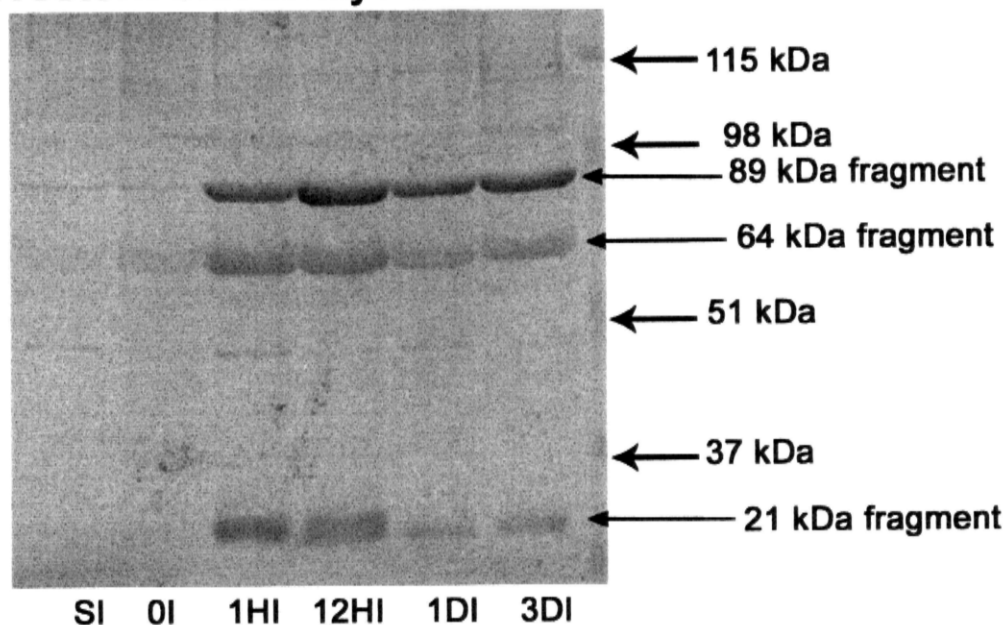
Densitometric analysis of PARP 89 and 64 kDa fragments

Ischemic brain tissue lysates

■ 89 kDa fragment
▨ 64 kDa fragment
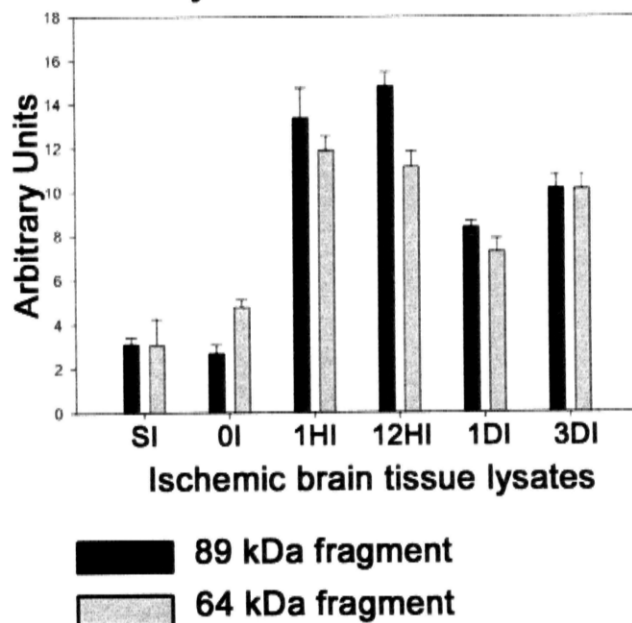
Fig-51: Double immunofluorescence analysis of PARP and gra-b. FITC was conjugated to secondary antibody specific for PARP primary antibody and TRITC was conjugated to secondary antibody specific for Gra-b. The sections were counterstained with DAPI. Immunofluorescence of PARP was depicted in green, immunofluorescence of gra-b was depicted in red, merged image showing co-localization of gra-b with PARP in ischemic infarct. We hadn't found any co-localization of gra-b with PARP in the contralateral hemisphere.

Fig-51

Double immunohistochemistry of PARP and gra-b

DAPI PARP Gra-b Merge

Contralateral hemisphere

DAPI PARP Gra-b Merge

DAPI PARP Gra-b Merge

Ipsilateral hemisphere
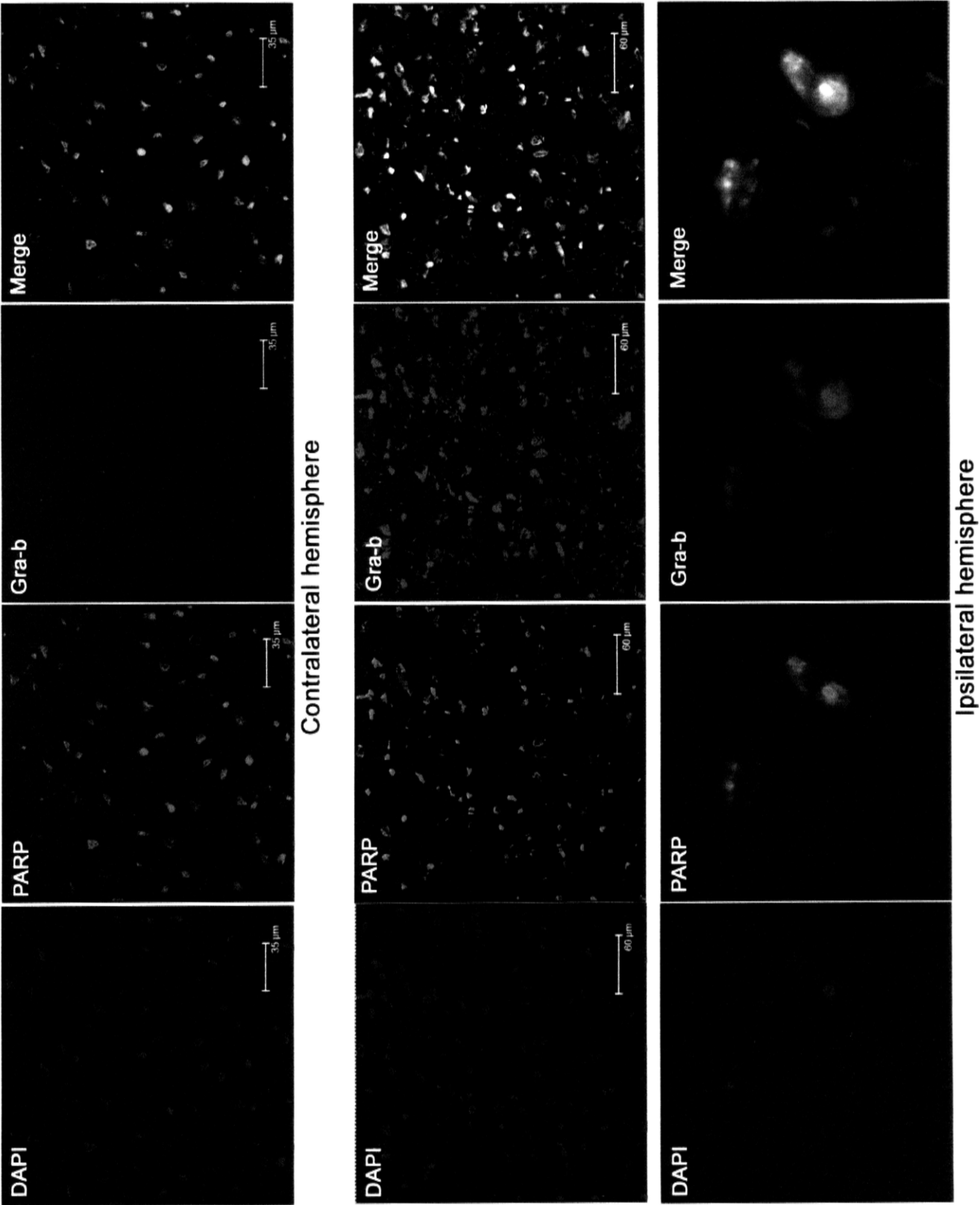
Fig-52: Co-immunoprecipitation of Bid with gra-b. Gra-b antibody was used to isolate the antibody-antigen complex and Western blot analysis was performed to identify the interacting proteins. Western blot analysis showed the presence of Bid as one of the proteins interacting with gra-b during cerebral ischemia. S) Sham-operated tissue lysate. I) Tissue lysate from 1-hour reperfused ischemic sample. TL) Whole tissue lysate without immunoprecipitation used as positive control.

Fig-53: Co-immunoprecipitation of PARP with gra-b. Gra-b antibody was used to isolate the antibody-antigen complex and Western blot analysis was performed to identify the interacting proteins. Western blot analysis showed the presence of PARP as another protein interacting with gra-b during cerebral ischemia. S) Sham-operated tissue lysate. I) Tissue lysate from 1-hour reperfused ischemic sample. TL) Whole tissue lysate without immunoprecipitation used as positive control.

Fig-54: Co-immunoprecipitation of caspase-3 with gra-b. Gra-b antibody was used to isolate the antibody-antigen complex and Western blot analysis was performed to identify the interacting proteins. Western blot analysis showed the presence of caspase-3 as another protein interacting with gra-b during cerebral ischemia. S) Sham-operated tissue lysate. I) Tissue lysate from 1-hour reperfused ischemic sample. TL) Whole tissue lysate without immunoprecipitation used as positive control.

Fig-52

Co-Immunoprecipitation of Bid with gra-b
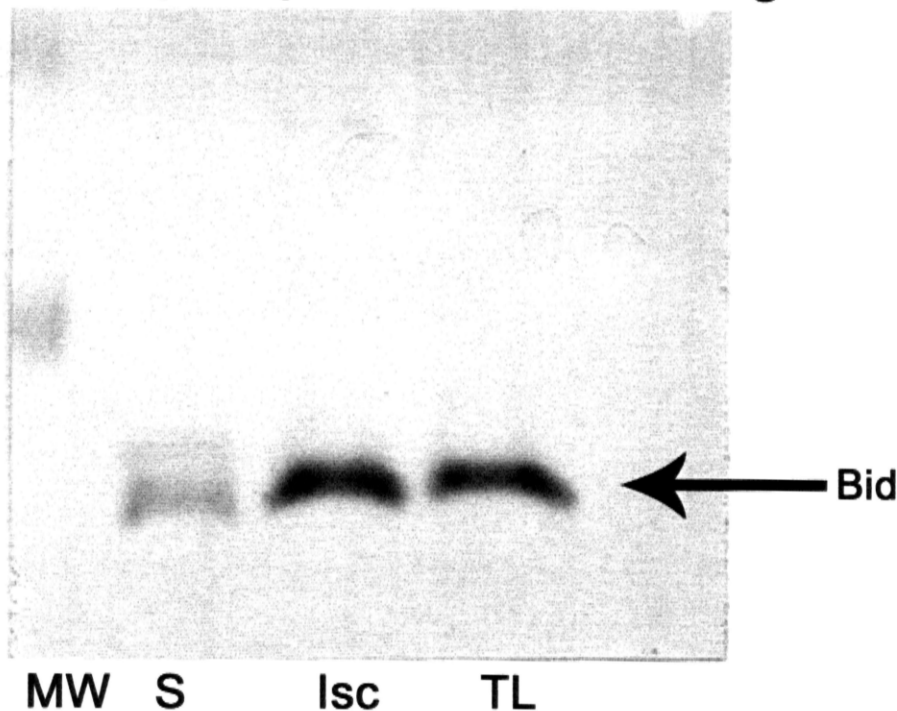
MW   S   Isc   TL

Fig- 53

Co-Immunoprecipitation of PARP with gra-b

S   Isc   TL   MW

Fig-54

Co-Immunoprecipitation of caspase-3 with gra-b

S   Isc   TL
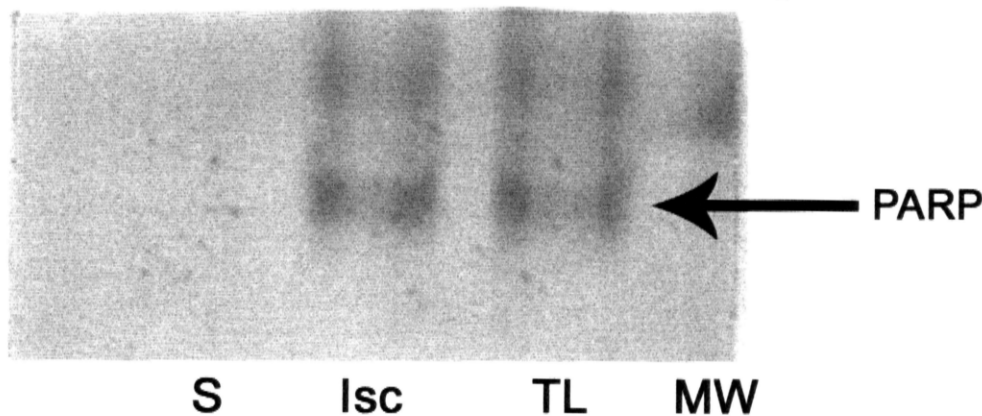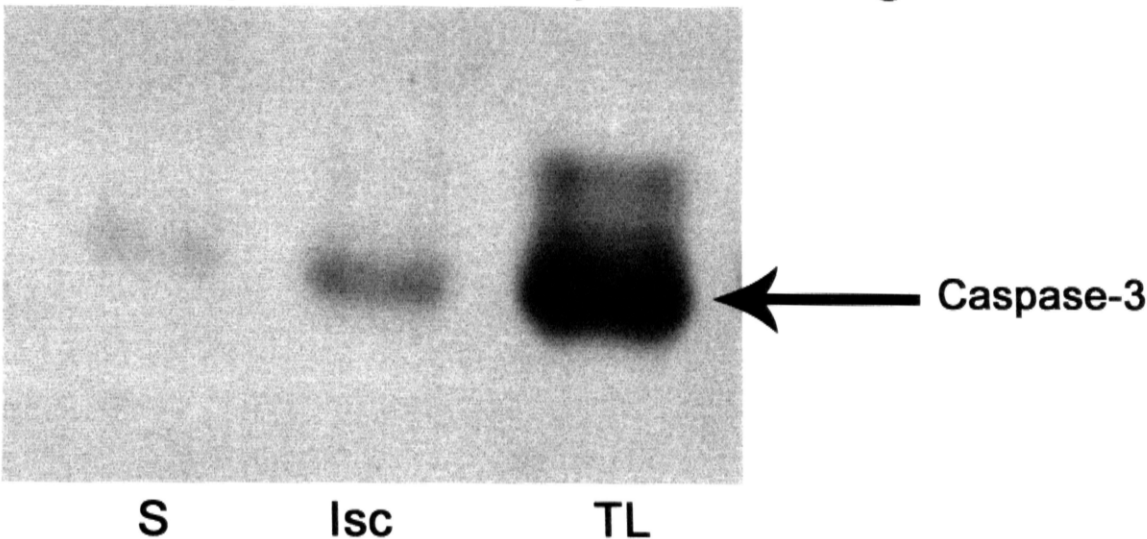
Fig-55: Co-immunoprecipitation of HSP-70 with granzyme-b. Granzyme-b antibody was used to isolate the antibody-antigen complex and western blot analysis was performed to identify the interacting proteins. Western blot analysis showed the presence of HSP-70 interacting with granzyme-b in the ipsilateral hemisphere during cerebral ischemia. S-denotes sham operated ipsilateral hemisphere, I denotes ischemic ipsilateral hemisphere, TL denotes whole tissue lysate of ipsilateral hemisphere. TL without immunoprecipitation was used as positive control.

Fig-56: Western blot analysis of HSP-70 in sham and ischemic rat brain homogenates. Representative western blot of 3 individual blots of HSP-70. Increased levels of HSP-70 was observed in the from 1 hr reperfusion time period till 3rd day of reperfusion. Further 40 kDa fragment known to be liberated by the action of granzyme-b on HSP-70 was found to be elevated from 1hr till 3rd day of reperfusion. The break down of HSP-70 correlated with the elevated levels of granzyme-b during ischemic/reperfusion conditions.

Fig-55

Co-immunoprecipitation of HSP-70 with gra-b

HSP-70
72 kDa

S   I   TL

Fig-56

Western blot analysis of HSP-70

HSP-70

40 kda
fragment

SI   0I   1HI   12HI   1DI   3DI
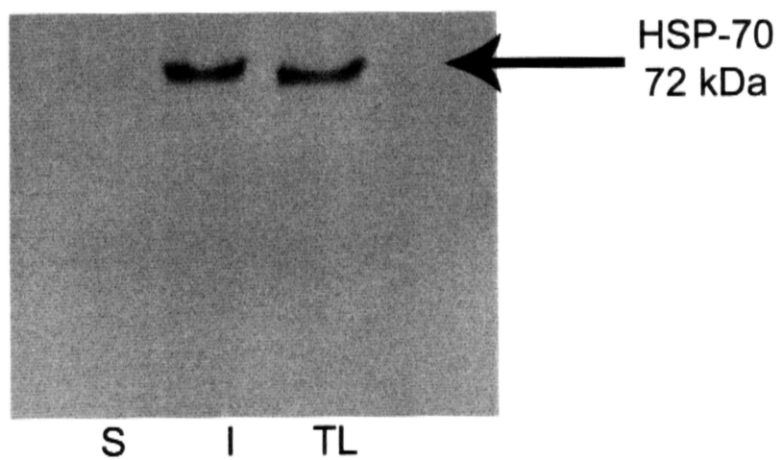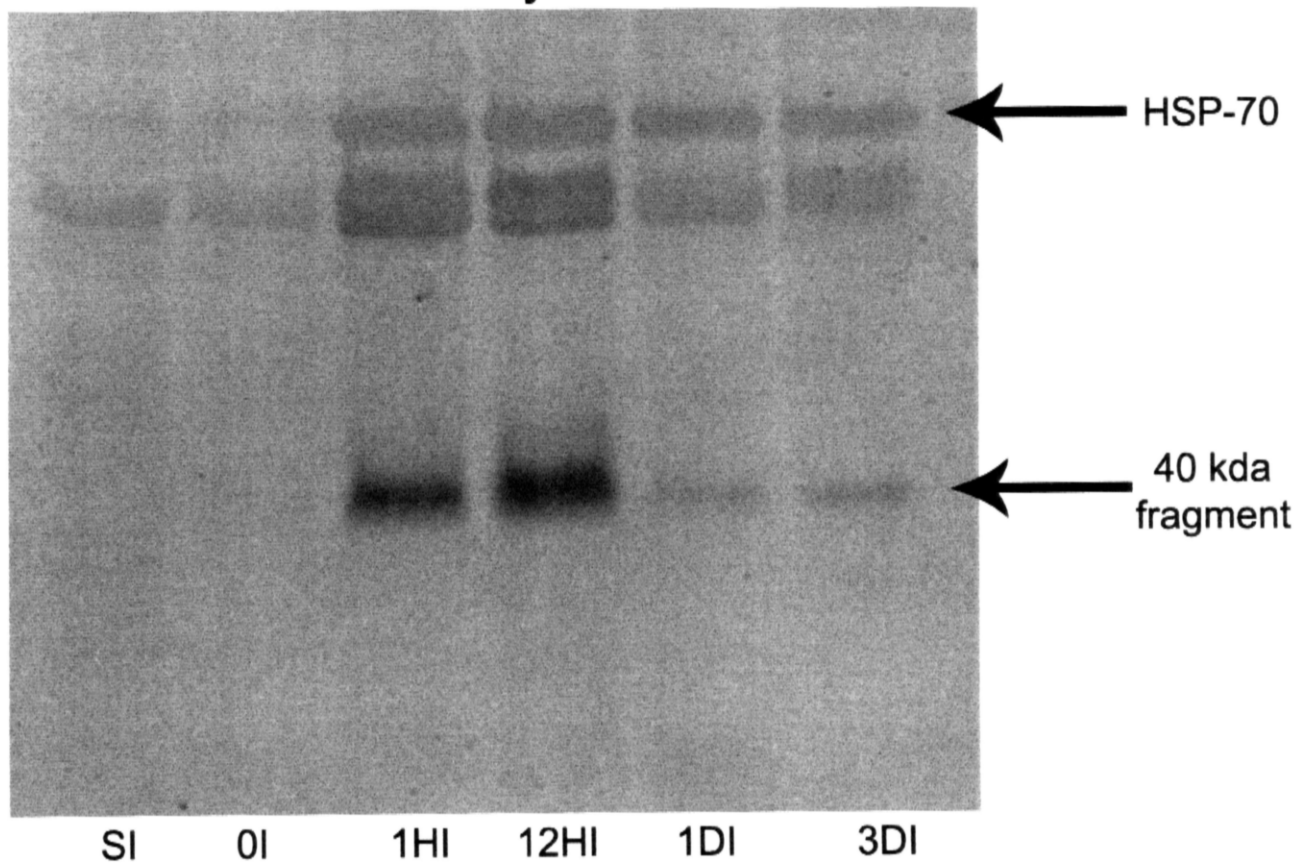
Fig-57: Western blot analysis of AIF levels in the nuclear fraction of ischemic rat brain. Representative blot of 3 individual western blots of AIF. A significant increase in the AIF level was observed in ischemic samples as compared to the sham-operated samples at 1HI (1hr ischemic), 12HI (12 hr ischemic) reperfused ischemic ipsilateral samples respectively, Densitometric analysis was performed using NIH image analysis software.

Fig-58: Immunohistochemical localization of AIF in the ischemic rat brain. A significant increase in the nuclear localization of AIF in the ipsilateral hemisphere compared to the contralateral hemisphere is observed. Arrows point to the degenerating cells, which were highly immunoreactive for nuclear AIF. Immunoreactivity was confined to the mitochondrial fraction mostly present outside to the nucleus in the contralateral hemisphere. Images were taken under a magnification of 1000x. Bright field images were taken with an Olympus UCTR30-2 fluorescent microscope.

Fig-57

Western blot analysis of Apoptosis Inducing Factor

← AIF

SI   0I   1HI   12HI   1DI   3DI

Densitometric analysis of AIF

Arbitrary Units

SI   0I   1HI   12HI   1DI   3DI
Ischemic Brain tissue lysates
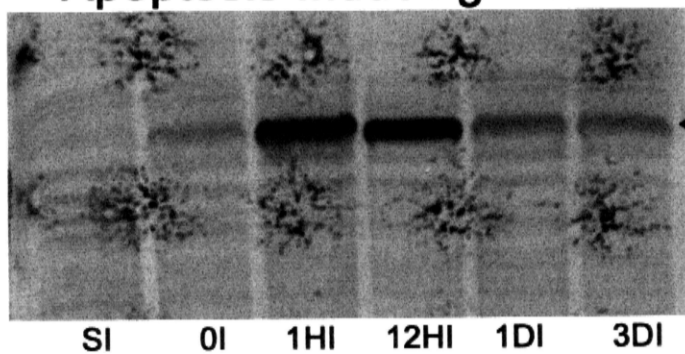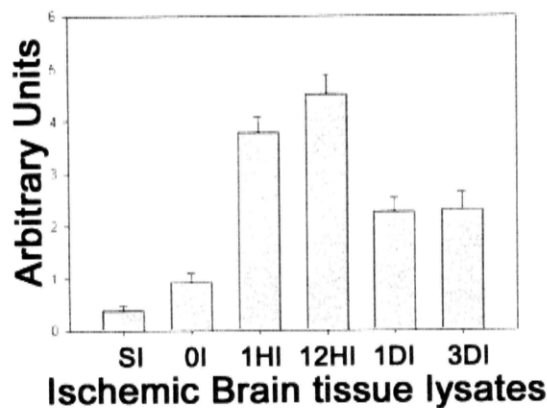
Fig- 58

Immunohistochemistry of AIF

Contralateral hemisphere 1000x
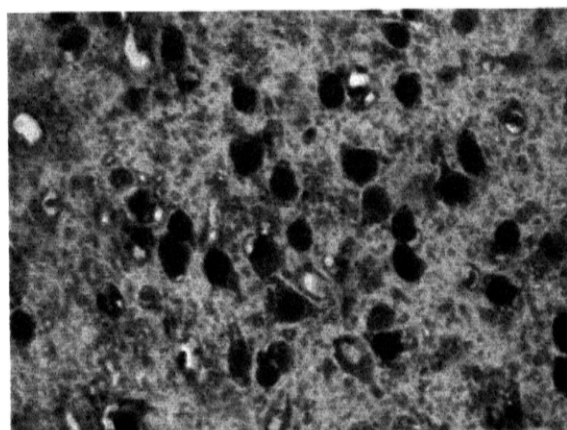
Ipsilateral heimsphere 1000x
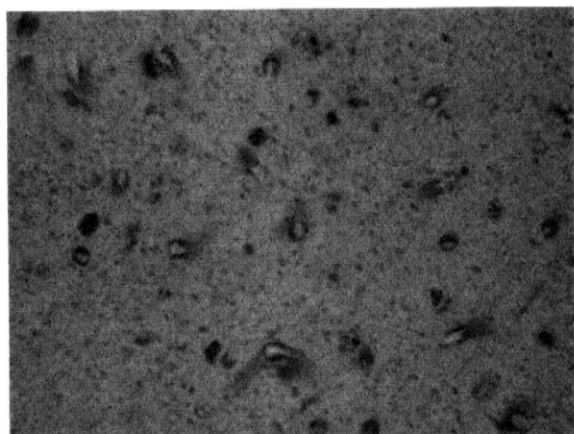
Contralateral hemisphere 1000x
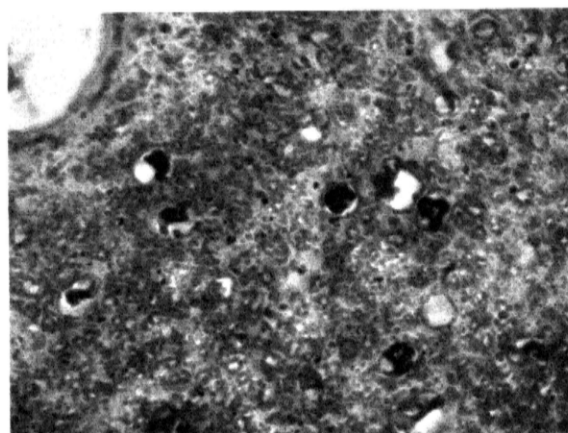
Ipsilateral heimsphere 1000x

Fig-59: Co-localization of gra-b with TUNEL. TRITC was conjugated to secondary antibody specific for gra-b primary antibody and FITC conjugated to BrdU primary antibody was obtained in Apo-Alert DNA fragmentation kit. Arrows point to TUNEL- and gra-b-positive cells undergoing apoptosis. Arrowheads point to non-apoptotic cells positive for TUNEL (diffused TUNEL staining in the cytosol). Images were taken under a Leica confocal microscope.

Fig- 59

Immunofluorescence of gra-b and TUNEL
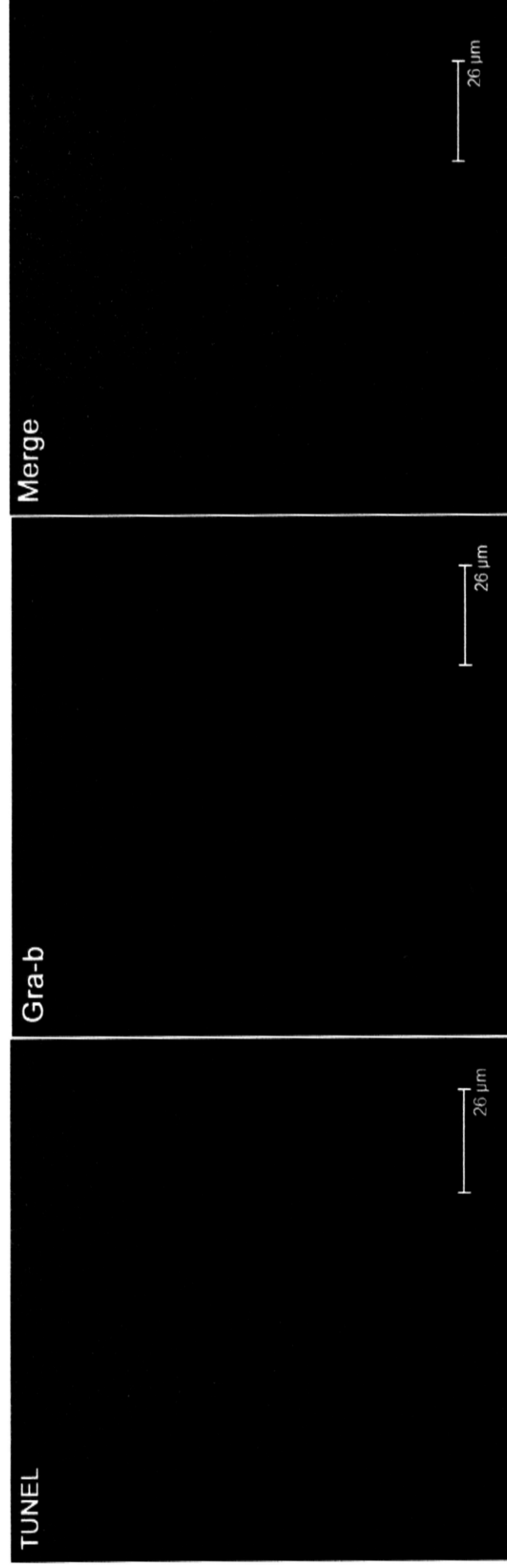
Contralateral hemisphere
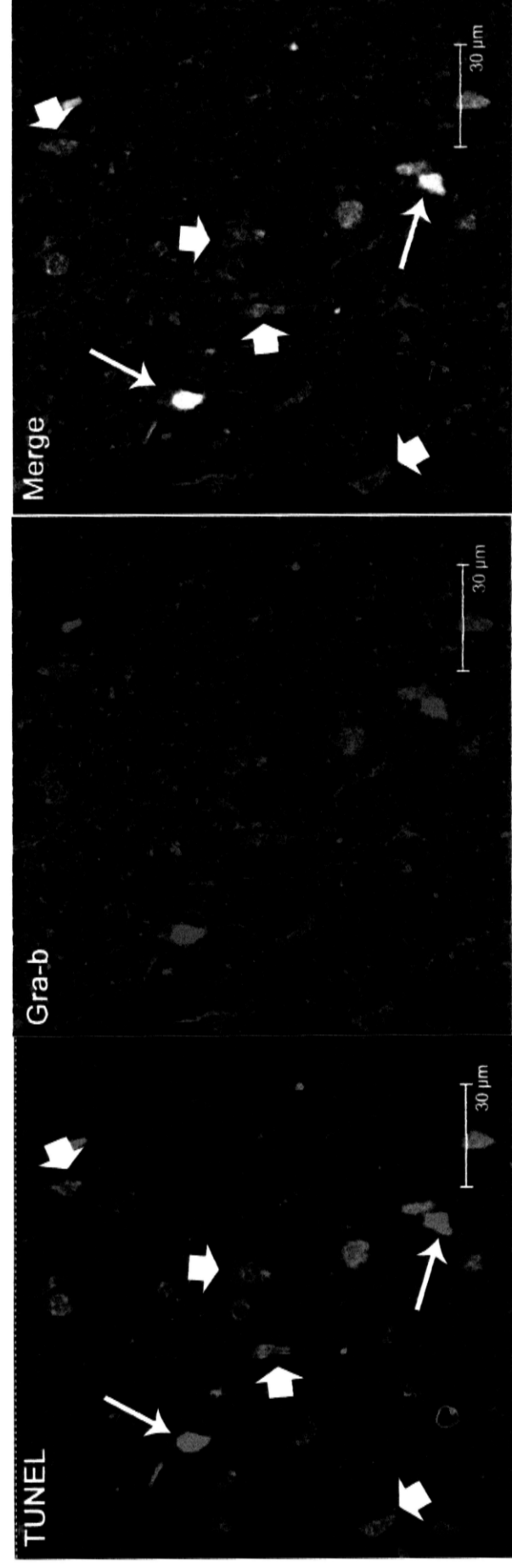
Ipsilateral hemisphere

various toxic mediators like TNF-α, Fas ligand or granzymes and perforins into the vicinity of the target cells.

Gra-b belongs to serine protease family, which is secreted by activated CTLs an NK cells (Trapani 2001). Gra-b shares similar substrate specificity with caspase-3 having the ability to cleave PARP to 72, 64 kDa signature fragments (Froelich et al., 1996), cleave Bid to tBid which translocates to mitochondria and activates intrinsic cell death pathway (Waterhouse et al., 2005), activate caspase-3 ((Metkar et al., 2003) or cleave lamins or ICAD (Enari et al., 1998). Further the ability of gra-b to mediate cell death by DNA fragmentation independent of caspase-3 makes it a crucial protease of the apoptotic cell death machinery. We observed a significant increase in the levels of gra-b from after 1 hr of reperfusion and which lasted until the 3rd day, although levels begin to decrease by the 3rd day. The observed increase in the gra-b levels correlated with the infiltration of CD-8$^+$ cells and with the increase in chemokines such as IL-2, IP-10/CXCL10, and TNF-α. A high increase in the intensity of gra–b was observed in the striatum and cortex of the ipsilateral hemisphere. Double immunofluorescence analysis showed that gra-b was localized in the nuclear and cytosolic fraction of the degenerating neurons.

Gra-b has the strongest apoptotic activity, showing caspase-like activity and the ability to activate several caspases and cleave caspase substrates such as PARP, Bid, ICAD, lamins, and HSP-70 etc., (Trapani 2001). Furthermore, gra-b induces both caspase-dependent and -independent modes of cell death (Sutton et al., 2000, Cullen and Martin 2008, Metkar et al., 2003). Gra-b can cleave Bid or directly activate caspase-3 in a caspase-dependent apoptotic cell death pathway. Though it has been shown that gra-b can induce cell death even in the absence of caspase-3, the mechanism underlying the

caspase-independent cell death pathway is not clearly understood. In vitro, the CTLs induce DNA fragmentation in the target cell much slower in gra-b deficient mice than the CTLs in wild-type littermates (Heusse et al., 1994). This study indicates that gra-b acts directly through DNA fragmentation via the caspase-independent cell death mechanism. Co-immunoprecipitation experiments revealed that gra-b interacts with PARP, Bid and caspase-3, which points towards its ability to interact with other pro-apoptotic proteins during the pathology. However, the morphology of some cells, which stained positive for TUNEL and gra-b, resembled non-apoptotic cell death because of the diffused TUNEL staining in the cytosol (Gao et al., 2005). Our results are interesting in light of the work done by Young et al, who observed that gra-b induces necrotic cell death in NK cell lymphoma (Young et al., 2007). Their results are in line with the type of cell death we observed in ischemic infarct mediated by gra-b. The increased levels of gra-b, production of 89-, and 64-kDa PARP fragments, interaction with caspase-3, and Bid indicate that a large number of proteases and their potentially synergistic cross talk are involved in the etiology of cerebral ischemia (Froelich et al., 1996, Young et al., 2007). Furthermore, neuronal death mediated by CTLs and apoptotic and non-apoptotic cell death mediated by gra-b indicate that different modes of cell death play a role in the etiology of cerebral ischemia.

The role of immune responses in cerebral ischemia is still a matter of debate. Our study suggests that CTLs and gra-b mediate deleterious effects by contributing to neuronal death during the onset of cerebral ischemia. Further, the mode of cell death mediated by gra-b becomes ambiguous due to its presence in both apoptotic and non-apoptotic cell death. This study provides the basis for investigating the modes of cell

death and for elucidating the situations that lead to the preferential activation of specific cell death paths. According to our data it is conceivable that, in addition to cell death mediated by T cells via contact-dependent mechanisms, release of gra-b by activated CTLs is also responsible for neuronal death. To the best of our knowledge this is the first report to show neuronal death to be mediated by direct contact with CTLs and by the release of gra-b, which further activates various cellular proapoptotic proteins during cerebral ischemia.

Cleavage of HSP-70 by gra-b contributes to the nuclear translocation of AIF in ischemic infarct

Of the preferred substrates of gra-b, HSP-70 stands in the front row. It has been shown by (Loeb et al., 2006) that gra-b cleaves HSP-70 to 40, 30 kDa signature fragments. We too observed similar fragmentation pattern during cerebral ischemia. Further in order to check whether gra-b interacts with HSP-70, which might lead to its fragmentation, we performed co-immunoprecipitation analysis by pulling down gra-b and checking for the association of HSP-70 by western blot analysis. We observed the interaction of gra-b with HSP-70 in the ischemic samples over the sham operated thereby mediating its cleavage during the pathology.

HSP-70 is one of the potent cell death inhibitory factors that protect cells from an array of stressful stimuli like cerebral ischemia (Zheng et al., 2007). HSP-70 over expressing HSPtg mice were shown to contain decreased infarct size over the wild type mice during cerebral ischemia and was also less susceptible for neonatal hypoxic/ischemic injury (Tsuchiya et al., 2003). The protective effect of HSP-70 is associated with the reduction of nuclear translocation of AIF (Matsumori et al., 2005).

AIF a mitochondrial protein was shown to translocate form mitochondria into the cytosol and to nucleus upon various cellular insults in a caspase independent fashion. The nuclear translocation of AIF results in large scale DNA fragmentation or chromatin condensation. It has been shown that AIF participates in chromatin condensation apart from cathepsin and ACINUS during various apoptotic or necrotic stimuli (Zamami and Kroemer 1999). However the role of HSP-70 induction in the wild type mice in mitigating nuclear translocation is of question. In the present study we are able to demonstrate that the inability of the HSP-70 despite its increased levels during cerebral ischemia in male Wistar rats to inhibit the nuclear translocation of AIF might be due to its cleavage by the secreted gra-b. We observed elevated levels of HSP-70 during the reperfusion hrs of cerebral ischemia as well as its breakdown correlating with the elevated levels of gra-b. The break down of HSP-70 by gra-b might facilitate the translocation of AIF into the nucleus thereby exerting its pathological effects. Thus the beneficial effect of HSP-70 in inhibiting the nuclear translocation of AIF might be compromised by the action of gra-b during cerebral ischemia.

Cell death in cerebral ischemia is extremely complex and is disordered, due to the involvement of large number of proteases and their cross talks. The nature of these proteases in mediating cell death individually and in synergic manner with proteases of other families makes the understanding of the molecular and biochemical events extremely difficult. Our study suggests that gra-b secreted by activated CTLs mediate deleterious effects by cleaving various anti-apoptotic mediators like HSP-70 and thus allowing the translocation of AIF into the nucleus. Further the involvement of other proteases like calpains, cathepsin, their interacting with mitochondrial membranes also

contributes to the release of AIF from mitochondrial membrane into the cytosol. Elevated levels of HSP-70 can inhibit the nuclear translocation of AIF from cytosol, however breakdown of HSP-70 by gra-b leads to the nuclear translocation of AIF thus contributing to the pathology of cerebral ischemia. This finding clearly indicates the detrimental role of gra-b contributing to ischemic damage during cerebral ischemia. The overall proposed pathway depicting the role of gra-b during cerebral ischemia is depicted in Fig-60.

Fig-60: Schematic representation of the gra-b pathway during transient focal cerebral ischemia. Based on the results obtained from the above work a path way was constructed to show gra-b mediated cell death during focal cerebral ischemia in rat. Translocation of NF-κB into the neuronal nucleus results in the elevation of various chemokines. In addition break down of blood brain barrier results in the infiltration of CTLs into the ischemic infarct. CTLs secrete granzymes and perforins into the vicinity of target cell. Gra-b enter the target cell either dependent or independent of perforins and interacts with substrates like PARP, Bid, HSp-70 and cleaves them into 64 kDa PARP fragment, active tBid, and 40 kDa HSP-70 fragment respectively. Elevation of tBid levels results in intrinsic cell death pathway. Further interaction of gra-b with caspase-3 results in the direct execution of caspase-3 mediated apoptotic cell death pathway. Cleavage of HSP-70 by gra-b facilitates the nuclear translocation of AIF resulting in caspase independent non-apoptotic cell death also.

Fig-60   Schematic representation of the proposed Granzyme b pathway
during cerebral Ischemia
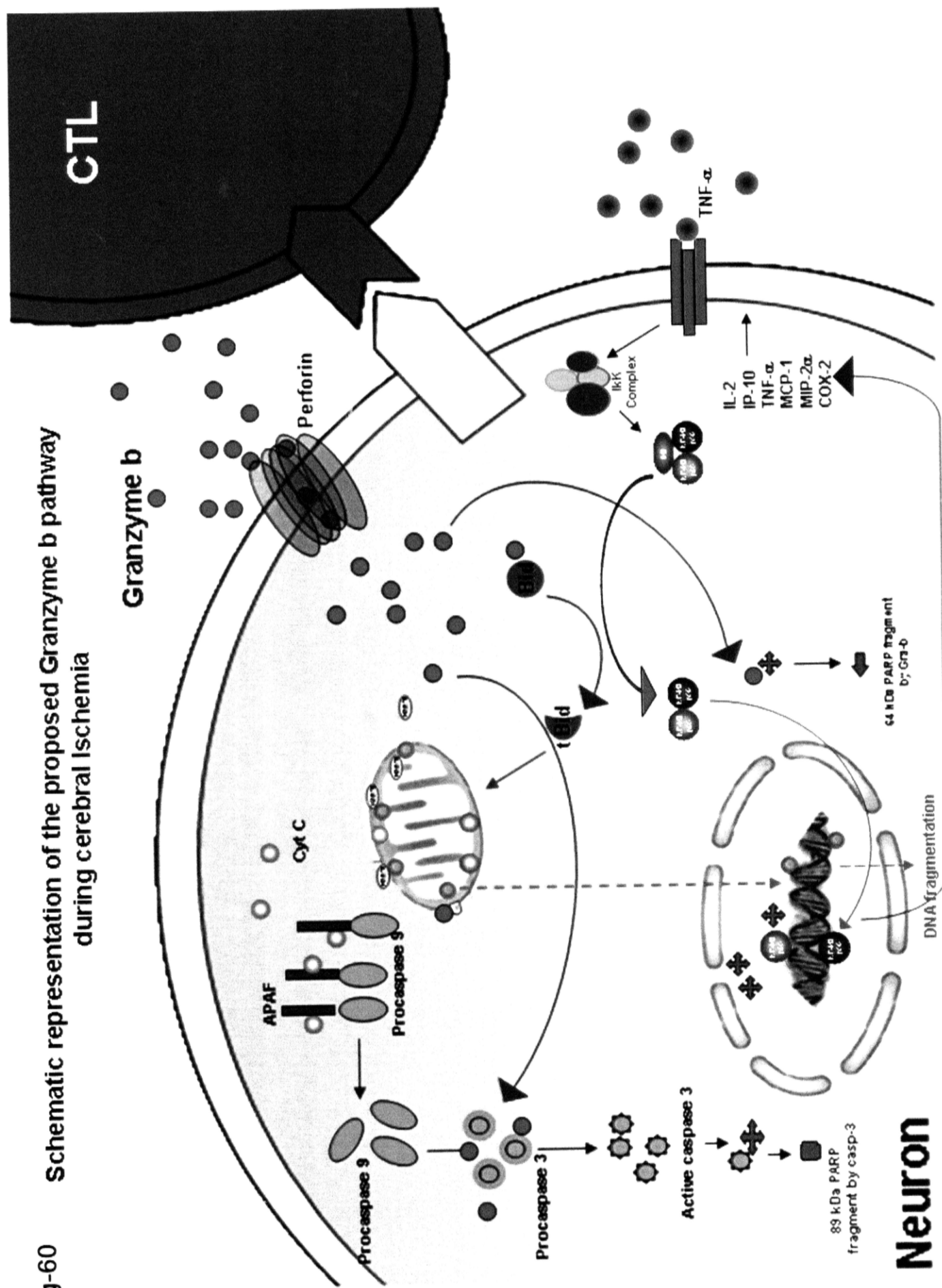
References

Aloisi F, Ria F, Adorini L. Regualation of T- Cell responses by CNS presenting cells: different roles of microglia and astrocytes. Immunol Today. 2000;21:141-147.

Babcock AA, Kuziel WA, Rivest S, Owens T. Chemokine expression by glial cells directs leukocytes to sites of axonal injury in the CNS. The Journal of Neuroscience. 2003;23:7922-7930

Baird AE. Forgotten lymphocyte. Circulation. 2006;113:2035-2036.

Bajetto A, Bonavia R, Barbero S, Schettini G, Characterization of chemokines and their receptors in the central nervous system: physiopathological implications, J. Neurochem. 2002;82:1311-29

Barkla DH, Gibson PR. The fate of epithelial cells in the human large intestine. *Pathology.* 1999;31:230–238.

Barry M, Bleackley RC. Cytotoxic T lymphocytes: all roads lead to death. Nat Rev Immunol. 2002;2:401-409.

Barry M, Heibein JA, Pinkoski MJ, Lee SF, Moyer RW, Green DR, Bleackley RC. Granzyme B short-circuits the need for caspase 8 activity during granule-mediated cytotoxic T-lymphocyte killing by directly cleaving Bid. Mol Cell Biol. 2000;20:3781-3794.

Basu S, Binder RJ, Suto R, Anderson KM, Srivastava PK. Necrotic but not apoptotic cell death releases heat shock proteins, which deliver a partial maturation signal to dendritic cells and activate the NF-kappa B pathway. Int Immunol. 2000;12:1539-1546.

Beadling CB, Smith KA. "DNA array analysis of interleukin-2-regulated immediate/early genes". Med Immunol. 2002;18:2.

Beauvillain C, Donnou S, Jarry U, Scotet M, Gascan H, Delneste Y, Guermonprez P, Jeannin P, Couez D. Neonatal and adult microglia cross-present exogenous antigens. Glia. 2008;56:69-77.

Beinke S, Ley SC. Functions of NF-kappaB1 and NF-kappaB2 in immune cell biology. Biochem J. 2004 382):393-409.

Benedek A, Moricz K, Juranyi Z, Gigler G, Levay G, Harsing LG Jr, Matyus P, Szenasi G and Albert M. Use of TTC staining for the evaluation of tissue injury in the early phases of reperfusion after focal cerebral ischemia in rats. Brain Res. 2006 ;1116:159-65.

Berthier VO, Bermond F, Flacher V, Massacrier C, Schmitt D, Peguet NJ. TNF-alpha enhances phenotypic and functional maturation of human epidermal Langerhans cells and induces IL-12 p40 and IP-10/CXCL10 production. FEBS Lett. 2005;579:3660-3668.

Bloom WM, De Bont HJ, Meijerman I, Kuppen PJ, Mulder GJ, Nagelkerke JF.Interleukin-2-activated natural killer cells can induce both apoptosis and necrosis in rat hepatocytes. Hepatology. 1999;29:785-92

Browne KA, Johnstone RW, Jans DA, Trapani JA. Filamin (280-kDa actin-binding protein) is a caspase substrate and is also cleaved directly by the cytotoxic T lymphocyte protease granzyme B during apoptosis. J Biol Chem. 2000;275:39262-39266.

Budihardjo I, Oliver H, Lutter M, Luo X, Wang X. Biochemical pathways of caspase ativation during apoptosis. Annu. Rev. Cell. Dev. Biol. 1999;15:269-290.

Cash E, Rott O. Microglial cells qualify as the stimulators of unprimed CD4+ and CD8+ T lymphocytes in the central nervous system. Clin Exp Immunol. 1994;98:313-318.

Chaitanya Vijay G, Prakash Babu P. Activation of calpain, cathepsin-b and caspase-3 during transient focal cerebral ischemia in rat model. (In Press) Neurochemical Research. 2008.

Charriaut-Marlangue C, Margaill I, Represa A, Popovici T, Plotkine M, Ben-Ari Y. Apoptosis and necrosis after reversible focal ischemia: an in situ DNA fragmentation analysis. J Cereb Blood Flow Metab. 1996;16:186–194.

Constantinescu CS, Tani M, Ransohoff RM, Wysocka M, Hilliard B, Fujioka T, Murphy S, Tighe PJ, Sarma JD, Trinchieri G, Rostami A. Astrocytes as antigen-presenting cells: expression of IL-12/IL-23. J Neurochem. 2005;95:331-340.

Cullen SP, Adrain C, Lüthi AU, Duriez PJ, Martin SJ. Human and murine granzyme B exhibit divergent substrate preferences. J Cell Biol. 2007;12:435-444.

Cullen SP, Martin SJ. Mechanisms of granule-dependent killing. Cell Death Differ. 2008; 15: 251-262.

Culmsee C, Zhu C, Landshamer S, Becattini B, Wagner E, Pellecchia M, Blomgren K, Plesnila N. Apoptosis-inducing factor triggered by poly (ADP-ribose) polymerase and Bid mediates neuronal cell death after oxygen-glucose deprivation and focal cerebral ischemia. J Neurosci. 2005;25:10262-10272.

Dai WJ, Kohler G, Brombacher F. Both innate and acquired immunity to infection are increased in IL-10-deficient mice, J. Immunol. 1997; 158:2259–2267

Denker SP, Ji S, Dingman A, Lee SY, Derugin N, Wendland MF, Vexler ZS. Macrophages are comprised of resident brain microglia not infiltrating peripheral monocytes acutely after neonatal stroke. J Neurochem. 2007;100:893-904.

Diaz A, Chepenik KP, Korn JH, Reginato AM, Jimenez SA. Differential regulation of cyclooxygenases 1 and 2 by interleukin-1 beta, tumor necrosis factor-alpha, and transforming growth factor-beta 1 in human lung fibroblasts. Exp Cell Res 1998;241:222-9.

Duckworth EA, Butler T, Collier L, Collier S, Pennypacker KR. NF-kappaB protects neurons from ischemic injury after middle cerebral artery occlusion in mice. Brain Res. 2006;1088:167-75.

Dufour H, Dziejman M, Liu MT, Leung JH, Lane TE, Luster AD. IFN-gamma-inducible protein 10 (IP-10; CXCL10)-deficient mice reveal a role for IP-10 in effector T cell generation and trafficking. J. Immunol. 2002;168:3195–3204

Ebnet K, Chluba-de Tapia J, Hurtenbach U, Kramer MD, Simon MM. In vivo primed mouse T cells selectively express T cell-specific serine proteinase-1 and the proteinase-like molecules granzyme B and C. Int Immunol. 1991;3:9-19.

Enari M, Sakahira H, Yokoyama H, Okawa K, Iwamatsu A, Nagata S. A caspase-activated DNase that degrades DNA during apoptosis, and its inhibitor ICAD. Nature. 1998;391:43-50.

Engelhardt JI. Lymphocytic infiltrates in the spinal cord in amyotrophic lateral sclerosis. Arch Neurol. 1993;50:30-36.

Fabry Z, Raine CS, Hart MN. Nervous tissue as an immune compartment: the dialect of the immune responses in CNS. Immunol today. 1994;15:218-224.

Fadok VA, Voelker DR, Campbell PA, Cohen JJ, Bratton DL, Henson PM. Exposure of phosphotidyl serine on the surface of apoptotic lymphocytes triggers specific recognition and removal by macrophages. J. Immunol. 1992;148:2207-2216.

Falsig J, Porzgen P, Lund S, Schrattenholz A, Leist M. The inflammatory transcriptome of reactive murine astrocytes and implications for their innate immune function. J Neurochem. 2006;96:893-907

Fillit H, Ding WH, Buee L, Kalman J, Altstiel L, Lawlor B, Wolf-Klein G. Elevated circulating tumor necrosis factor levels in Alzheimer's disease. Neurosci. Lett. 1991;129: 318–320

Froelich CJ, Hanna WL, Poirier GG, Duriez PJ, Amours DD, Salvesen GS, Alnemri ES, Earnshaw WC, Shah GM. Granzyme B/perforin-mediated apoptosis of Jurkat cells results in cleavage of poly (ADP-ribose) polymerase to the 89-kDa apoptotic fragment and less abundant 64-kDa fragment. Biochem Biophys Res Commun. 1996;23:658-65.

Gao Y, Signore AP, Yin W, Cao G, Yin XM, Sun F, Luo Y, Graham SH, Chen J. Neuroprotection against focal ischemic brain injury by inhibition of c-Jun N-terminal kinase and attenuation of the mitochondrial apoptosis-signaling pathway. J Cereb Blood Flow Metab. 2005;25:694-712.

Garcia-Sanz JA, MacDonald HR, Jenne DE, Tschopp J, Nabholz M. Cell specificity of granzyme gene expression. J Immunol. 1990;145:3111-3118.

Gardiner CM, Reen DJ. Differential cytokine regulation of natural killer cell-mediated necrotic and apoptotic cytotoxicity.Immunology. 1998;93:511-517.

Ghosh S, Karin M. Missing pieces in the NF-kappaB puzzle. M. Cell. 2002, 109 Supp:S81-96

Giffard, RG, Xu L, Zhao H, Carrico W, Ouyang Y, Qiao Y, Sapolsky R, Steinberg G, Hu B, Yenari MA. Chaperones, protein aggregation, and brain protection from hypoxic/ischemic injury. J Exp Biol. 2004;207:3213-3220.

Giulian D, Corpuz M, Chapman S, Mansouri M, Robertson C. Reactive mononuclear phagocytes release neurotoxins after ischemic and traumatic injury to the central nervous system. J. Neurosci. Res. 1993;36:681–693

Giuliani F, Goodyer CG, Antel JP, Yong VW. Vulnerability of human neurons to T- cell mediated cytotoxicity. J of Immunol. 2003;171:368-379.

Gobeil, S., Boucher, C.C., Nadeau, D., Poirier, G.G. Characterization of the necrotic cleavage of poly(ADP-ribose) polymerase (PARP-1): implication of lysosomal proteases. Cell Death Differ. 2001;8:588-94.

Goppelt-Struebe M, Rehm M, Schaefers HJ. Induction of cyclooxygenase-2 by platelet-derived growth factor (PDGF) and its inhibition by dexamethasone are independent of NF-kappaB/IkappaB transcription factors. Naunyn Schmiedebergs Arch Pharmacol

2000;361:636-45.

Hakim AM. The cerebral ischemic penumbra. Can J Neurol Sci. 1987;14:557-559.

Haunstetter A and Izumo S. Apoptosis: basic mechanisms and implications for cardiovascular disease. Circ Res. 1998;82:111–1129.

Heusse JW, Wesselschmidt RL, Shresta S, Russel JH, Ley TJ. Cytotoxic lymphocytes require granzyme-b for the rapid induction of DNA fragmentation and apoptosis in allergenic target cells. Cell. 1994;76:977-987.

Isabelle M, Marianne Martinic A, Hartmut Wekerle, Harald Neumann. Transection of Major Histocompatibility Complex Class I-Induced Neurites by Cytotoxic T Lymphocytes. American Journal of Pathology. 2001;159:809-815.

Isabelle MM, Gallimore A, Oxenius A, Martinic MM, Wekerle H, Neumann H. MHC class I restricted killing of neurons by virus specific CD8+ T lymphocytes is effected through Fas/Fas-L but not perforin pathway. Eur J Immunol. 2000;30:3623-3633.

Ishimaru N, Kishimoto H, Hayashi Y, Sprent J. Regulation of naive T cell function by the NF-kappaB2 pathway. Nat Immunol. 2006 7:763-772.

Jacobson MD, Weil M, Raff MC. Programmed cell death in animal development. Cell. 1997;88:347-354.

Janas ML, Groves P, Kienzle N, Kelso A. IL-2 regulates perforin and granzyme gene expression in CD8+ T cells independently of its effects on survival and proliferation. J Immunol. 2005;175:8003-8010.

Jane FA, Ning Q, Edra SL, Krister K, Miles H. Induced neuronal expression of class I major histocompatibility complex mRNA in acute and chronic inflammation models. Journal of Neuroimmunology. 2002;131:83-91.

Jenne DE, Tschopp J. Granzymes, a family of serine proteases released from granules of cytolytic T lymphocytes upon T cell receptor stimulation. Immunol Rev. 1988;103:53-71.

Kato H, Kogure K, Liu XH, Araki T, Itoyama Y. Progressive expression of immuno-molecules on activated microglia and invading leukocytes following focal cerebral ischemia in the rat. Brain Res. 1996;23:203-212.

Kato M, Nonaka T, Maki M, Kikuchi H and Imajoh-Ohmi S. Caspases cleaves the amino-terminal calpain inhibitory unit of calpastatin during apoptosis in human jurkat T cells.J. Biochem. 2000;127:297–305.

Kerr JF, Wylie AH, Currie AR. Apotosis: a basic biological phenomenon with wide ranging implications in tissue kinetics. Br. J. Cancer. 1972;26:239-257.

Kleinschnitz C, Bendszus M, Frank M, Solymosi L, Toyka KV, Stoll G. In vivo monitoring of macrophage infiltration in experimental brain lesion by MRI. J cereb blood flow and metab. 2003;23:1356-1361.

Kluck RM, Esposti MD, Perkins G, Renken C, Kuwana T, Bossy-Wetzel E, Goldberg M, Allen T, Barber MJ, Green DR, Newmeyer DD. The pro-apoptotic proteins, Bid and Bax, cause a limited permeabilization of the mitochondrial outer membrane that is enhanced by cytosol. J. Cell Biol. 1999;147:809-822.

Kriz J. Inflammation in ischemia brain injury: timing is important. Crit Rev Neurocrit Care. 2006;18:145-157.

Kumiko S, Shigenobu T, Timothy JK, Masato E, Hideki S, Carol AC, Françoise D, Luis MM, Shigekazu N, Scott HK, William CE. Transition from Caspase-dependent to Caspase-independent Mechanisms at the Onset of Apoptotic Execution. J. Cell Biol. 1998;143:225-239.

Kuwana T, Mackey MR, Perkins G, Ellisman MH, Latterich M, Schneiter R, Green DR, Newmeyer DD. Bid, Bax, and lipids cooperate to form supramolecular openings in the outer mitochondrial membrane. Cell. 2002;111:331-342.

Laouini D, Elkhal A, Yalcindag A, Kawamoto S, Oettgen H, Geha RS. COX-2 inhibition enhances the TH2 immune response to epicutaneous sensitization. J Allergy Clin Immunol. 2005;116:390-396

Liu CC, Jiang S, Persechini PM, Zychlinsky A, Kaufmann Y, Young JD. Resistance of cytolytic lymphocytes to perforin-mediated killing. Induction of resistance correlates with increase in cytotoxicity. J Exp Med. 1989;169:2211-2225.

Loeb CR, Harris JL, Craik CS. Granzyme B proteolyzes receptors important to proliferation and survival, tipping the balance toward apoptosis. J Biol Chem. 2006;281:28326-28335.

Lomgren K, Zhu C, Wang X, Karlsson JO, Leverin AL, Bahr BA, Mallard C and Hagberg H. synergistic activation of caspase-3 by m-calpain after neonatal hypoxia-ischemia: A mechanism of "pathologic apoptosis". J. Biol. Chem. 2001;276:10191–10198.

Longa EZ, Weinstein PR, Carlson S and Cummins R. Reversible middle cerebral artery occlusion without craniectomy in rats. Stroke. 1989;20:84-91.

Majno G, Joris I. Apoptosis, oncosis and necrosis. An overview of cell death. Am J Pathol. 1995;146:3-15

Marta Artal-sanz., Chrysanthi Samara, Popi Syntichki and Nektarios Tavernarakis 2006. Lysosomal biogenesis and function is critical for necrotic cell death in Caenorhabditis elegans. The journal of Cell Biology 173:231-239.

Masabumi M, Takahiro K, Masamichi S. Brain cytokines and chemokines: roles in ischemia injury and pain. J Pharmacol Sci. 2006;100:461-470.

Matsumori Y, Hong SM, Aoyama K, Fan Y, Kayama T, Sheldon RA, Vexler ZS, Ferriero DM, Weinstein PR, Liu J. Hsp70 overexpression sequesters AIF and reduces neonatal hypoxic/ischemic brain injury. J Cereb Blood Flow Metab. 2005;25:899-910.

May MJ, Ghosh S. Signal transduction through NF-kB. Immunol. Today. 1998;19: 80-88.

Mayer MP, Bukau B. Hsp70 chaperones: cellular functions and molecular mechanism. Cell Mol Life Sci. 2005;62:670-684.

Mc Conkey DJ. Biochemical determinants of apoptosis and necrosis. Toxicol Lett 1998;99:157–168.

Mc Tigue DM, Tani M, Krivacic K, Chernosky A, Kelner GS, Maciejewski D, Maki R, Ransohoff RM, Stokes BT. Selective chemokine mRNA accumulation in the rat spinal cord after contusion injury, J. Neurosci. Res.1998;53:368–376

McGuire MJ, Lipsky PE, Thiele DL. Generation of active myeloid and lymphoid granule serine proteases requires processing by the granule thiol protease dipeptidyl peptidase I. J Biol Chem. 1993;268:2458-2467.

McMahon EJ, Bailey SL, Miller SD. CNS dendritic cells: critical participants in CNS inflammation? Neurochem Int. 2006;49:195-203

Merrill JE. Proinflammatory and anti-inflammatory cytokines in multiple sclerosis and central nervous system acquired immunodeficiency syndrome. J. Immunother. 1992;12: 167–170

Metkar SS, Wang B, Ebbs ML, Kim JH, Lee YJ, Raja SM, Froelich CJ. Granzyme B activates procaspase-3 which signals a mitochondrial amplification loop for maximal

apoptosis. J Cell Biol. 2003;160:875-885.

Michael JM, You-Sun K, Zheng GL. TNF-α and reactive oxygen species in necrotic cell death. Cell Research 2008;18:343-349.

Morgan MJ, Kim YS, Liu ZG. TNF and reactive oxygen species in necrotic cell death. Cell Res. 2008;18:343-9.

Moroni F, Meli E, Peruginelli F, Chiarugi A, Cozzi A, Picca R, Romagnoli P, Pellicciari R, Pellegrini-Giampietro DE. Poly(ADP-ribose) polymerase inhibitors attenuate necrotic but not apoptotic neuronal death in experimental models of cerebral ischemia. Cell Death Differ. 2001;8:921-932.

Moubarak RS, Yuste VJ, Artus C, Bouharrour A, Greer PA, Menissier-de Murcia J, Susin SA. Sequential activation of poly(ADP-ribose) polymerase 1, calpains, and Bax is essential in apoptosis-inducing factor-mediated programmed necrosis. Mol Cell Biol. 2007;27:4844-4862.

Zamzami N, Kroemer G. Condensed matter in cell death. Nature 1999; 401:127-128.

Neumann H, Medana IM, Bauer J, Lassmann H. Cytotoxic T Lymphocytes in autotimmune and degenerative CNS diseases. Trends in Neurosci. 2002;25:313-319.

Nicotera Peirluigi, Marcel leist, Elisa Ferrando-may Intracellular ATP, a switch in the decision between apoptosis and necrosis. Toxicol lett. 1998;102-103:139-142.

Nijboer CH, Heijnen CJ, Groenendaal F, May MJ, van Bel F, Kavelaars A. A Dual Role of the NF {kappa}B Pathway in Neonatal Hypoxic-Ischemic Brain Damage. Stroke. 2008;17. [Epub ahead of print]

Nitsch Robert, Elena PE, Alina Smorodchenko, Carmen ID, Orhan Aktas, Frauke Zipp. Direct impact of T cells on neurons revealed by two-photon microscopy in living brain tissue. J Neurosci. 2004;24:2458-2464

O'Neill LA, Kaltschmidt C. NF-kB: a crucial transcription factor for glial and neuronal cell function. Trends Neurosci. 1997;20:252-258

Patricia HD, Sandhya S, Susan PM, Michael AE,Laurie KJ, Arthur VA, Halina OT. B cell deficient mice with experimental stroke have reduced lesion size and inflammation. J Cereb Blood Flow Metab. 2007;27:1798-1805

Pimentel-Muinaos FX, Munaoz-Fernaandez MA, Fresno M. Control of T lymphocyte activation and interleukin 2 receptor expression by endogenously secreted lymphokines.

J. Immunol. 1994;152:5714-5722.

Pinkoski MJ, Waterhouse NJ, Heibein JA, Wolf BB, Kuwana T, Goldstein JC, Newmeyer DD, Bleackley RC, Green DR. Granzyme B-mediated apoptosis proceeds predominantly through a Bcl-2-inhibitable mitochondrial pathway. J Biol Chem. 2001;276:12060-12067.

Popovich PG, Stuckman S, Gienapp IE, Whitacre CC. Alterations in immune cell phenotype and function after experimental spinal cord injury. J.Neurotrauma. 2001;18: 957–966.

Quan LT, Tewari M, O'Rourke K, Dixit V, Snipas SJ, Poirier GG, Ray C, Pickup DJ, Salvesen GS. Proteolytic activation of the cell death protease Yama/ CPP32 by granzyme B. Proc Natl Acad Sci U.S.A. 1996;93:1972-1976.

Radons J, Multhoff G. Immunostimulatory functions of membrane-bound and exported heat shock protein 70. Exerc Immunol Rev. 2005;11:17-33

Rami A. Ischemic neuronal death in the rat hippocampus: the calpain-calpastatin-caspase hypothesis. Neurobiology of Disease. 2003;13:75-88.

Rensing-Ehl A, Malipiero U, Irmler M, Tschopp J, Constam D, Fontana A. Neurons induced to express MHC complex I are killed via the perforin and not the Fas-L (Apo-1/CD95) pathway. Eur J Immunol. 1996;26:2271-2274.

Robinson Agramonte M, Dorta-Contreras AJ, Lorigados Pedre L. Immune events in central nervous system of early and late onset Alzheimers disease patients Rev.neurol. 2001;32:901-904

Sahara S, Aoto M, Eguchi Y, Imamoto N, Yoneda Y, Tsujimoto Y. Acinus is a caspase-3-activated protein required for apoptotic chromatin condensation. Nature. 1999;401:168-173.

Sapolsky RM, Trafton J and Tombaugh GC. Excitotoxic neuron death, acidotic endangerment, and the paradox of acidotic protection. Adv. Neurol. 1996;71:237–244.

Schroeter M, Jander S, Witte OW, Stoll G. Local immune responses in the rat middle cerebral artery occlusion. J Neuroimmunology. 1994;55:195-203

Sergey YP, Anatoli GK, Vladimir LG. Necrosis: a specific form of cell death? Experimental Cell Research. 2003;283:1-16.

Sergey YP, Anatoli GK, Vladimir LG. Necrosis: a specific form of programmed cell

death? Exp Cell Res.2003;283:1-16

Sha WC. Regulation of Immune Responses by NF-kappa B/Rel Transcription Factors. J. Exp. Med. 1998;187:143-146

Shacter E, Williams JA, Hinson RM, Senturker S, Lee YJ,.Oxidative stress interferes with cancer chemotherapy: inhibition of lymphoma cell apoptosis and phagocytosis. Blood 2000;96:307-313

Sharif-Askari E, Alam A, Rhéaume E, Beresford PJ, Scotto C, Sharma K, Lee D, DeWolf WE, Nuttall ME, Lieberman J, Sékaly RP. Direct cleavage of the human DNA fragmentation factor-45 by granzyme B induces caspase-activated DNase release and DNA fragmentation. EMBO J. 2001;20:3101-3113.

Slee EA, Harte MT, Kluck RM, Wolf BB, Casiano CA, Newmeyer DD, Wang HG, Reed JC, Nicholson DW, Alnemri ES, Green DR, Martin SJ. Ordering the cytochrome c-initiated caspase cascade: hierarchical activation of caspases-2, -3, -6, -7, -8, and -10 in a caspase-9-dependent manner. J Cell Biol. 1999;144:281-292.

Soren B, Steven CL. Functions of NF-kB1 and NF-kB2 in immune cell biology. Biochem. J. 2004;382:393-409.

Stefan JR, Yigong S. Molecular mechanisms of caspase regulation during apoptosis. Nature Reviews, Molecular Cell Biology. 2004;5:897-907.

Stoll G. Inflammatory cytokines in the nervous system: Multi functional mediators in the autoimmunity and cerebra ischemia. Rev Neurol. 2002;158:887-891.

Sun DY, Jiang S, Zeng LM, Ojcius DM, Ding E, Young J. Separate metabolic pathways leading to DNA fragmentation and apoptopic chromatin chromatin condensation. J. Exp. Med.1994; 179: 559–568.

Susin SA, Lorenzo HK, Zamzami N, Marzo I, Snow BE, Brothers GM, Mangion J, Jacotot E, Costantini P, Loeffler M, Larochette N, Goodlett DR, Aebersold R, Siderovski DP, Penninger JM, Kroemer G. Molecular characterization of mitochondrial apoptosis-inducing factor. Nature. 1999;397:441-446.

Sutton VR, Davis JE, Cancilla M, Johnstone RW, Ruefli AA, Sedelies K, Browne KA, Trapani JA. Initiation of apoptosis by granzyme B requires direct cleavage of bid, but not direct granzyme B-mediated caspase activation. J Exp Med. 2000;192:1403-1414.

Syntichaki P and Tavernarakis N. The biochemistry of neuronal necrosis: rogue biology?

Nat. Rev. Neurosci. 2003;4:672–684.

Syntichaki P, Samara C and Tavernarakis N. The vacuolar H+ ATPase mediates intracellular acidification required for neurodegeneration in C.elegans.Curr.Biol. 2005;15:1249-1254.

Syntichaki Popi and Nektarios Tavernarakis. Death by necrosis: Uncontrollable catastrophe, or is there order behind the chaos. 2002;3:604-609.

Tanuma N, Sakuma H, Sasaki A, Matsumoto Y. Chemokine expression by astrocytes plays a role in microglia/macrophage activation and subsequent neurodegeneration in secondary progressive multiple sclerosis. Acta Neuropathol. 2006;112:195-204.

Thomas DA, Du C, Xu M, Wang X, Ley TJ. DFF45/ICAD can be directly processed by granzyme B during the induction of apoptosis. Immunity. 2000;12:621-632.

Torriglia A, Paolo P, Jean YB, Elisabeth C, Jacques T, Yves C, Marie-France C. L-DNase II, a Molecule That Links Proteases and Endonucleases in Apoptosis, Derives from the Ubiquitous Serpin Leukocyte Elastase Inhibitor. Mol Cell Biol. 1998;18:3612-3619.

Trapani JA, Smyth MJ. Functional significance of the perforin/granzyme cell death pathway. Nat Rev Immunol. 2002;2:735-747.

Trapani JA. Granzymes: a family of lymphocyte granule serine proteases. Genome Biol. 2001;2:3014.1-3014.7.

Tsuchiya D, Hong S, Matsumori Y, Shiina H, Kayama T, Swanson RA, Dillman H, Liu J, Scott PS, Wienstein PROver expression of rat heat shock protein 70 is associated with reduction of early mitochondrial cytochrome c release and subsequent DNA fragmentation after permanent focal ischemia. J Cereb Blood Flow and Metab. 2003;23:718-727.

Vancompernolle K, Van Herreweghe F, Pynaert G, Van de Craen M, De Vos K, Totty N, Sterling A, Fiers W, Vandenabeele P, Grooten J. Atractyloside-induced release of cathepsin B, a protease with caspase-processing activity. FEBS Lett. 1998;6:150-158.

Vercammen D, Brouckaert G, Denecker G, Van de Craen M, Declercq W, Fiers W, Vandenabeele P. Dual signaling of Fas receptor: initiation of both apoptotic and necrotic cell death pathways. J Exp Med 1998;188:919-930.

Wallach, D. TNF: a decade of accumulated knowledge and emerging answers. Eur.

Cytokine Netw. 1996;7:713-724.

Wang H, Shimoji M, Yu SW, Dawson TM, Dawson VL Apoptosis inducing factor and PARP-mediated injury in the MPTP mouse model of Parkinson's disease. Ann NY Acad Sci. 2003;991:132-139.

Wang KK. Calpain and caspase: can you tell the difference? Trends Neurosci. 2000;23:20-26.

Waterhouse NJ, Sedelies KA, Browne KA, Wowk ME, Newbold A, Sutton VR, Clarke CJ, Oliaro J, Lindemann RK, Bird PI, Johnstone RW, Trapani JA. A central role for Bid in granzyme B-induced apoptosis. J Biol Chem. 2005;280:4476-4482.

Wise RJ, Rhodes CG, Gibbs JM, Disturbance of oxidative metabolism of glucose in recent human cerebral infarcts. Ann Neurol. 1983;14:627-637.

Xiuli Liu, Terry Van Vleet and Rick G Schnellmann. The role of Calpain in oncotic cell death. Annu.Rev.Pharmacol.Toxicol. 2004;44:349-370.

Yamashima T, Tonchev AB, Tsukada T, Saido TC, Imajoh-Ohmi S, Momoi T and Kominami E. Sustained calpain activation is associated with lysosomal rupture executes necrosis of the post ischemic CA1 neurons in primates. Hippocampus. 2003;13:791–800.

Yamashima T. Implication of cysteine proteases calpain, cathepsin and caspase in ischemic neuronal death of primates. Prog.Neurobiol. 2000;62:273–295.

Yeager MP, De Leo JA, Hoopes PJ, Hartov A, Hildebrandt L, Hickey WF. Trauma and inflammation modulate lymphocyte localization in vivo; quantitation of tissue entry and retention using indium-111-labeled lymphocytes. Crit Care Med. 2000;28:1477-1482.

Yilmaz G, Arumugam TV, Stokes KY, Granger DN. Role of T lymphocytes and interferon-gamma in ischemic stroke. Circulation 2006;113:2105-2112.

Young-Hyeh Ko, Sanghui Park, Heekyung Jin, Heesook Woo, Hyunseop Lee, Chaewha Park, Kihyun Kim. Granzyme B leakage-induced apoptosis is a crucial mechanism of cell death in nasal-type NK/T-cell lymphoma. Laboratory Investigation. 2007;87:241–250.

Youssef S, Steinman L. At one harmful and beneficial: the dual properties of NF-kB. Nature immunol. 2006;7:901-902

Zamzami N, Kroemer G. Condensed matter in cell death. Nature. 1999;401:127-128.

Zhang C, Lam TT, Tso MO. Heterogeneous populations of microglia/macrophages in the retina and their activation after retinal ischemia and reperfusion injury. Exp Eye Res.

2005;81:70070-9.

Zhang D, Beresford PJ, Greenberg AH, Lieberman J. Granzymes A and B directly cleave lamins and disrupt the nuclear lamina during granule-mediated cytolysis. Proc Natl Acad Sci U S A. 2001;98:5746-5751.

Zhang L, Schallert T, Zhang ZG, Jiang Q, Arniego P, Li Q, Lu M and Chopp M. A test for detecting long-term sensorimotor dysfunction in the mouse after focal cerebral ischemia. J. Neurosci. Meth. 2002;117:207-214.

Zhang W, Potrovita I, Tarabin V, Herrmann O, Beer V, Weih F, Schneider A, Schwaninger M. Neuronal activation of NF-kappaB contributes to cell death in cerebral ischemia. J Cereb Blood Flow Metab. 2005;25:30-40.

Zhang X, Chen J, Graham SH, Du L, Kochanek PM, Draviam R, Guo F, Nathaniel PD, Szabo C, Watkins SC, Clark RS. Intranuclear localization of apoptosis-inducing factor (AIF) and large scale DNA fragmentation after traumatic brain injury in rats and in neuronal cultures exposed to peroxynitrite. J Neurochem. 2002;82:181–191.

Zheng Z, Kim JY, Ma H, Lee JE. Yenari MA. Anti-inflammatory effects of 70 kDa Heat shock protein in experimental stroke. J Cereb Blood Flow and Metab. 2007;28:53-63.

Zhu C, Wang X, Qiu L, Peeters-Scholte C, Hagberg H, Blomgren K. Nitrosylation precedes caspase-3 activation and translocation of apoptosis inducing factor in neonatal rat cerebral hypoxia-ischaemia. J Neurochem. 2004;90:462-471.

Publications

ORIGINAL PAPER

Activation of Calpain, Cathepsin-b and Caspase-3 during Transient Focal Cerebral Ischemia in Rat Model

Ganta Vijay Chaitanya · Phanithi Prakash Babu

Abstract Calpains, cathepsins and caspases play crucial role in mediating cell death. In the present study we observed a cascade of events involving the three proteases during middle cerebral artery occlusion (MCAo) in Wistar rats. The rats were MCA occluded and reperfused at various time points. We observed a maximal increase in the levels of calpains during 1h and 12 h after reperfusion than permanently occluded rats. Further, these levels were reduced by 1st and 3rd day of reperfusion. Similarly the cathepsin-b levels were significantly increased during 1h and 12 h, of reperfusion, followed by activation of caspase-3 which reached maximal levels by 1st and 3rd day of reperfusion. The sequential activation of calpains, cathepsin-b and cleaved caspase-3 is evident by the Western blot analysis which was further confirmed by the cleavage of substrates like PSD-95 and spectrin. The differences in the regional distribution and elevation of these proteases at different reperfusion time periods indicates that differential mode of cell death occur in the brain during cerebral ischemia in rat model.

Keywords Calpain · Cathepsin-b · Active caspase-3 · PSD-95 · Spectrin · Middle cerebral artery occlusion · Focal cerebral ischemia · Apoptosis · Necrosis

Introduction

Ischemic cell death is often considered to be chaotic due to involvement of many proteases belonging to various families, and their cross talks. Ischemic brain injury after ischemia-reperfusion is modulated by at least two morphologically distinct cell death pathways, namely necrosis and apoptosis. The induction of apoptosis and necrosis is tightly regulated process by several biochemical intermediates, including alterations in high-energy phosphates, intracellular calcium accumulation and reactive oxygen species etc. [1–3].

Apoptosis is an evolutionarily conserved mode of cell death characterized by a discrete set of biochemical and morphological events through the members of caspase family. Necrosis has been defined as a type of cell death that lacks the features of apoptosis and autophagy and is considered to be uncontrolled initiated by noncellular mechanisms such as ischemia, trauma and thrombosis. These events ultimately lead to irreversible cell death with depletion of high energy stores, and disruption of the cellular membrane involving fluid and electrolyte imbalance, cell swelling, loss of potassium and magnesium ions and accumulation of intracellular water, sodium chloride, hydrogen and calcium [3–5]. However, recent research suggests that its occurrence and course might be tightly regulated. The acidification of cytoplasm is required for necrotic cell death though the reason for the acidification remains unclear [5, 6]. Investigations in both nematodes and mammals converge to implicate specific calpain and lysosomal proteases (cathepsins) in the execution of necrotic cell death [7, 8].

Caspases belong to the cysteine protease family, which are specifically activated during apoptotic stimuli. Caspase-activated and caspase-mediated cell death is marked by the fragmentation of nuclear DNA and the generation of internucleosomal fragments (mono- and/or oligomers of 200 bp, DNA ladders), whereas DNA degradation in necrosis is random and nonspecific. While caspase

G. V. Chaitanya · P. P. Babu (✉)
Centre for Biotechnology and Department of Animal Sciences, School of Life sciences, University of Hyderabad, Hyderabad, AP 500046, India
e-mail: ppbsl@uohyd.ernet.in; pbphanithi@yahoo.com

activation is specific to apoptosis, calpains and cathepsin activation occurs during both apoptosis and necrosis. Recent data suggest that necrosis rather than apoptosis appear to be the crucial component of the damage to the nervous system during human ischemic injuries and neurodegenerative diseases [3].

Studies in primates indicate that damage to the lysosomal membrane is inflicted enzymatically by activated calpains, which localize to lysosomal membranes after the onset of ischemic episodes, with subsequent spillage of cathepsins into the cytoplasm. This observation led to the formulation of the "Calpain–Cathepsin hypothesis," whereby the calcium-mediated activation of calpains results in the rupture of lysosomes and leakage of killer cathepsins that eventually dismantle the cell [9].

The relative role of these proteases, which mediate necrosis and apoptosis, remains unclear in transient fore brain ischemia. Determining the relative roles of calpains, caspases and cathepsins in post-ischemic neuronal death is further complicated by potential cross talk between these proteolytic systems. Calpains and caspases cleave many common substrates including cytoskeletal and regulatory proteins [10]. In addition, these protease systems appear to modulate each other via calpain-mediated cleavage of caspases 3, 7, 8, 9, cathepsin [10, 11] and caspase-3-mediated cleavage of calpastatin [12], which is an endogenous inhibitor of calpain, there by activating calpain. These potential interactions amplify the importance of understanding the spatio-temporal distribution of calpain, caspase and cathepsin-b activity in the post-ischemic brain. In the present study we compared the relative activity, localization, and time course of calpain, active caspase-3 and cathepsin-b and proteolysis mediated by them on various substrates in the adult rat brain following middle cerebral artery occlusion in rat.

Experimental Procedure

Antibodies

Calpain antibody used for immunohistochemical analysis was purchased from Research Diagnostics Inc. (RDI) Flanders, NJ, for Western blot analysis gift from Dr. Spencer, University of California, Los Angeles. Cathepsin-b antibody was purchased from Oncogene, Sandiego, CA. Cleaved Caspase-3 antibody, which detects p-20 fragment, used for immunohistochemical analysis and caspase-3 antibody for Western blot analysis, was purchased from Cell Signaling and Technology (CST) Beverly, MA. PSD-95 and Spectrin antibodies were gift from Prof. Emmanuel Brouillet, Service Hospitalier Frédéric Joliot, France.

Surgical Procedure

All experiments were performed according to the guidelines of Institutional Animal Ethical Committee (IAEC). Male Wistar rats, weighing 300–350 g, were used in the present study. Rats were randomly divided into 6 groups. 1, sham group; 2, permanently occluded for 3 h; 3, 1 h reperfused; 4, 12 h reperfused; 5, 1 day reperfused; 6, 3 days reperfused groups which were 3 h MCA occluded. MCAo was achieved by the nylon suture method [13], in which the left middle cerebral artery (MCA) was occluded by inserting a nylon monofilament through the external carotid artery to occlude origin of MCA for 3 h. The animals were anesthetized using N_2O-halothane mixture through facemask. Briefly, the bifurcation of the left common carotid artery, the bifurcation of the left internal carotid artery, and the left external carotid artery were exposed through a midline neck incision. The external carotid artery was ligated distally. A 3–0 monofilament suture (50 mm in length), was inserted through an arteriectomy of the external carotid artery. The nylon suture was gently advanced from the external carotid artery into the internal carotid artery. The path of the suture towards the base of the skull was visualized. Approximately 17.5–18 mm of suture was inserted past the common carotid artery bifurcation to block the origin of the left MCA. The occlusion of the MCA was felt. For the sham-operated rats, the carotid arteries were exposed; suture was inserted but was not extended to occlude the MCA. The animal was allowed to recover from anesthesia. After the occlusion period the animal was re-anesthetized and the filament was removed from the artery.

Three rats from 1 h reperfusion time period were perfusion-fixed with saline followed by 4% paraformaldehyde and the brains were dissected out for immunohistochemical analysis. Group of 4 rats from each group were killed with an overdose of pentobarbital, brains were removed quickly and the ipsilateral ischemic regions were processed for immunoblotting.

Behavioral Tests

After the recovery of the animal from anesthesia an observer who was masked to the experimental conditions performed two types of behavioral functional tests. Neurological deficits were scored as follows; no neurological deficit normal (0); failure to extend the right forepaw fully (1); circling to the right (2); unable to walk spontaneously (3) and dead (4). The second test, the corner test, which is a sensorimotor functional assessment, was performed in ischemic animals as described previously [14]. In this test, the ischemic rat turns preferentially toward the non-impaired side. The turns in one versus the other direction

were recorded from 10 trials for each test. The animals, which exhibited only 2nd or 3rd degree of behavioral deficit, were taken in this study.

Western Blots

After decapitation, rat brains ($n = 4$) were dissected immediately and ipsilateral hemispheres were separated, snap frozen in liquid nitrogen and stored at $-80°C$ until analysis. Tissues were homogenized in the radio immunoprecipitation assay buffer containing 50 mM Tris–HCl pH 8.0, 150 mM NaCl, 1 mM EDTA, 0.4% deoxy chlolate, 1% non-idet P-40 containing protease inhibitors including 1 mM PMSF and phosphatase inhibitors including 10 mM β-glycerophosphate, 10 mM NaF, 0.3 mM Na_3VO_4. The lysates were sonicated for 2 min in the equal intervals of time period and then centrifuged at 14,000g for 15 min at 4°C. Supernatants were collected into pre-chilled eppendorfs and used as protein samples for further analysis. Equal amounts of protein were separated using SDS-PAGE and further transferred onto nitro-cellulose membrane. The transferred immunoblots were blocked in non-fat skimmed milk (5%) in tris buffer saline (TBS; 10 mM Tris pH 7.5, 150 mM NaCl) for 1 h. The membranes were incubated for 12–14 h in primary antibodies raised against calpain, cleaved caspase-3, cathepsin-b, PSD-95 and spectrin. Blots were re-incubated with secondary antibodies conjugated to alkaline peroxidase (ALP) (anti-rabbit and anti-mouse IgG conjugated to ALP obtained from Genei Pvt. Ltd., Bangalore, India), for 1 h at room temperature. Before and after incubation of blots with secondary antibodies, blots were washed with TBS and TBST (TBS containing 0.1% Tween 20). Immunoreactivity was visualized by incubating the blots in BCIP/NBT substrate.

Cresyl Violet Staining

Formalin fixed, paraffin embedded ischemic rat brain sections were deparaffinized in xylene, rehydrated in alcohol series and incubated in 0.1% Cresyl violet solution for 3–5 min. The sections were then rinsed in distilled water and differentiated in 95% alcohol, followed by dehydration in 100% alcohol. The sections were then cleared in xylene and mounted using DPX mounting medium.

TTC Staining

After decapitation ischemic rat brains were dissected immediately and chilled in ice-cold saline for 5 min. The brain was sliced into 2 mm thick slices with the help of brain matrices. The slices were then incubated in phosphate-buffered saline (pH 7.4) containing 2% TTC at 37°C

for 20 min and then stored in 10% neutral-buffered formalin [15]. Slices were photographed with the help of Nikon camera.

Immunohistochemistry

For immunohistochemical analysis ($n = 3$), rats after MCA occlusion were perfusion-fixed with saline and then with 4% paraformaldehyde solution by overdose of pentobarbital. Brains were removed and post-fixed in the same fixative for another 24 h. Then each tissue block was dehydrated, embedded in paraffin, and cut into 3–4 μm thick coronal sections. Paraffin was removed from slides using xylene, followed by rehydration in an alcohol dilution series. Antigen retrieval was performed using a microwave method. Slides were incubated for 20 min after slow boiling for 10 min and rinsed in PBS. Slides were soaked in 0.1% Triton-X 100 in PBS for 5 min to increase permeability of fixed tissue, followed by rinsing in 1X PBS. Endogenous peroxidase was blocked by incubation for 45 min in methanol containing 1.5% hydrogen peroxide and blocked using 10% normal goat serum for 1 h. The sections were then stained with monoclonal antibodies raised against calpain, cleaved caspase-3 (p-20 fragment) and cathepsin-b (diluted 1:100). After they were washed, the sections were overlaid for 1 h with peroxidase goat anti-mouse and anti-rabbit antibodies followed by developing with DAB complex (DAKO-kit). All incubations were performed under humidified conditions, and slides were washed 4 times for 5 min each in PBS between steps. Contralateral hemisphere, omission of primary or secondary antibody served as negative controls.

Results

Elevation of Calpain and Cathepsin-b Levels

The intensity of the calpain and cathepsin-b levels evident by the Western blot analysis showed a significant increase from 0 h reperfusion till the 3 day (Figs. 1 and 2). However a maximal increase was observed during 1 and 12 h indicating the contribution of reperfusion injury in the pathology of cerebral ischemia at these time points. Serial sections probed with calpain in order to check its localization in the brain during ischemia revealed a significant increase and localization in the striatum of the infarct in the ipsilateral hemisphere of the rat brain (Fig. 3), compared with the contralateral hemisphere. Immunohistochemical analysis for cathepsin-b showed a clear increase in the levels of cathepsin-b in the ischemic region (Fig. 4) over the contra lateral hemisphere, which correlated with the localization of calpains. Immunohistochemical analysis was performed on
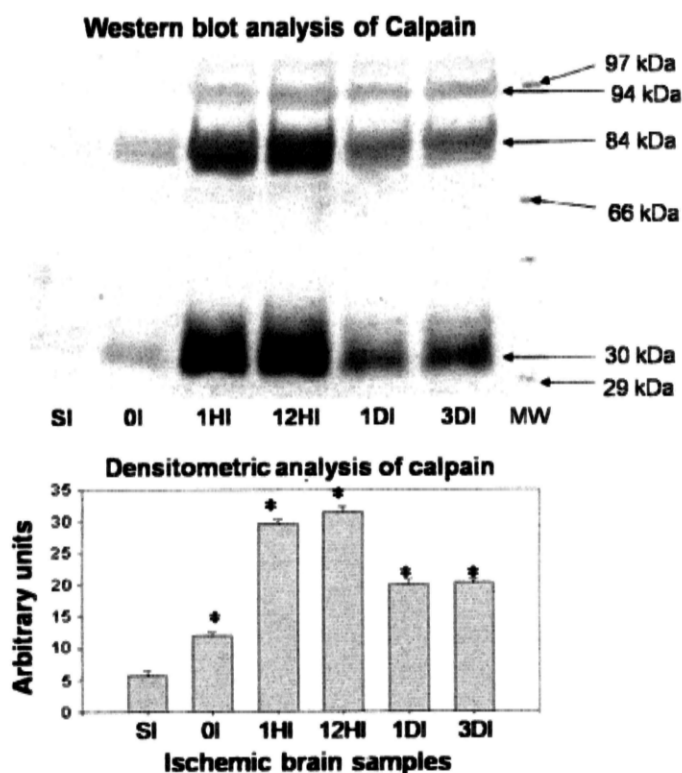
Western blot analysis of Calpain

97 kDa
94 kDa
84 kDa
66 kDa
30 kDa
29 kDa

SI   OI   1HI   12HI   1DI   3DI   MW

Densitometric analysis of calpain

Fig. 1 Western blot and densitometric analysis of calpain levels during cerebral ischemia in rat brain. A significant increase in the calpain levels were observed in ischemic samples over the sham operated samples starting from the permanent occlusion for 3 h time period till the 3 day of reperfusion. SI (Sham ischemic), OI (0 h ischemic), 1HI (1 h ischemic), 12HI (12 h ischemic), 1DI (1 day ischemic), 3DI (3 days ischemic) reperfused ischemic ipsilateral samples respectively after 3 h occlusion. P > 0.05

1 h reperfused brain samples. However, during later time periods, correlating with the activation of caspases the presence or localization of calpains and cathepsins varied due to the decrease in the intensity of insult.

Elevation of Cleaved Caspase-3 Levels

Apoptosis is a highly regulated programmed cell death mediated by activated caspases. We observed a significant increase in the cleaved active form of caspases-3 from 1 h of reperfusion till the 3, 1 and 3 day time periods being the maximal intensity observed (Fig. 5).

Further, in order to check the localization of active caspases-3 in the tissue section we performed immuno-histochemical analysis. We observed a significant increase in the active caspases-3 immunoreactivity around the infarct maximum in the cortical regions compared to striatum (Fig. 6). We did not observe any significant increase in the contralateral hemisphere. Though we observed some immunoreactivity in the striatum, it might be due to some of the cells, which might have undergone secondary necrosis failing to execute the apoptotic program.
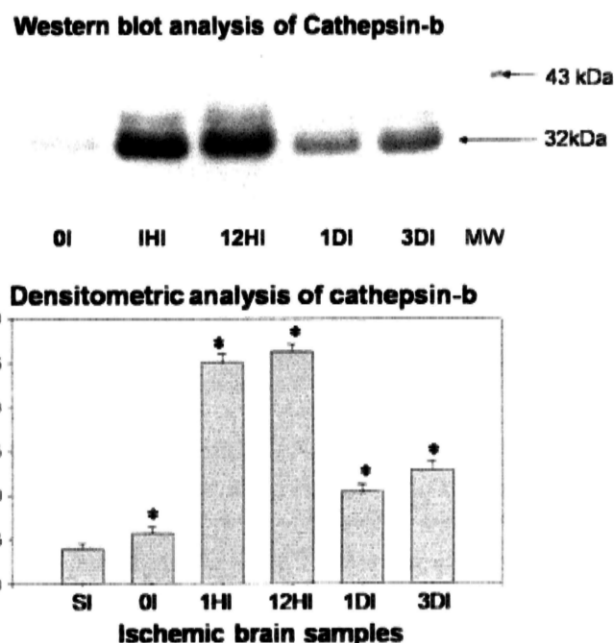
Western blot analysis of Cathepsin-b

43 kDa
32 kDa

SI   OI   IHI   12HI   1DI   3DI   MW

Densitometric analysis of cathepsin-b

Fig. 2 Western blot and densitometric analysis of cathepsin-b levels during cerebral ischemia in rat brain. A significant increase in the cathepsin-b levels was observed in ischemic samples over the sham operated, starting from 1 h reperfused time period till the 3 day of reperfusion. SI (Sham ischemic), OI (0 h ischemic), 1HI (1 h ischemic), 12HI (12 h ischemic), 1DI (1 day ischemic), 3DI (3 days ischemic) reperfused ischemic ipsilateral samples respectively after 3 h of occlusion. P > 0.05

Differential Breakdown of Spectrin by Caspases and Calpains

α-Spectrin is cyto-skeletal protein, which is known to produce signature fragments of 145, 150 and 120 kDa upon cleavage respectively by calpain and caspases respectively. In our study consistent with other reports we observed significant increase in the breakdown products of α-Spectrin to 150 and 145 kDa signature fragments produced by calpains and 120 kDa signature fragment produced by caspase-3 during cerebral ischemia (Fig. 7). The intensity of the Spectrin Break Down Products (SBDP) significantly increased during the reperfusion period, indicating the involvement of both proteases in the ischemic injury and also the impact of reperfusion injury during cerebral ischemia. Western blot analysis of actin was performed to confirm equal loading (Fig. 8).

Cleavage of PSD-95 by Calpains

PSD-95 belongs to Membrane Associated Guanylate Kinase (MAGUK) family. Alterations in the calcium concentration, plays an important role in the activation of calpains thereby acting upon many of its substrates of which PSD-95 is one. We observed two truncated products migrating at 50 and 36 kDa, respectively generated from
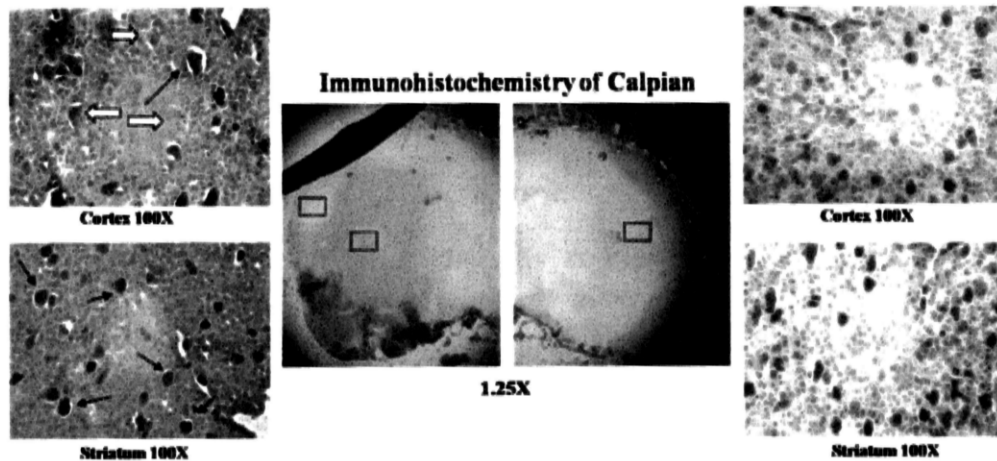
Immunohistochemistry of Calpian

1.25X

Cortex 100X

Striatum 100X

Cortex 100X

Striatum 100X

Fig. 3 Immunohistochemical localization of calpain in the ischemic rat brain. A significant increase in the localization of calpain in the ipsilateral cortex than contralateral is visible. Images were taken under a magnification of 1.25X and 100X to have a clear view of regional and cellular localization of calpains in the infarct. Pyknotic cells and few shrunken cells resembling apoptotic cells stained positive for calpain in striatum and cortex respectively. White arrows point the less immunoreactive cells and black arrows point the degenerating cells, which were highly immunoreactive for calpain. Photographs were taken with Nikon Alphaphot YS2 microscope
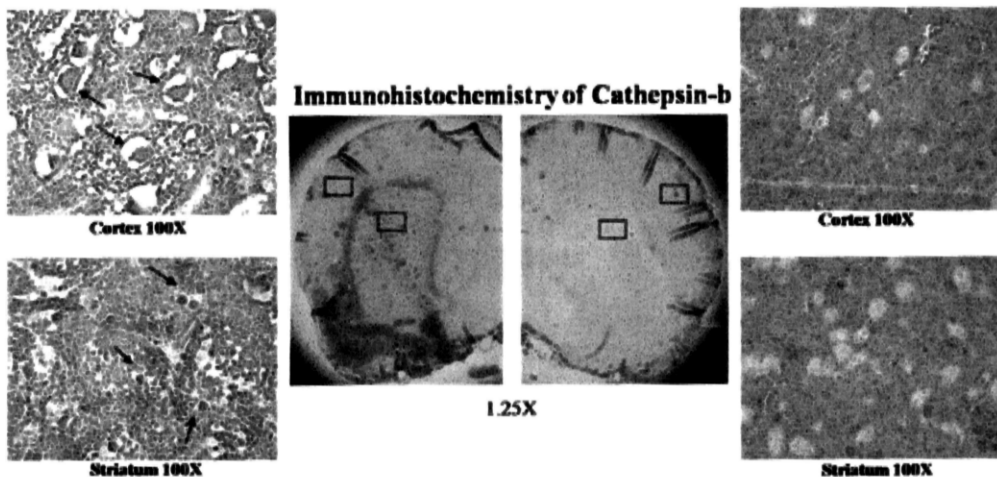

Immunohistochemistry of Cathepsin-b

1.25X

Cortex 100X

Striatum 100X

Cortex 100X

Striatum 100X

Fig. 4 Immunohistochemical localization of cathepsin-b in the ischemic rat brain. A significant increase in the localization of cathepsin-b in the ipsilateral cortex than contralateral is visible. Black arrows point the degenerating cells, which were highly immunoreactive for cathepsin-b. Images were taken under a magnification of 1.25X and 100X to have a clear view of regional and cellular localization of calpains in the infarct. Bright field Images were taken with Olympus UCTR30-2 fluorescent microscope

PSD-95 (Fig. 9) during cerebral ischemia. The intensity of cleaved products was almost in a similar manner with that of the elevated levels of calpain. We observed a significant increase in the intensity of the cleaved PSD-95 starting from 0 h till the 3rd day, of which 1 and 12 h reperfusion samples being the maximum intensity over the sham operated ischemic brain region.

Discussion

Cerebral ischemia results in an infarct comprising of central necrotic core and a physiologically ill penumbra, which gradually merges into the core. Calpains and cathepsin-b are known to mediate necrotic cell death and apoptotic cell death independent or dependent of caspases [16–18]. Even though a substantial amount of literature is available on the involvement of various proteases and cell death mechanisms during cerebral ischemia, their time periods of activation, regional localization and their cross talks are sparse. Therefore in the present study, we investigated the role of these protease systems during middle cerebral artery occlusion.

Focal cerebral ischemia model has been standardized for 3 h occlusion in rat model and studied reperfusion induced cell death at different time periods and localization of the proteases in and around the infarct as well as the status of some of their substrates like, PSD 95 and α-Spectrin during the reperfusion period of cerebral ischemia. We observed a significant increase in the levels of calpains, cathepsin-b
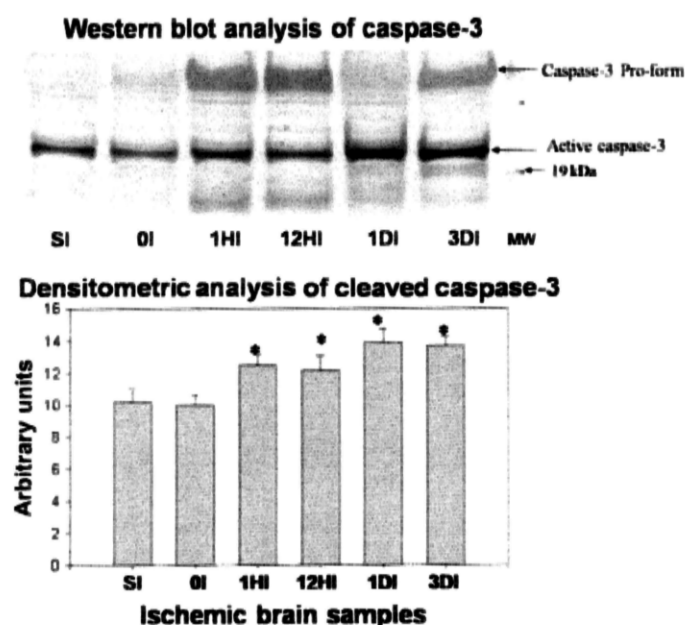
Western blot analysis of caspase-3

Densitometric analysis of cleaved caspase-3

Fig. 5 Western blot and densitometric analysis of cleaved caspase-3 levels during cerebral ischemia in rat brain. A significant increase in the cleaved caspase levels were observed in ischemic samples over the sham operated, starting from 1 h reperfused time period till the 3 day of reperfusion. However there was a significant increase in the levels of active caspase-3 starting from 1-day reperfusion time period till 3 day indicating the contribution of apoptotic cell death from these time periods. SI (Sham ischemic), 0I (0 h ischemic), 1HI (1 h ischemic), 12HI (12 h ischemic), 1DI (1 day ischemic), 3DI (3 days ischemic) reperfused ischemic ipsilateral samples respectively after 3 h of occlusion. $P \geq 0.05$

and cleaved caspases-3 respectively. Disturbances in the cellular calcium levels results in a fast and transient over activation of calpains. The time course of their activation mainly depends on the intensity of the insult. We observed a significant increase in calpain levels starting from 0 h
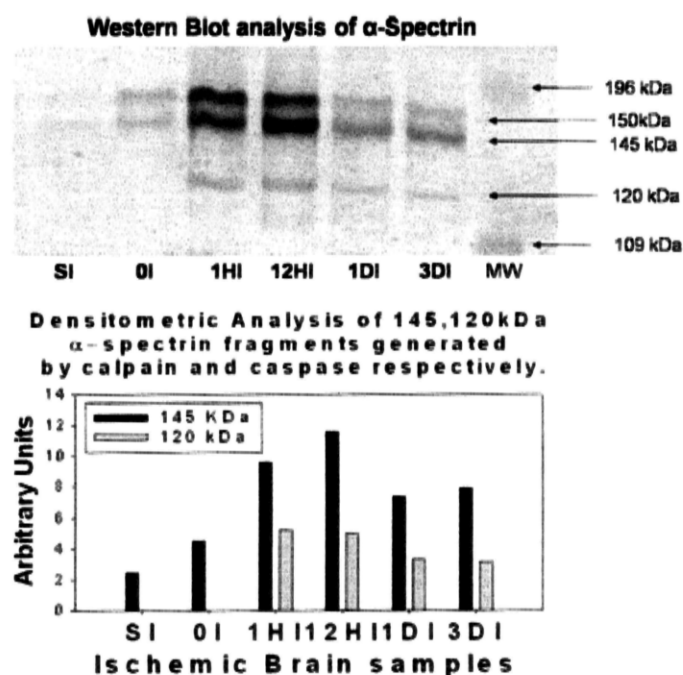
Western Blot analysis of α-Spectrin

Densitometric Analysis of 145,120kDa α-spectrin fragments generated by calpain and caspase respectively.

Fig. 7 Western blot and densitometric analysis of spectrin cleavage pattern during cerebral ischemia in rat brain. A Differential cleavage pattern of spectrin is observed in the form of 150, 145 and 120 kDa produced by calpains and active caspase-3 respectively. Significant increase in the 150 and 145 kDa fragment levels were observed in ischemic samples over the sham operated, starting from 0 h reperfused time period till the 3 day of reperfusion. However 120 kDa fragment showed an increase starting from 1 h reperfusion time period. SI (Sham ischemic), 0I (0 h ischemic), 1HI (1 h ischemic), 12HI (12 h ischemic), 1DI (1 day ischemic), 3DI (3 days ischemic) reperfused ischemic ipsilateral samples respectively after 3 h of occlusion

reperfusion period, which peaked by 1 h. Over activation of calpains, might be the key and first step in the cell death during cerebral ischemia. Cathepsin-b levels were also
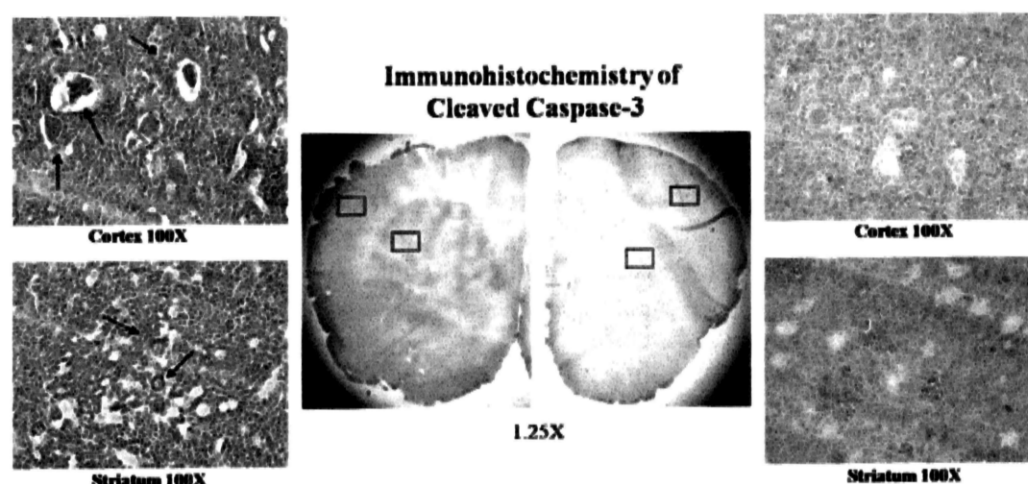
Immunohistochemistry of Cleaved Caspase-3

Fig. 6 Immunohistochemical localization of cleaved caspase-3 in the ischemic rat brain. A significant increase in the localization of active caspase-3 in the ipsilateral cortex than contralateral is visible. However increase in the immunoreactivity is mostly confined to apoptotic cells in the cortex than the pyknotic cells in the striatum. White arrows point the less immunoreactive cells and black arrows

point the degenerating cells, which were highly immunoreactive for cleaved caspse-3. Images were taken under a magnification of 1.25X and 100X to have a clear view of regional and cellular localization of active caspase-3 in the infarct. Bright field Images were taken with Olympus UCTR30-2 fluorescent microscope
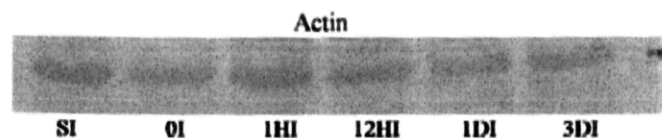
Actin

SI   OI   1HI   12HI   1DI   3DI

Fig. 8 Western blot of Actin showing equal loading

Western blot analysis of PSD-95

95 kDa

51 kDa
50 kDa

36 kDa

SI   OI   1HI   12HI   1DI 3DI   MW

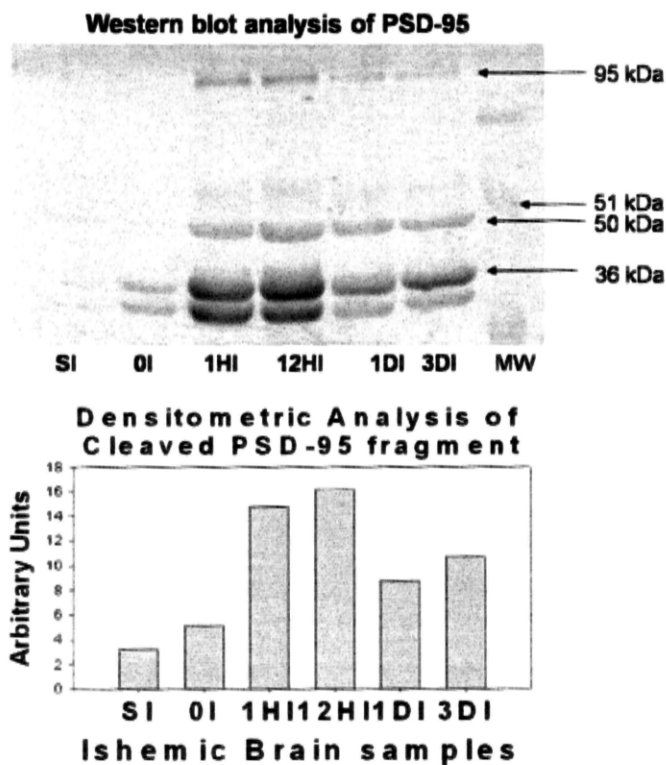**Densitometric Analysis of Cleaved PSD-95 fragment**

Fig. 9 Western blot and densitometric analysis of PSD-95 levels during cerebral ischemia in rat brain. A significant increase in the cleavage of PSD-95 was observed in ischemic samples over the sham operated, starting from permanent occlusion for 3 h time period till the 3rd day of reperfusion. We observed the cleavage products 50 and 36 kDa produced by the action of calpains. SI (Sham ischemic), OI (0 h ischemic), 1HI (1 h ischemic), 12HI (12 h ischemic), 1DI (1 day ischemic), 3DI (3 days ischemic) reperfused ischemic ipsilateral samples respectively after 3 h of occlusion

significantly increased by 1 h reperfusion period. Over production of free radicals might damage the lysosomal membrane there by contributing to the spillage of cathepsin-b during the reperfusion phase of cerebral ischemia. Moreover, interaction of calpains with the lysosomal membranes also exacerbates this process [8]. The elevation and activation of calpains and cathepsin-b provides clear information about their crucial role in mediating necrosis during the initial hours of the insult. However, the extent they mediate the necrotic cell death independently, during cerebral ischemia needs to be elucidated.

Cell death in penumbra is known to be apoptotic, mediated by caspases [19]. Though we observed an increase in the levels of active caspase-3 from 1 h

reperfusion period, its intensity was at peak only from 1 day after reperfusion indicating that apoptosis might be a late event in the pathology of cerebral ischemia [15]. We observed a clear presence of calpains and cathepsin-b in the infarct presumably in the necrotic core during the initial hours. However, caspases were mainly confined to the periphery presumably penumbra, though a small increase in its intensity in core is observed. Caspases are not implicated in necrotic cell death and are strict regulators of apoptosis. The presence of caspase activity amidst necrotic cells might be due to the execution of both apoptotic and necrotic cell death mechanisms in the same cell. Further apoptosis of immune cells infiltrating the infarct also might contribute to the caspase positivity in the necrotic core of the infarct [20, 21]. Further the cell death morphology observed by staining the sections with Cresyl violet showed necrotizing and pyknotic cells in striatum and apoptotic cells in the cortical region, correlating with the increase immunoreactivity of calpains and cathepsin-b in striatum and cortex respectively (Fig. 10). The morphological features of cell death resembled same as the morphology observed in immunohistochemical analysis of calpain, cathepsin-b and cleaved caspase-3, which showed pyknotic cells and apoptotic, cells respectively. Moreover, calpains and cathepsin-b immunostaining correlated with the white colored region of the TTC stained ischemic rat brain and caspase-3 immunostaining correlated with the red colored region (Fig. 11).

Activation of these proteases brings about the breakdown of wide range of substrates like PARP, which is a substrate of caspases, calpains, cathepsin-b and granzymes, spectrin a substrate for calpains and caspases and PSD-95 a substrate for calpain alone. PARP generates an array of signature fragments of 89, 21, 72, 64 and 50 kDa when acted upon by caspases, granzymes and cathepsin-b respectively [10, 22]. We observed a significant increase in the break down products of spectrin to 150 and 145 kDa belonging to calpain and 120 kDa belonging to caspases respectively. However, the intensity of calpain derived fragments over the caspase derived fragment was significantly high implicating a prominent role of calpains during cerebral ischemia. It has been observed that PSD-95 is cleaved by calpains to 50 and 30 kDa during developing and adult rat brain [23]. We observed a significant increase in the 50 and 30 kDa-truncated products generated by calpain during middle cerebral artery occluded rat model. While 150 and 145 kDa spectrin fragments were increased from 0 h reperfusion period correlating with the increase of calpains, 120 kDa fragment was observed only after the reperfusion has started even the intensity is low indicating that the calpains might be the first proteases to be activated in the molecular events leading to cellular demise in cerebral ischemia.
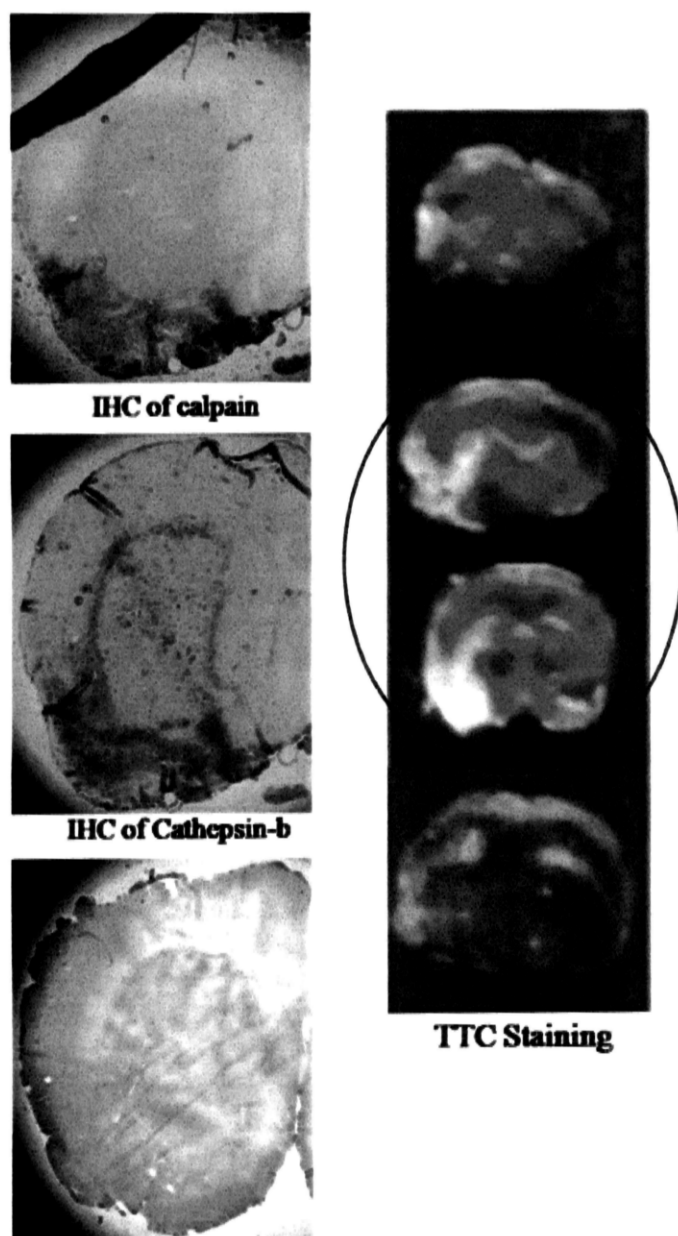
IHC of calpain

IHC of Cathepsin-b

TTC Staining

Cresyl Violet Staining

Necrotic neurons in ipsilateral Striatum. 100X

Neurons in Contralateral striatum 100X

Pyknotic neurons in ipsilateral striatum. 100X

Neurons in Contralateral striatum 100X

Apoptotic neurons in ipsilateral Cortex. 100X

Neurons in Contralateral cortex 100X

Fig. 11 Cresyl violet stained rat brain sections. Cresyl violet stains the nissil granules of the neurons and renders purple colour to neurons (**a**) necrotizing neurons in the striatum of ipsilateral hemisphere. (**b**) Pyknotic cells in the striatum of ipsilateral hemisphere. (**c**) Apoptotic neurons in the cortex of the ipsilateral hemisphere. (**d**, **e**, and **f**) Normal neurons in the striatum and cortex of contralateral hemisphere. Bright field Images were taken with Olympus UCTR30-2 fluorescent microscope

Fig. 10 TTC stained rat brain sections. Ischemic rat brain was cut into 2 mm thick slices and incubated in TTC solution for 15–20 min at 37°C. Ischemic regions appeared white in colour and non-ischemic region red in colour. Immunohistochemical analysis was performed on other ($n = 3$) ischemic rat brain sections correlating with the encircled TTC stained ischemic brain slices

Cell death in cerebral ischemia is extremely complex and is disordered, due to the involvement of large number of proteases [24, 25]. The nature of these proteases in mediating cell death individually and in synergic manner with proteases of other families makes the understanding of the molecular and biochemical events extremely difficult. The time dependent elevation and activation of these proteases makes pharmaceutical intervention in cerebral ischemia extremely difficult. A combination of drugs aimed at suitable time periods depending on activation time periods of these proteases might be of potential use.
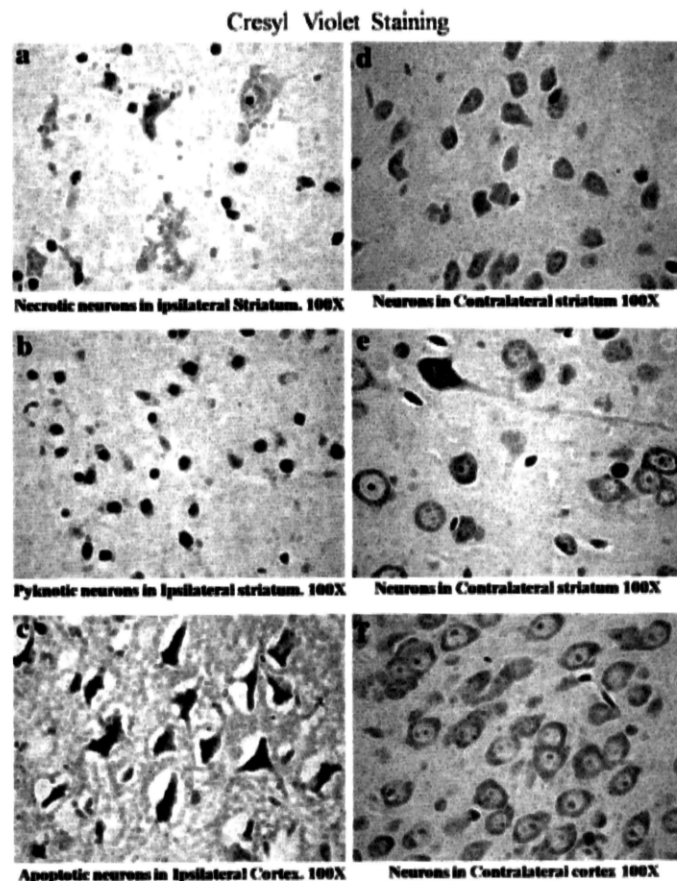
However, studies in this direction to elucidate the molecular events during focal cerebral ischemia are necessary.

References

1. Mc Conkey DJ (1998) Biochemical determinants of apoptosis and necrosis. Toxicol Lett 99:157–168
2. Haunstetter A, Izumo S (1998) Apoptosis: basic mechanisms and implications for cardiovascular disease. Circ Res 82:111–1129
3. Syntichaki P, Tavernarakis N (2003) The biochemistry of neuronal necrosis: rogue biology? Nat Rev Neurosci 4:672–684
4. Nicotera P, Leist M, Ferrando-may E (1998) Intracellular ATP, a switch in the decision between apoptosis and necrosis. Toxicol lett 102–103:139–142
5. Sapolsky RM, Trafton J, Tombaugh GC (1996) Excitotoxic neuron death, acidotic endangerment, and the paradox of acidotic protection. Adv Neurol 71:237–244